ADSORPTION OF BINARY VAPOR MIXTURES ONTO SOLIDS

by

Gracia Ann Perfetti

Dissertation submitted to the Graduate Faculty of the

Virginia Polytechnic Institute and State University

in partial fulfillment of the requirements for the degree of

DOCTOR OF PHILOSOPHY

in

Chemistry

APPROVED:

J. P. Wightman, Chairman

J. G. Mason

M. A. Ogliaruso

T. C. Ward

J. W. Viers

May, 1975

Blacksburg, Virginia

DEDICATION

To My Parents and My Husband

ACKNOWLEDGMENTS

I am deeply grateful to my research director, Dr. James P. Wightman, for his guidance and encouragement during the course of this investigation. His patience and his friendship have been instrumental in bringing this work to a successful conclusion.

I am indebted to the members of my committee, Dr. John Mason, Dr. Michael Ogliaruso, Dr. Thomas Ward, and Dr. James Viers, not only for their helpful suggestions in the preparation of this dissertation, but also for their friendship during the past four years.

I would like to thank those persons who have assisted in the construction and repair of the experimental equipment, especially Andy Mollick of the glassblowing shop and Dave McCommon and Rick Miller of the electronics shop.

I wish to acknowledge the National Science Foundation for financial support of this investigation.

TABLE OF CONTENTS

LIST OF TABLES

LIST OF FIGURES

I. INTRODUCTION

Physical adsorption of pure gases and vapors onto solids has been studied extensively (1, 2). In contrast, data on adsorption from gas mixtures are scarce (3). There is no simple function which relates adsorption from gas mixtures to adsorption of the pure components. When a gas mixture is adsorbed on a solid, the components compete for the surface. Since the strengths of the gas-solid interactions are different for the various components, selective adsorption can occur. It is this selectivity that makes adsorption onto solids a potential method of separation.

Separation of gas mixtures on an industrial scale by adsorption is often more economical than separation by more conventional methods. For this reason there is a large amount of interest in adsorption of mixtures by solids in the hydrocarbon industry. Lewis et al. (4) have shown that mixtures of low-boiling hydrocarbons are readily separated by adsorption onto solids at ordinary temperatures and pressures; separation by distillation requires high pressure units and refrigeration. Separation of constant-boiling mixtures is often readily performed by adsorption onto solids (5). There has also been an increased use of adsorption for removal of trace impurities from gases (6).

There is considerable interest in adsorption onto solids as a means of reducing air pollution. For example, adsorption onto carbon is being used to remove vinyl chloride from the air in polyvinyl chloride factories (7). Not only are health standards improved, but valuable starting material is recovered.

To determine if separations by adsorption are feasible, data on adsorption of mixtures onto solids are required. While pure vapor adsorption data are easily obtained, measurement of adsorption of vapor mixtures is complicated and time-consuming. It would, therefore, be advantageous to be able to calculate mixed vapor adsorption from adsorption data for the pure components. Several models have been developed for this purpose. But because of the scarcity of mixed vapor adsorption data, the validity of these models has not been adequately investigated.

This work was undertaken to obtain experimental adsorption isotherms for binary vapor mixtures onto solids, along with pure component adsorption data. The adsorbates chosen for study were ethanol, benzene, and cyclohexane. The adsorbents used were silica and carbon. A wide variety of adsorbate-adsorbent interactions are possible with these choices. Heats of adsorption and adsorbate cross-sectional areas were obtained from the pure component isotherms. Finally, the isotherms obtained for the binary vapor mixtures were compared to those calculated from the pure component isotherms using several thermodynamic models.

II. HISTORICAL

Young and Crowell's "Physical Adsorption of Gases" (2) contains a general review of the literature on adsorption of binary vapor mixtures onto solids prior to 1957. For the most part, the following survey will be limited to systems in which the adsorbate is a mixture of organic vapors and the adsorbent is silica or carbon. Several models for calculating binary vapor adsorption from the isotherms of the pure components will also be presented.

Adsorption Isotherms

Innes and Rowley (8) have studied the adsorption of methanol-carbon tetrachloride vapor mixtures onto activated charcoal at 25°C. Isotherms of the amounts of each component adsorbed versus partial pressure for several constant adsorbed phase compositions were measured. Preferential adsorption of methanol occurred. Values of ϕ, the total number of moles adsorbed at monolayer coverage, were obtained for each adsorbed phase composition. If normal liquid packing is assumed for the adsorbed phase, the ratio of the monolayer values for pure methanol and carbon tetrachloride, ϕ_M/ϕ_C, should be equal to the ratio of the molecular areas of carbon tetrachloride and methanol calculated from their molar volumes, $\bar{V}$:

$$\frac{\phi M}{\phi C} = \left[\frac{\bar{V}_C}{\bar{V}_M}\right]^{2/3} \qquad (1)$$

The ratio ϕ_M/ϕ_C calculated from Equation (1) is 1.77; the experimental

ratio was 2.31. Since carbon tetrachloride is a symmetric molecule, it was expected to occupy the area based on its molar volume. The authors, therefore, concluded that the discrepancy in the ratios was caused by methanol occupying less than its normal area. The authors postulated that since charcoal is hydrophobic, methanol is vertically oriented with the methyl group lying on the surface. With this type of orientation, the hydroxyl groups would be free to hydrogen bond, which would account for the evidence of lateral interaction observed in the pure methanol isotherm. The ratio ϕ_M/ϕ_C calculated from Equation (1) with the methanol molecules so oriented is 2.31, in excellent agreement with experiment. The experimental values of ϕ for the mixtures agreed well with the following equation:

$$\frac{1}{\phi} = \frac{x_C}{\phi_C} + \frac{x_M}{\phi_M} \qquad (2)$$

where x_i is the mole fraction of component i in the adsorbed phase. Thus, the areas occupied by methanol and carbon tetrachloride were mutually independent. Since Equation (2) was valid, the authors concluded that methanol is also vertically oriented in the mixtures.

A similar study was made for adsorption of methanol-benzene vapor mixtures on charcoal at 25°C by Innes, Olney, and Rowley (9). Preferential adsorption of methanol was observed. The experimental data were in good agreement with an expression analogous to Equation (2). Assuming that the methanol molecules are vertically oriented with the methyl groups lying on the surface, the ratio ϕ_M/ϕ_B calculated from Equation (1) is 2.17. Since the experimental ratio was 2.42, the

authors postulated that benzene molecules lie flat on the surface and, thus, occupy more than the area based on molar volume.

Cines and Ruehlen (10) have studied the effect of surface coverage and multilayer formation on selective adsorption by measuring adsorption of benzene-2,4-dimethylpentane vapor mixtures on two different silica gels at 65.6°C. Silica gel I showed only monolayer adsorption; silica gel II exhibited multilayer adsorption. Isotherms of amounts adsorbed versus pressure for three different equilibrium* vapor phase compositions were obtained on silica gel I. Benzene was selectively adsorbed from the mixtures. The dependence of selective adsorption on surface coverage was investigated by plotting the selectivity versus total pressure. Selectivity, α, is defined as:

$$\alpha = \frac{x_1/y_1}{x_2/y_2} \qquad (3)$$

where x_i and y_i are mole fractions in the adsorbed and vapor phases, respectively. Selectivity increased with increasing pressure, indicating that benzene replaced dimethylpentane in the adsorbed phase as surface coverage increased.

One mixed vapor isotherm was measured on silica gel II. A plot of α versus total pressure for this isotherm went through a maximum at a pressure corresponding to monolayer coverage. It was, therefore, concluded that selectivity occurred primarily in the monolayer.

A similar observation was made by Pavlyuchenko (11) for adsorption

---

*The term "equilibrium" will be implicit hereafter in all references to the vapor phase.

of acetone-chloroform vapor mixtures on carbon black at 30 and 50°C. Isotherms of amounts adsorbed versus pressure for several different vapor phase compositions were measured. For each isotherm, the composition of the adsorbed phase became equal to the composition of the liquid phase in the multilayer region. Thus, the influence of the adsorbent on the composition of the adsorbed phase did not extend very far into the multilayer region.

The adsorption of benzene-methanol vapor mixtures on porous Vycor glass at 15, 25, and 35°C has been studied by Reeds and Kammermeyer (12). Isotherms were measured at constant total pressure. In this temperature range, a vapor-liquid azeotrope occurs. At 25°C benzene was selectively adsorbed from mixtures having a methanol vapor mole fraction ≤ 0.68; at higher mole fractions methanol was selectively adsorbed. Thus, an adsorption azeotrope occurred, which did not coincide with the vapor-liquid azeotrope. An adsorption azeotrope has also been observed by Ellis and Thompson (5) in the ethanol-acetone/activated carbon system at 105°C.

Lewis *et al.* (4) have obtained adsorption data for binary mixtures of the lower gaseous hydrocarbons on silica and on activated carbon. Isotherms were measured at 25°C and at a total pressure of one atmosphere. For mixtures involving components with the same degree of unsaturation but different vapor pressures, both carbon and silica selectively adsorbed the less volatile component. For mixtures involving components with nearly equal vapor pressures but different degrees of unsaturation, it was observed that the less volatile component was selectively adsorbed on carbon. Silica, however, selectively

adsorbed the more unsaturated component. The authors concluded that degree of unsaturation is unimportant as a factor controlling selective adsorption on carbon, but it is very important with silica. Similar trends in adsorption behavior have been observed by Thomas and Lombardi (13) for benzene-toluene mixtures on carbon and by Szepesy and Illes (14, 15) for a series of binary hydrocarbon mixtures on carbon.

Lewis et al. (4) have also determined isotherms for three mixtures at a series of different total pressures ranging from 0.33 to 19.2 atmospheres. In all three cases, selectivity decreased with increasing total pressure, but a significant change in selectivity was observed only for large changes in total pressure. Two systems were investigated over a temperature range from 0 to 40°C. In both cases selectivity decreased slightly with increasing temperature.

Chernyshev, Kel'tsev, and Khalif (16) have studied the adsorption of propane-butane gas mixtures on activated carbon at 20 and 100°C. Butane was selectively adsorbed at both temperatures. The variation of selectivity with temperature was very slight and followed no particular trend, as shown in Table 1 for different vapor mole fractions (y) of propane.

Actually, it can be shown that the variation of selectivity with temperature is related to heats of adsorption. Hill (17) has developed the thermodynamics of adsorption of pure vapors onto solids. The treatment is readily extended to adsorption of binary mixtures. For example, the isosteric heat of adsorption of a component in a mixture, q_{st}^{i}, is obtained from the following equation:

TABLE 1

VARIATION OF SELECTIVITY WITH TEMPERATURE (16)

$y_{C_3H_8}$	20°C α	100°C α
0.4030	3.89	3.87
0.5880	4.63	3.31
0.7710	4.93	4.28
0.8765	4.03	4.35

$$q_{st}^{\,i} = -R \left(\frac{\partial \ln P_i}{\partial 1/T} \right)_{n_i,\, n_j} \qquad (4)$$

where P_i is the partial pressure and n_i, n_j are the numbers of moles of each component adsorbed. From a knowledge of two or more isotherms, isosteric heats of adsorption may be calculated. To obtain data at constant n_i and n_j, the adsorption isotherms must be measured in either of two ways. Amounts of each component adsorbed can be measured as a function of total pressure for several constant vapor phase compositions, or as a function of vapor phase composition for several constant total pressures. Bering, Pavlyuchenko, and Serpinskii (18) have obtained heats and entropies of adsorption for chloroform-acetone/carbon (11) from a knowledge of several adsorption isobars at two temperatures.

Bering, Serpinskii, and Surinova (19) have shown that the temperature dependence of the selectivity is related to the isosteric heats of adsorption of the components in the mixture. Equation (3) for the selectivity can be written as:

$$\alpha = \frac{n_1}{n_2} \frac{P_2}{P_1} \qquad (5)$$

Differentiating ln α with respect to 1/T at constant n_1 and n_2 gives:

$$\left(\frac{\partial \ln \alpha}{\partial 1/T} \right)_{n_1,\, n_2} = \left(\frac{\partial \ln P_2}{\partial 1/T} \right)_{n_1,\, n_2} - \left(\frac{\partial \ln P_1}{\partial 1/T} \right)_{n_1,\, n_2}$$

$$= \frac{q_{st}^{\,1} - q_{st}^{\,2}}{R} \qquad (6)$$

The second line follows directly from Equation (4). Thus, if $q_{st}^{1} > q_{st}^{2}$, α decreases with increasing temperature, and vice versa.

Shen and Smith (20) have studied adsorption of benzene-hexane mixtures on silica at low surface coverage ($\theta \leq 0.1$) from 70 to 130°C. Amounts adsorbed were measured as a function of pressure for several constant vapor phase compositions. Preferential adsorption of benzene occurred. Isosteric heats of adsorption for benzene and hexane, from the pure states and from the mixtures, were calculated. For the pure components, q_{st} decreased rapidly with increasing surface coverage, indicating that the silica surface was heterogeneous. The heat of adsorption of benzene from the mixture, q_{st}^{b}, was independent of the amount of hexane adsorbed. But q_{st}^{h} decreased as the amount of adsorbed benzene increased. The authors, therefore, concluded that benzene occupied the most energetic sites on the surface, leaving the low energy sites for hexane. The heat of adsorption of hexane from the mixtures was independent of the amount of hexane present, which indicated that the sites available for hexane all had about the same energy. It was postulated that selective adsorption of benzene was due to interactions between its π electrons and the hydroxyl groups on the silica surface.

Models

Many models for predicting binary vapor adsorption from the isotherms of the pure components have been proposed. These models have been reviewed by Buelow, Grossmann, and Schirmer (21) and by Sircar and Myers (22).

The earliest models for predicting binary vapor adsorption were extensions of pure gas models. Hill (23) extended the BET theory to the case of a binary mixture. The Langmuir model was extended to mixtures by Markham and Benton (24) and by Gonzalez and Holland (25). The parameters obtained by applying a model to the pure component isotherms are used to calculate the mixed vapor isotherms. These models have the advantage that the binary vapor adsorption isotherms are analytical equations. The chief disadvantage is that the models usually do not accurately describe the pure vapor isotherms. Even if the models fit the pure vapor data, there is no guarantee that the models will fit the mixed vapor data. For example, the mixed Langmuir model (24) did not accurately predict the benzene-2,4-dimethylpentane/silica isotherms obtained by Cines and Ruehlen (10) even though the model was in excellent agreement with the pure component isotherms.

Another group of models was based on the Polanyi potential theory of adsorption. Polanyi theory states that the volume of gas adsorbed, V, is a function only of the adsorption potential, ε, and is independent of the temperature:

$$\varepsilon = RT \ln P^S/P \qquad (7a)$$

$$V = n\bar{V} \qquad (7b)$$

where P is the equilibrium pressure, P^S is the saturation vapor pressure of the adsorbate at temperature T, n is the number of moles adsorbed, and $\bar{V}$ is the molar volume of the liquid adsorbate at temperature T. Isotherms for a particular adsorbate-adsorbent system can, thus, be

collapsed to a single characteristic curve by plotting V versus ε. In the Dubinin modification of the Polanyi theory, isotherms of all adsorbates on a particular adsorbent are collapsible to a single curve by application of a correlating divisor β:

$$\varepsilon = \frac{RT}{\beta} \ln P^s/P \qquad (8)$$

The correlating divisor is usually the molar volume of the liquid. The Polanyi-Dubinin theory has been shown to be valid for many systems.

The Polanyi-Dubinin theory was first extended to binary mixtures by Lewis et al. (4). The model gave good agreement only for systems in which the selectivity was independent of composition. The model developed by Grant and Manes (26) is applicable to systems of variable selectivity. The adsorbate is assumed to be a mixture in which the potential of each component is determined by the adsorbate volume of the mixture. The potential of a component in a mixture is given by an equation similar to Equation (8), the only difference being that P must be replaced by P_i^*, the pressure that would be exerted by pure component i at the same adsorbate volume as that of the mixture:

$$\varepsilon_i = \frac{RT}{\beta_i} \ln \left(\frac{P^s}{P^*} \right)_i \qquad (9)$$

It is assumed that the partial pressure of a component in the mixture, P_i, is related to P_i^* through an expression analogous to Raoult's Law:

$$P_i = P_i^* x_i \qquad (10)$$

where x_i is the mole fraction in the adsorbed phase. Combining Equations (9) and (10) gives, at constant temperature:

$$\varepsilon_1 = \varepsilon_2 = \frac{1}{\beta_1} \ln x_1 \left(\frac{P^s}{P}\right)_1 = \frac{1}{\beta_2} \ln x_2 \left(\frac{P^s}{P}\right)_2 \quad (11)$$

Equation (11) and the relation $x_1 + x_2 = 1$ are sufficient to calculate x_1 from the constants β_i and P_i^s, and chosen values of P_1. This value of x_1 is then used to calculate the adsorption potential of the components in the mixture from Equation (11), and the corresponding adsorbate volume of the mixture is read from the characteristic curve. Assuming that adsorbate volumes are additive, the total number of moles adsorbed, n_t, and the number of moles of each component adsorbed may be calculated from the following equations:

$$n_t = \frac{V}{x_1\bar{V}_1 + x_2\bar{V}_2} \quad (12a)$$

$$n_i = x_i n_t \quad (12b)$$

The model was successfully applied to several binary mixtures of hydrocarbons onto carbon. There are two main disadvantages to this model. First, it is applicable only to systems whose pure component isotherms are collapsible to a single characteristic curve. Secondly, Equation (11) must be solved for x_1 by successive approximations.

Myers and Prausnitz (27, 28) have developed the ideal adsorbed solution model. The authors defined an adsorbed solution analogous to a liquid solution:

$$Py_i = P_i^* \gamma_i x_i \qquad (13)$$

where x_i and y_i are the mole fractions in the adsorbed and vapor phases, respectively, γ_i is the activity coefficient for component i in the adsorbed phase, P is the total vapor phase pressure, and P_i^* is the pressure of component i at the same temperature and spreading pressure π as that of the adsorbed solution. If the adsorbed solution is ideal, Equation (13) reduces to:

$$Py_i = P_i^* x_i \qquad (14)$$

and the binary vapor isotherms can be calculated from the pure component isotherms. Spreading pressure curves (graphs of π versus P) are obtained for the pure components by application of the Gibbs adsorption equation to the pure vapor isotherms:

$$\frac{\pi}{RT} = \int_0^P \frac{N}{P}\, dP \qquad (15)$$

where N is the number of moles adsorbed per unit area of adsorbent. Values of P_i^* at a particular value of π may then be read from the spreading pressure curves. If binary vapor isotherms of amounts adsorbed versus pressure for constant vapor phase composition are desired, the total pressure is first calculated from:

$$\frac{1}{P} = \frac{y_1}{P_1^*} + \frac{y_2}{P_2^*} \qquad (16a)$$

The corresponding value of x_i is then calculated from Equation (14). If the binary vapor isotherm is desired at constant total pressure, x_1 is first calculated from:

$$x_1 = \frac{P - P_2^*}{P_1^* - P_2^*} \qquad (16b)$$

and y_1 is calculated from Equation (14). If desired, the number of moles of each component adsorbed may then be calculated from:

$$\frac{1}{N_t} = \frac{x_1}{N_1^*} + \frac{x_2}{N_2^*} \qquad (17a)$$

$$N_i = x_i N_t \qquad (17b)$$

where N_i^* is the number of moles of pure component i adsorbed per unit area at P_i^*.

The ideal adsorbed solution model has been applied to a variety of literature data with good results. Therefore, Myers and Prausnitz postulated that the assumption of an ideal adsorbed solution is valid for many systems. However, when Henson and Kabel (29) applied the model to the data of Reeds and Kammermeyer (12), agreement between experimental and calculated isotherms was poor. The authors postulated that since the isotherms were obtained at pressures close to saturation, multilayer adsorption took place. In the multilayer region, the adsorbed molecules would interact with each other largely in the manner of the liquid phase, making the assumption of ideality invalid unless the liquid solution were ideal. Adsorption activity coefficients were calculated,

and were found to behave similarly to solution activity coefficients.

Bering, Serpinskii, and Surinova (30) have calculated adsorption activity coefficients for benzene-trimethylpentane mixtures on carbon black at 45°C, from low coverage to saturation. Adsorbed solutions were ideal in the monolayer region; as surface coverage increased the adsorption activity coefficients became larger than one, and gradually approached the solution activity coefficients. For systems showing positive deviations from Raoult's Law, the authors proposed that the adsorbed solutions would be more ideal than the liquid solutions. Intermolecular interactions in the adsorbed phase would be lower than in the liquid solution as a result of the decrease in the number of nearest neighbors for each molecule. The activity coefficients for adsorption would be lower and closer to unity.

Kidnay and Myers (31) have presented a simplified version of the ideal adsorbed solution model which may be used under certain conditions. Equation (15) may be rewritten by transforming the independent variable from P to N:

$$\frac{\pi}{RT} = \int_0^N \frac{d \ln P}{d \ln N} \, dN \qquad (18)$$

If the slopes (d ln P)/(d ln N) of the pure component isotherms coincide at all values of N, the spreading pressure curves will coincide, and the term $P_i^*(\pi)$ in Equation (14) can be replaced by $P_i^*(N)$. Examination of log-log plots of the pure component isotherms will determine if this condition applies. The binary vapor isotherm can then be calculated directly from Equations (14) and (16) and the pure component data;

calculation of spreading pressure curves is not necessary. The authors found this condition to be fulfilled for several systems below monolayer coverage.

In another simplification of the ideal adsorbed solution model developed by Fernbacher and Wenzel (32), P_i^* in Equation (14) is defined as the pressure of component i at the same adsorbate volume, V, as that of the mixture. The method is valid only if the spreading pressures of the pure components coincide at all values of V. This will be true if the pure component isotherms, V versus P, can be made to coincide. The model proposed by Grant and Manes (26) is, therefore, a special case of this model, in which the pure vapor isotherms are made to coincide by using the Polanyi-Dubinin theory. The model of Fernbacher and Wenzel is much easier to use. The pure vapor isotherms are plotted as V versus P; values of P_i^* are read from these graphs and used in Equations (14) and (16).

Sircar and Myers (22) have pointed out that the ideal adsorbed solution model sometimes cannot be used for cases in which one of the components of the mixture is close to saturation. The reason for the failure is illustrated in Figure 1, where π_i^s is the spreading pressure of component i at saturation. To use the ideal adsorbed solution model, the pressures of the pure components at the same spreading pressure as that of the adsorbed solution, P_i^*, must be known. For adsorbed phase compositions having spreading pressures greater than π_2^s, the spreading pressure of component 2 and, therefore, P_2^* is not defined. Sircar and Myers have developed an extension of the ideal adsorbed solution model which may be used when one of the components of a mixture is near

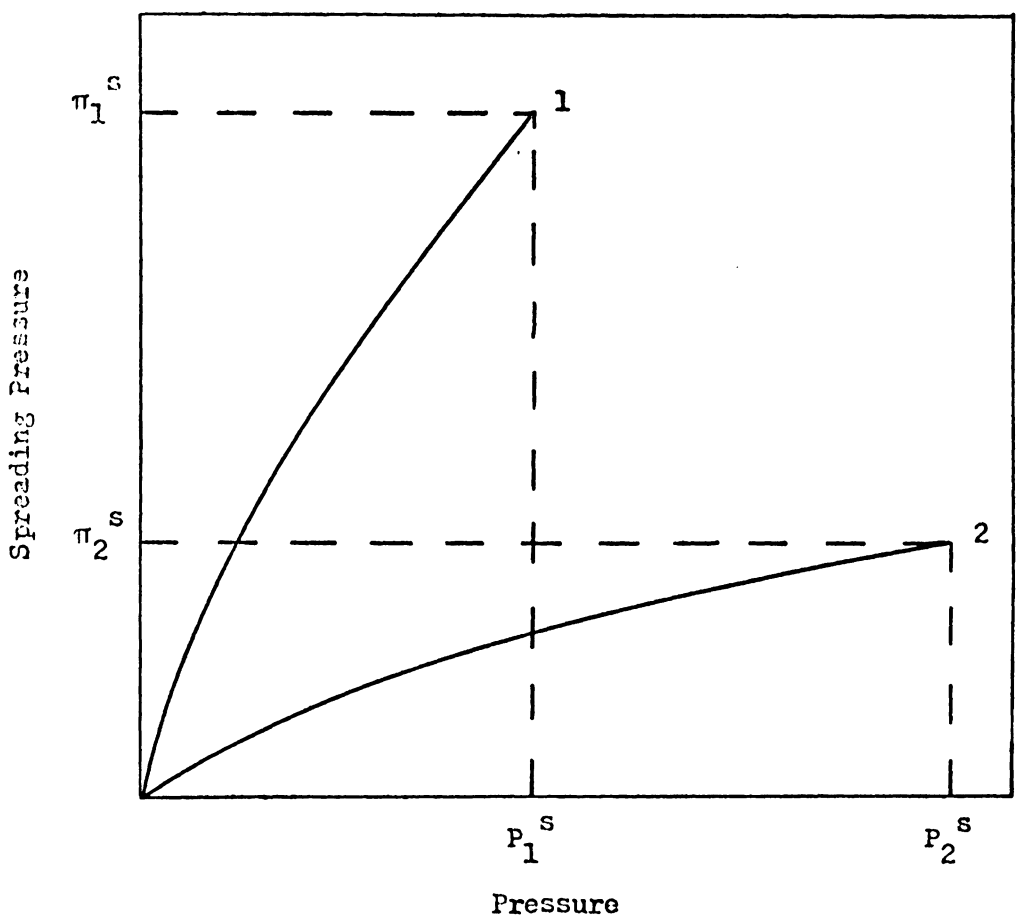

Figure 1. Limitation of the Ideal Adsorbed Solution Model

saturation. The binary vapor isotherms are calculated from:

$$\frac{1}{P} = \sum_i \frac{y_i}{P_i^*} \exp\left[\frac{\pi_r(\pi_i^s - \pi^s)}{N_i^* RT}\right] \qquad (19)$$

$$Py_i = P_i^* x_i \exp\left[\frac{-\pi_r(\pi_i^s - \pi^s)}{N_i^* RT}\right] \qquad (20)$$

where π_r, the reduced spreading pressure, is defined by:

$$\pi_r = \frac{\pi}{\pi^s} = \frac{\pi_i^*}{\pi_i^s} \qquad (21)$$

In Equation (21) π_i^* is the spreading pressure at P_i^*. The spreading pressures of the pure components at saturation, π_i^s, may be obtained from the pure vapor isotherms using Equation (15). The spreading pressure of the mixture at saturation, π^s, can be obtained from solution adsorption data for the same system:

$$\frac{\pi^s - \pi_2^s}{RT} = \int_0^{a_1} \frac{n_1}{(1-x_1')a_1} da_1 \qquad (22)$$

where n_1 is the number of moles of component 1 adsorbed from solution, x_1' is the mole fraction in the bulk liquid solution, and a_1 is the activity. Since a_1 is a function of vapor phase composition y_1, it follows that π^s is also a function of y_1. If solution adsorption data are not available, π^s can be estimated from:

$$\frac{1}{P^s} \exp\left(\frac{\pi^s}{n_m RT}\right) = \frac{y_1}{P_1^s} \exp\left(\frac{\pi_1^s}{n_m RT}\right) + \frac{y_2}{P_2^s} \exp\left(\frac{\pi_2^s}{n_m RT}\right) \quad (23)$$

where P^s is the saturation vapor pressure of the mixture, and n_m is the amount adsorbed at monolayer coverage for either pure component. The use of this model is straightforward if binary vapor isotherms of amounts adsorbed versus pressure for constant vapor phase composition are desired. If isotherms at constant total pressure are desired, Equation (19) must be solved for π_r by successive approximations. Sircar and Myers have applied this model to the data of Cines and Ruehlen (10) for adsorption of benzene-dimethylpentane mixtures onto silica with good results.

Van Ness (33) has shown that proper application of thermodynamics can reduce the amount of experimental data needed for determining binary vapor adsorption isotherms. At constant temperature, the spreading pressure of a mixture is given by:

$$-\frac{d\pi}{NRT} + d \ln P + \frac{x_1 - y_1}{y_1(1-y_1)} dy_1 = 0 \quad (24)$$

If y_1 is held constant, integration of Equation (24) gives:

$$\frac{\pi}{RT} = \int_0^P \frac{N}{P} dP \quad (25)$$

If π/RT is evaluated for different values of y_1, but all for the same pressure, then d ln P = 0 and Equation (24) may be solved for x_1:

$$x_1 = \frac{y_1(1-y_1)}{N}\left[\frac{\partial(\pi/RT)}{\partial y_1}\right]_{T,P} \qquad (26)$$

Thus, if N as a function of pressure is experimentally measured for several different constant values of y_1, there is no need to measure x_1; it may be calculated from Equation (26). π/RT is obtained as a function of pressure for each value of y_1 from Equation (25); the partial derivative in Equation (26) may then be evaluated.

Friederich and Mullins (34) have used the van Ness method to determine adsorption isotherms for ethylene-ethane, propylene-propane, and ethane-propane vapor mixtures on homogeneous carbon black at 25°C, at pressures ranging from 10 to 700 torr. The authors pointed out that the van Ness method is particularly useful for measuring binary vapor adsorption on low surface area adsorbents, for which the amount adsorbed is very small.

III. EXPERIMENTAL

The materials and the experimental methods that were used in this study are discussed in detail in the following section.

Adsorbates and Adsorbents

The adsorbates used were benzene (Fisher: 99 mole % grade), cyclohexane (Fisher: 99 mole % grade), and ethanol. Benzene and cyclohexane were used as received; ethanol was stored over Cab-O-Sil to remove trace quantities of water.

The adsorbents used were Cab-O-Sil and Graphon; both solids were obtained from Cabot Corporation. Graphon is a graphitized carbon black. Cab-O-Sil is a flame-hydrolyzed silica having a surface which is 25% hydroxylated (35, 36). Both solids were used as received. The surface areas of the two adsorbents were determined by the BET method using low temperature nitrogen adsorption (2). Surface areas of 214 ± 2 m^2/g and 89.0 ± 1.5 m^2/g were obtained for Cab-O-Sil and Graphon, respectively. These values agree well with the manufacturer's values of 200 ± 25 m^2/g for Cab-O-Sil and 89.4 m^2/g for Graphon.

Pure Vapor Adsorption Isotherms

The pure vapor adsorption isotherms were measured by a volumetric technique. The constant volume apparatus is shown schematically in Figure 2. A vacuum of 10^{-5} torr was obtained with a mechanical pump and a liquid nitrogen trapped mercury diffusion pump. Residual pressures were measured with a McLeod gauge (MG). The volume of the gas buret was determined before it was attached to the vacuum line. To ensure a

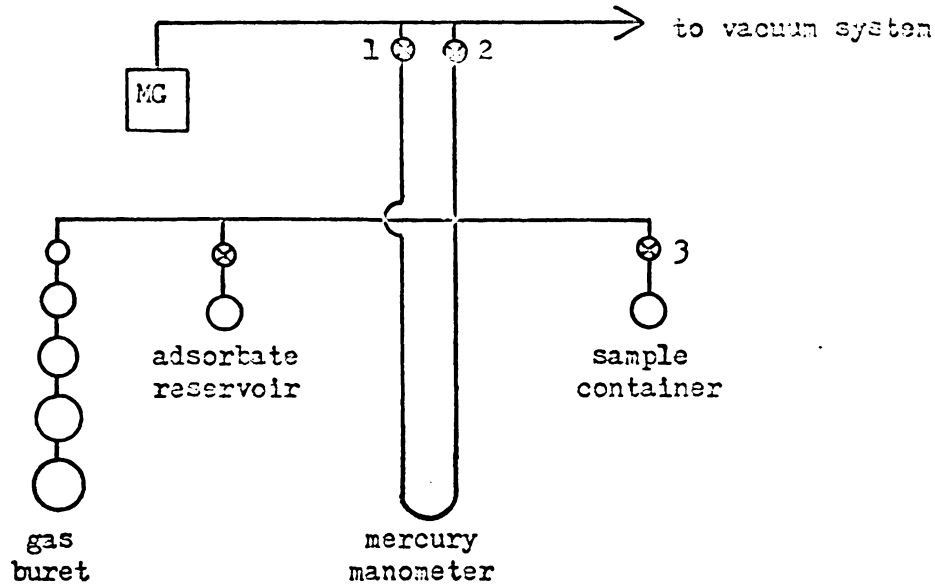

Figure 2. Pure Vapor Adsorption Apparatus

constant system volume, the mercury manometer was constructed so that a light would come on when the mercury in the right side reached a certain height. The mercury heights in the manometer were read to the nearest 0.01 cm with a cathetometer. The desired adsorbate was placed in the reservoir, and was degassed by four freeze-thaw cycles using liquid nitrogen with intermittent pumping. The desired adsorbent was placed in the sample container. The weights of the Cab-O-Sil and Graphon samples used for adsorption measurements were 0.0756 g and 0.1940 g, respectively. The entire adsorption system was surrounded by an air bath in which the temperature could be raised to 45°C.

To calculate the amount of vapor adsorbed, the volumes of two parts of the system must be known. To obtain V_1, the volume of the system excluding the adsorbent container, a series of pressure-volume measurements were made with helium using the calibrated gas buret. Once V_1 was known, the volume of the adsorbent container, V_2, was determined by helium expansion. Using this procedure V_1 was determined to be 155 ± 1 cc; V_2 was 36.0 ± 0.6 cc for the Cab-O-Sil isotherms and 36.2 ± 0.6 cc for the Graphon isotherms.

Prior to measuring each adsorption isotherm, the adsorbent was heated under vacuum to 110°C for one hour to remove any vapors already adsorbed on the surface. The adsorbent container was then immersed in a constant temperature bath for at least thirty minutes before adsorption measurements were begun. The water bath could be held to within 0.1°C of the desired adsorption temperature.

To measure an isotherm, all stopcocks were initially closed after evacuation. A small amount of adsorbate was allowed to expand into V_1,

and the pressure was read from the manometer. Assuming that the adsorbate is an ideal gas, the initial number of moles of adsorbate can be calculated from the measured pressure and V_1. Stopcock 3 was then opened, and the vapor was allowed to equilibrate with the solid. Although equilibrium appeared to be established within five minutes, an equilibration time of fifteen minutes was allowed. The final number of moles was then calculated from the measured equilibrium pressure and V_1 and V_2. The number of moles adsorbed is the difference between the initial and the final number of moles. To obtain the next point on the isotherm, stopcock 3 was closed and another sample of adsorbate was added to the system. In this case, the initial number of moles in the system is the sum of the number of moles in V_1 and the number of moles in both the vapor and adsorbed phases in V_2. Stopcock 3 was then opened and the final number of moles calculated from the equilibrium pressure. The same procedure was repeated until saturation vapor pressure was approached. Using this procedure, the number of moles of vapor adsorbed as a function of equilibrium pressure was obtained.

Adsorption isotherms at 20, 30, and 40°C for pure ethanol, benzene, and cyclohexane on Cab-O-Sil and on Graphon were measured. Data were obtained up to a relative pressure, P/P^s, of about 0.95 for each isotherm. The vapor pressures of the three adsorbates are given in Table 2 (37-40).

Binary Vapor Adsorption Isotherms

Adsorption isotherms for the binary vapor mixtures were measured by a modified volumetric technique. A schematic diagram of the apparatus

TABLE 2

ADSORBATE VAPOR PRESSURES

Adsorbate	Temperature (°C)	Vapor Pressure (torr)	Reference
Ethanol	20	44	37
	30	77	37
	40	135	37
Benzene	20	75	38
	30	119	38
	40	182	38
Cyclohexane	20	77	39
	30	121	39
	40	185	40

is given in Figure 3. To calculate adsorption of binary vapors, the partial pressure of each component before and after equilibration with the adsorbent must be known. To obtain these pressures, a Beckman GC-2A gas chromatograph equipped with a gas sampling valve was connected to the vacuum line. Vapor samples could be injected into the gas chromatograph directly from the vacuum line. Chromatograms were recorded on a Sargent Model SRG recorder.

It was found that chromatographic peak height was directly proportional to the pressure of the vapor injected into the gas chromatograph. Therefore, the partial pressure of each component in a vapor mixture could be determined. The column used to separate ethanol-cyclohexane and benzene-cyclohexane mixtures was 10% Carbowax 1540 on 60/80 mesh Chromosorb W. A second column consisting of 10% di(n-nonyl)phthalate (DNP) on 60/80 mesh Chromosorb W HP was used to separate ethanol-benzene mixtures. Both columns were obtained pre-packed from Supelco. Both chromatographic columns were operated at 70°C. Carrier gas (helium) flow rates of 24.5 ml/min for the DNP column and 21.6 ml/min for the Carbowax column gave good separations. Carrier gas pressures were approximately 30 and 35 psi for the DNP and Carbowax columns, respectively. The thermal conductivity detector was operated at a current of 175 ma.

The apparatus shown in Figure 3 was evacuated to a residual pressure of 10^{-5} torr with a mechanical pump and a liquid nitrogen trapped mercury diffusion pump. A Wallace & Tiernan absolute pressure gauge (PG) was used to measure pressures. The Toepler pump (TP) was necessary for mixing the vapors. Ethanol, cyclohexane, and benzene were placed in the

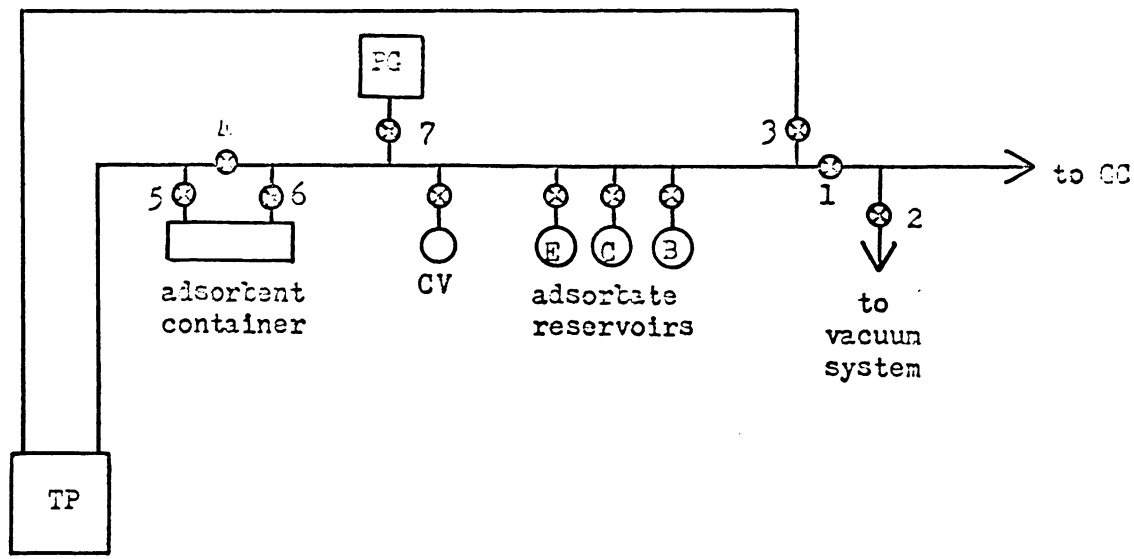

Figure 3. Binary Vapor Adsorption Apparatus

adsorbate reservoirs labeled E, C, and B, respectively. The adsorbates were degassed by several freeze-thaw cycles prior to use. The desired solid was placed in the adsorbent container. A 1.6264 g sample of Cab-O-Sil was used to obtain the 30°C isotherms of the three mixtures and the 40°C ethanol-benzene isotherm. For the remainder of the Cab-O-Sil isotherms, a 1.8646 g sample was used. A 4.0333 g sample of Graphon was used to obtain all of the Graphon isotherms. Volumes of various parts of the system were measured by helium expansion using the calibrated volume (CV).

Calibration curves of chromatographic peak height versus pressure for each adsorbate were first obtained. Referring to Figure 3, stopcocks 1-7 were open when the system was being evacuated. To obtain a calibration curve all but stopcocks 2 and 7 were closed. The desired adsorbate was allowed to expand into the system, and the pressure was read. Stopcocks 2 and 7 were closed; the vapor was then contained in volume V_1, where $V_1 = 202 \pm 5$ cc. Stopcock 1 was then opened, and the vapor expanded into $V_1 + V_2$, where $V_2 = 49.0 \pm 0.2$ cc. A one cc sample of this vapor was then injected into the gas chromatograph. From V_1, V_2, and the pressure read from PG, the pressure of the vapor injected into the gas chromatograph was calculated. In this manner, calibration curves of peak height versus pressure were obtained. The gas chromatograph was recalibrated periodically. Typical calibration curves of three adsorbates on the Carbowax column are shown in Figure 4.

Before making an adsorption measurement, the adsorbent was heated under vacuum to 110°C for one hour. The adsorbent container was then immersed in a water bath held to within 0.1°C of the desired adsorption

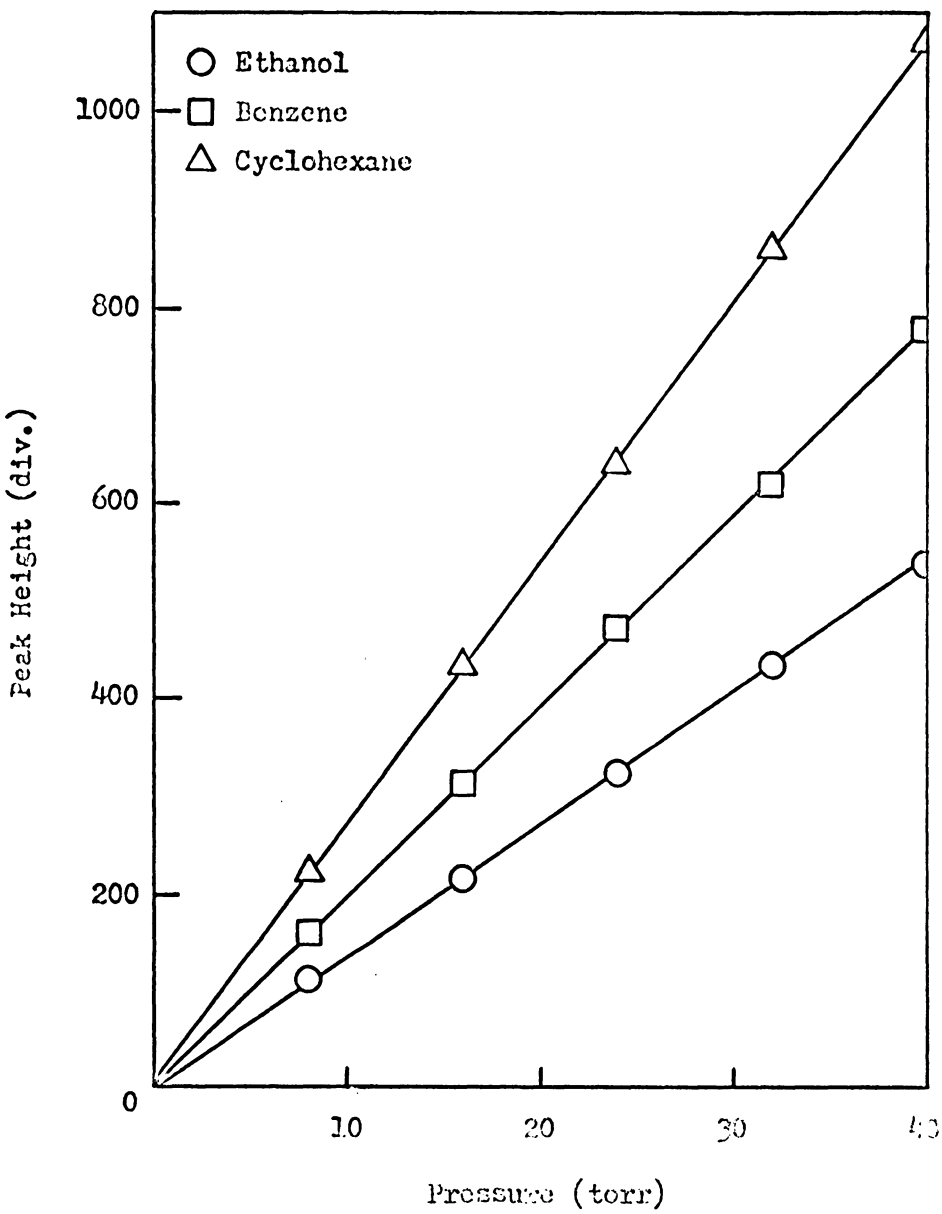

Figure 4. Typical Calibration Curves

temperature for at least thirty minutes prior to use. Following evacuation of the entire system stopcocks 1, 5, and 6 were closed; with the aid of the pressure gauge the desired approximate amounts of adsorbates were allowed to expand into the system. The vapors were then mixed with the Toepler pump for fifteen minutes, after which stopcock 7 was closed. The vapor mixture was then contained in volume V_3, where $V_3 = 6032 \pm 65$ cc. Stopcock 2 was then closed, stopcock 1 was opened, and a one cc sample of the vapor mixture was injected into the gas chromatograph. The partial pressures of the components were obtained from the calibration curves, and the initial number of moles of each component in V_3 was calculated. Stopcocks 5 and 6 were then opened, and the vapor mixture was allowed to equilibrate with the adsorbent for one hour. During equilibration the Toepler pump was operated to mix and circulate the vapors. Then stopcocks 2, 5, and 6 were closed, stopcock 1 was opened, and a one cc sample of the mixture was injected into the gas chromatograph. The partial pressures of the components contained in $V_2 + V_3$ were read from the calibration curves. The equilibrium partial pressures in V_3 were then calculated. The final number of moles of each component was then the sum of the number of moles in V_3 and the number of moles in the vapor phase in the sample container. The volume of the sample container was 304 ± 2 cc for the Cab-O-Sil isotherms, and 271 ± 2 cc for the Graphon isotherms. The number of moles of each component adsorbed is the difference between the initial and the final number of moles of each component. The entire system was then evacuated, and the adsorbent was prepared for the next run by heating to 110°C for an hour and then equilibrating the adsorbent for thirty minutes at the adsorption temperature.

Using this method the amounts of each component adsorbed were obtained as a function of vapor phase composition. Adsorption isotherms at 20, 30, and 40°C for ethanol-cyclohexane, ethanol-benzene, and benzene-cyclohexane vapor mixtures on Cab-O-Sil and on Graphon were measured at a total pressure of approximately 30 torr. For the three mixtures on Cab-O-Sil at 30°C, no attempt was made to hold the total pressure constant. The ethanol-benzene/Cab-O-Sil isotherm at 40°C was measured at a constant pressure of about 40 torr. The values of the total pressures for each isotherm are given in Table 3.

TABLE 3

AVERAGE TOTAL PRESSURES FOR BINARY VAPOR ADSORPTION ISOTHERMS

		Cab-O-Sil	Graphon
Mixture	T(°C)	Total Pressure (torr)	Total Pressure (torr)
Ethanol-Cyclohexane	20	27.4 ± 0.8	26.4 ± 1.6
	30	27.0 ± 2.3	30.2 ± 0.5
	40	30.7 ± 0.5	30.1 ± 0.6
Ethanol-Benzene	20	27.1 ± 0.7	25.8 ± 1.9
	30	26.7 ± 3.4	28.3 ± 0.5
	40	41.3 ± 0.8	28.9 ± 0.2
Benzene-Cyclohexane	20	28.3 ± 0.4	28.6 ± 0.8
	30	27.3 ± 3.9	28.9 ± 0.2
	40	31.2 ± 1.2	30.0 ± 0.7

IV. RESULTS AND DISCUSSION

In the following section the experimental pure and binary vapor adsorption isotherms are discussed. A thermodynamic analysis based on the pure vapor isotherms is included. Comparisons between the experimental binary vapor isotherms and those calculated from the pure vapor isotherms using various models are also presented.

Pure Vapor Adsorption Isotherms

The experimental pure vapor isotherms on Cab-O-Sil and on Graphon are presented graphically in the following sections. The experimental adsorption data and a sample calculation of pure vapor adsorption are given in Appendix I.

Cab-O-Sil isotherms

The adsorption isotherms at 20, 30, and 40°C for ethanol, benzene, and cyclohexane onto Cab-O-Sil are shown in Figures 5, 6, and 7, respectively. The isotherms have been plotted as N, the number of moles adsorbed per square meter of adsorbent, versus equilibrium pressure, P. The error in N for all of the pure vapor isotherms on Cab-O-Sil is about $\pm$ 0.3 x 10^{-6} mole/m^2. The shaded symbols in Figures 5 and 7 represent checks on reproducibility. Figures 5-7 show that the amount of vapor adsorbed decreases markedly with increasing adsorption temperature. This temperature dependence is generally observed for physical adsorption of pure vapors onto solids.

Figure 8 shows the 20°C adsorption isotherms for the three adsorbates on Cab-O-Sil. The data have been plotted as N versus relative

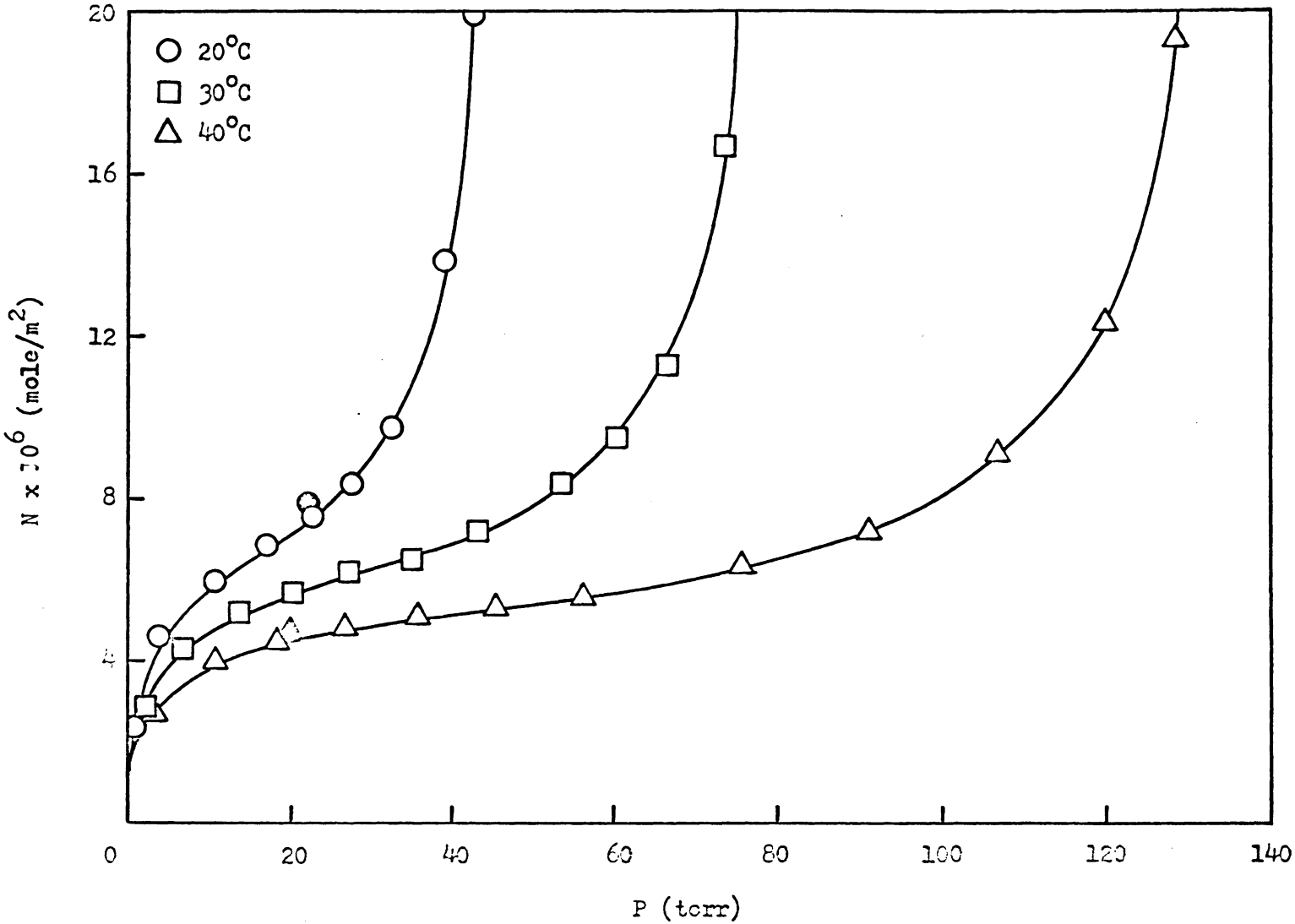

Figure 5. Ethanol/Cab-O-Sil Isotherms at 20, 30, and 40°C

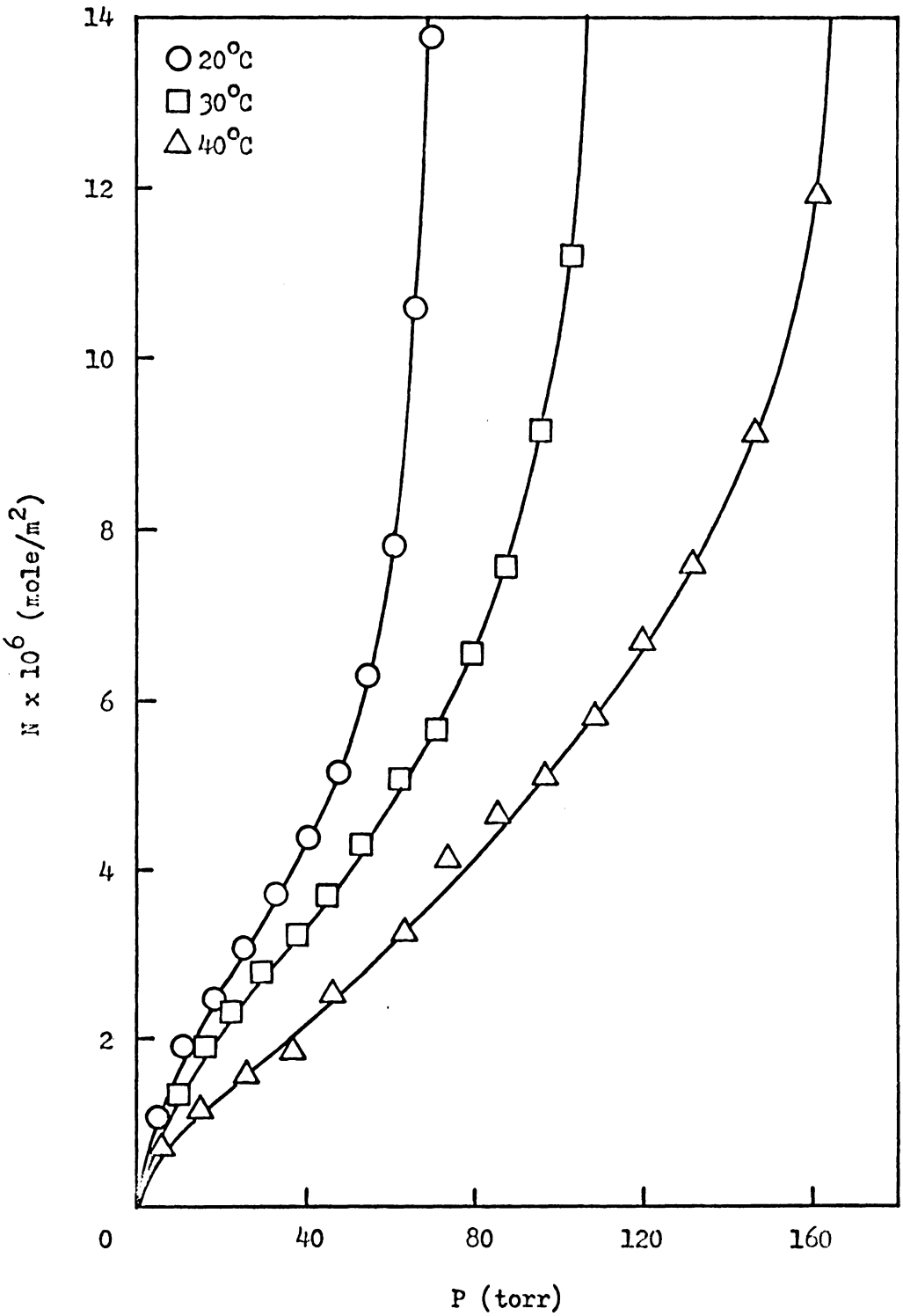

Figure 6. Benzene/Cab-O-Sil Isotherms at 20, 30, and 40°C

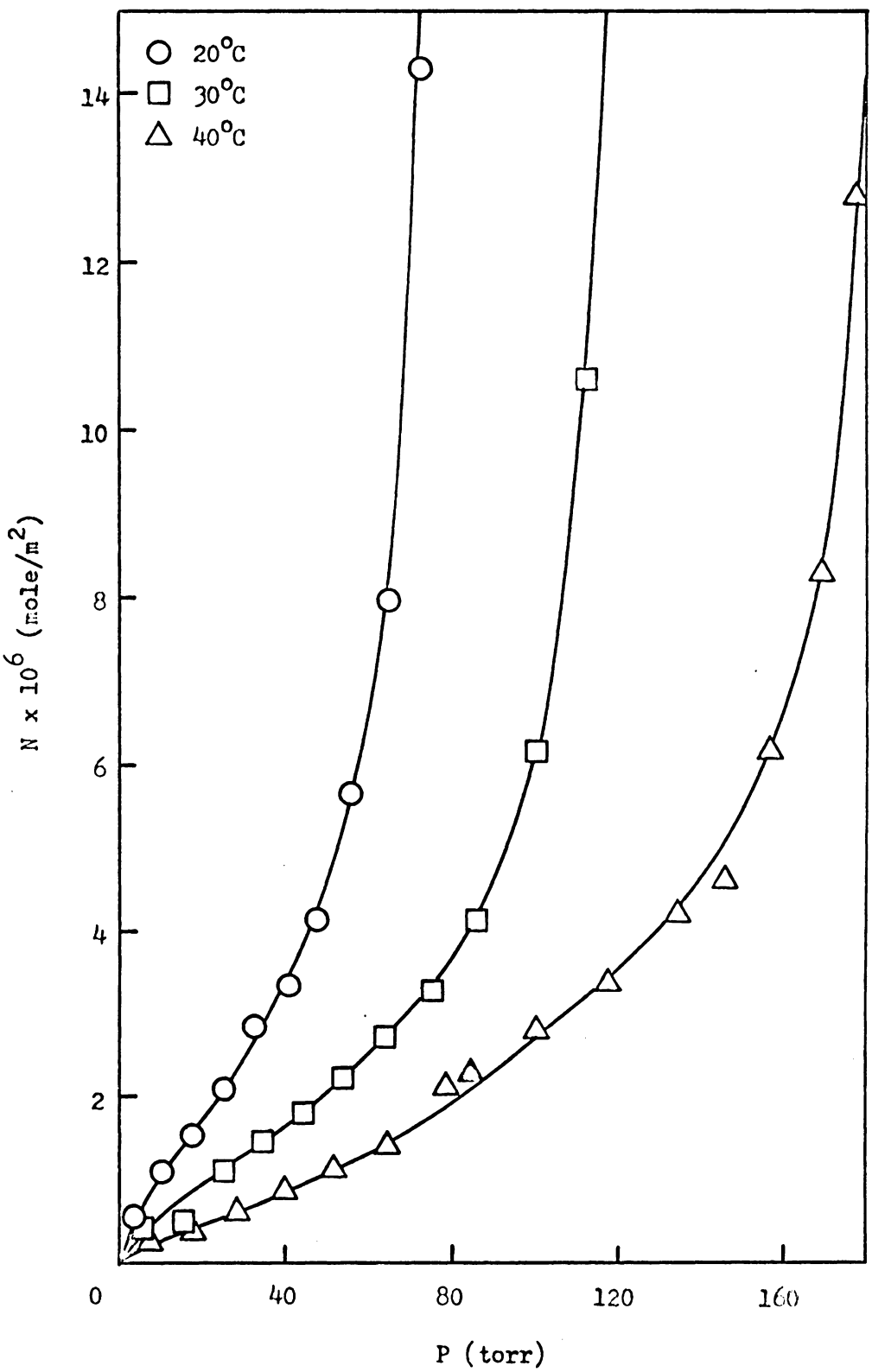

Figure 7. Cyclohexane/Cab-O-Sil Isotherms at 20, 30, and 40°C

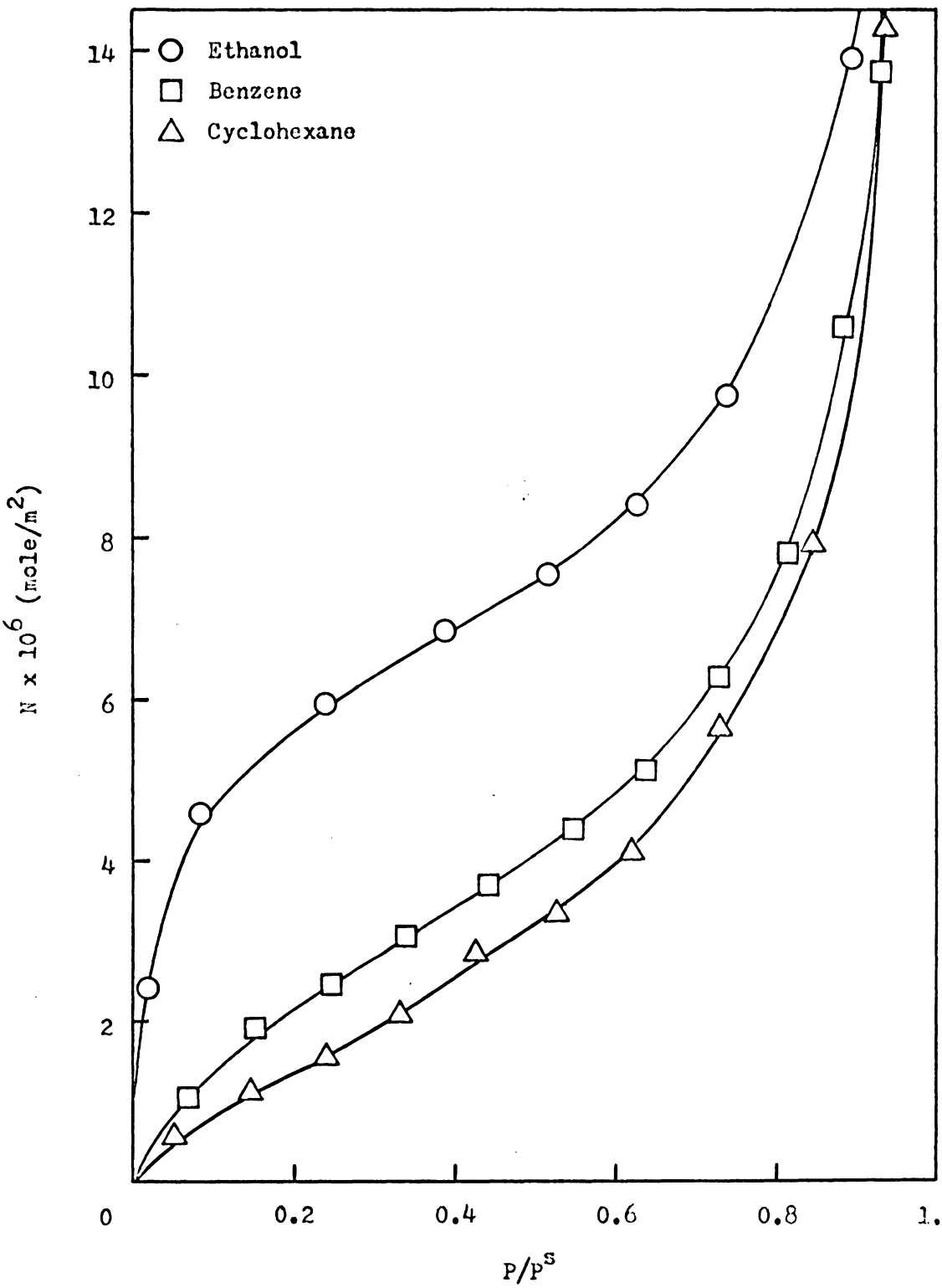

Figure 8. Pure Ethanol, Benzene, and Cyclohexane on Cab-O-Sil at 20°C

pressure, P/P^S. The amounts adsorbed follow the order ethanol > benzene > cyclohexane. All three isotherms are Type II or S-shaped (1). At relative pressures greater than about 0.7, the amounts of all three vapors adsorbed become very large. The very sharp rise in the initial part of the ethanol isotherm indicates a strong interaction with the high energy sites of the heterogeneous Cab-O-Sil surface. The adsorption isotherms for benzene and cyclohexane show much smaller initial rises, indicating weaker interactions with the surface for these adsorbates. Since Cab-O-Sil is polar, it would be expected to interact more strongly with polar adsorbate molecules like ethanol. The 30 and 40°C isotherms for the three adsorbates on Cab-O-Sil show similar trends in adsorption behavior.

The monolayer capacities and the cross-sectional areas of the three adsorbates were obtained from application of the BET model to the pure vapor isotherms. The linear form of the BET equation is:

$$\frac{P/P^S}{n(1-P/P^S)} = \left(\frac{c-1}{n_m c}\right)\frac{P}{P^S} + \frac{1}{n_m c} \qquad (27)$$

where n is the amount adsorbed in moles per gram of solid, c is a constant related to the average heat of adsorption in the first adsorbed layer, and n_m is the number of moles per gram corresponding to a monolayer. By plotting the left hand side of Equation (27) versus P/P^S a straight line is obtained, and n_m may be determined from the slope and the intercept of the graph. The cross-sectional area occupied by an adsorbate molecule, σ, may be calculated from:

$$\sigma = \frac{\Sigma}{n_m N_o} \qquad (28)$$

where Σ is the surface area of the adsorbent and N_o is Avogadro's number.

Table 4 lists the values of n_m and σ obtained for the three adsorbates onto Cab-O-Sil. The reported values of n_m are averages of the results obtained at the three adsorption temperatures. Cross-sectional areas (σ_L) based on liquid molar volumes (41) have also been included in Table 4. The experimental cross-sectional areas are all higher than the areas based on liquid packing. Whalen (42) has observed cross-sectional areas for benzene on silicas ranging from 50 to 119 A^2, and has proposed that benzene does not form complete monolayers in the region of BET applicability. Pierce and Ewing (43) have also observed such behavior, and have suggested that at apparent completion of the first layer, adsorbate molecules are not packed to liquid density. Further adsorption takes place by filling in the first layer and by starting the second layer. The large magnitudes of the cross-sectional areas for ethanol, benzene, and cyclohexane reported in Table 4 have been observed previously on other silica surfaces (44).

To further characterize adsorption of ethanol, benzene, and cyclohexane on Cab-O-Sil, heats of adsorption were obtained. The isosteric heat of adsorption, q_{st}, is defined by:

$$\left(\frac{\partial \ln P}{\partial 1/T}\right)_\theta = \frac{-q_{st}}{R} \qquad (29)$$

where $\theta = n/n_m$ is surface coverage. Isosteric heat of adsorption is determined from the slope of the line obtained by plotting ln P versus

TABLE 4

MONOLAYER CAPACITIES AND CROSS-SECTIONAL AREAS FOR THE THREE ADSORBATES ON CAB-O-SIL AND ON GRAPHON

		Cab-O-Sil		Graphon	
Adsorbate	$\sigma_L(A^2)$	$n_m \times 10^4$ (mole/g)	$\sigma(A^2)$	$n_m \times 10^4$ (mole/g)	$\sigma(A^2)$
Ethanol	21	9.50 ± 0.41	37.5	--	--
Benzene	28	6.00 ± 0.21	59.3	3.36 ± 0.04	44.0
Cyclohexane	32	3.45 ± 0.20	103	3.32 ± 0.12	44.5

1/T at constant θ. The slopes were determined from linear least squares fits of the data. Values of the isosteric heat of adsorption as a function of surface coverage for the three adsorbates on Cab-O-Sil are listed in Appendix II.

Figure 9 shows the isosteric heat of adsorption versus surface coverage for ethanol on Cab-O-Sil. The dashed line represents the heat of vaporization of ethanol. The behavior of q_{st} at low coverage ($\theta < 0.7$) could not be ascertained since data was not obtained for this region. The isosteric heat curve shows a pronounced maximum. Maxima in heat curves are attributed to lateral interactions in the adsorbed phase (45). For ethanol, the lateral interactions are probably caused by hydrogen bonding between adjacent adsorbate molecules. Isosteric heat curves for alcohols on fully hydroxylated silica surfaces do not contain maxima (46). For adsorption onto a fully hydroxylated surface, lateral interactions would not be important because ethanol would be hydrogen bonded to the surface hydroxyl groups. But the hydroxyl groups on the 25% hydroxylated Cab-O-Sil surface are isolated (35); adsorbed ethanol molecules would, thus, be free to interact laterally through hydrogen bonding.

For systems exhibiting lateral interactions, the isosteric heat of adsorption usually drops sharply near monolayer coverage (45). For ethanol on Cab-O-Sil, q_{st} starts to decrease around $\theta = 1.4$. The discrepancy could be related to the fact that ethanol is not packed to liquid density at monolayer coverage, as was concluded from the BET cross-sectional area for ethanol on Cab-O-Sil. If the number of moles adsorbed corresponding to $\theta = 1.4$ is used for n_m in Equation (28), σ for

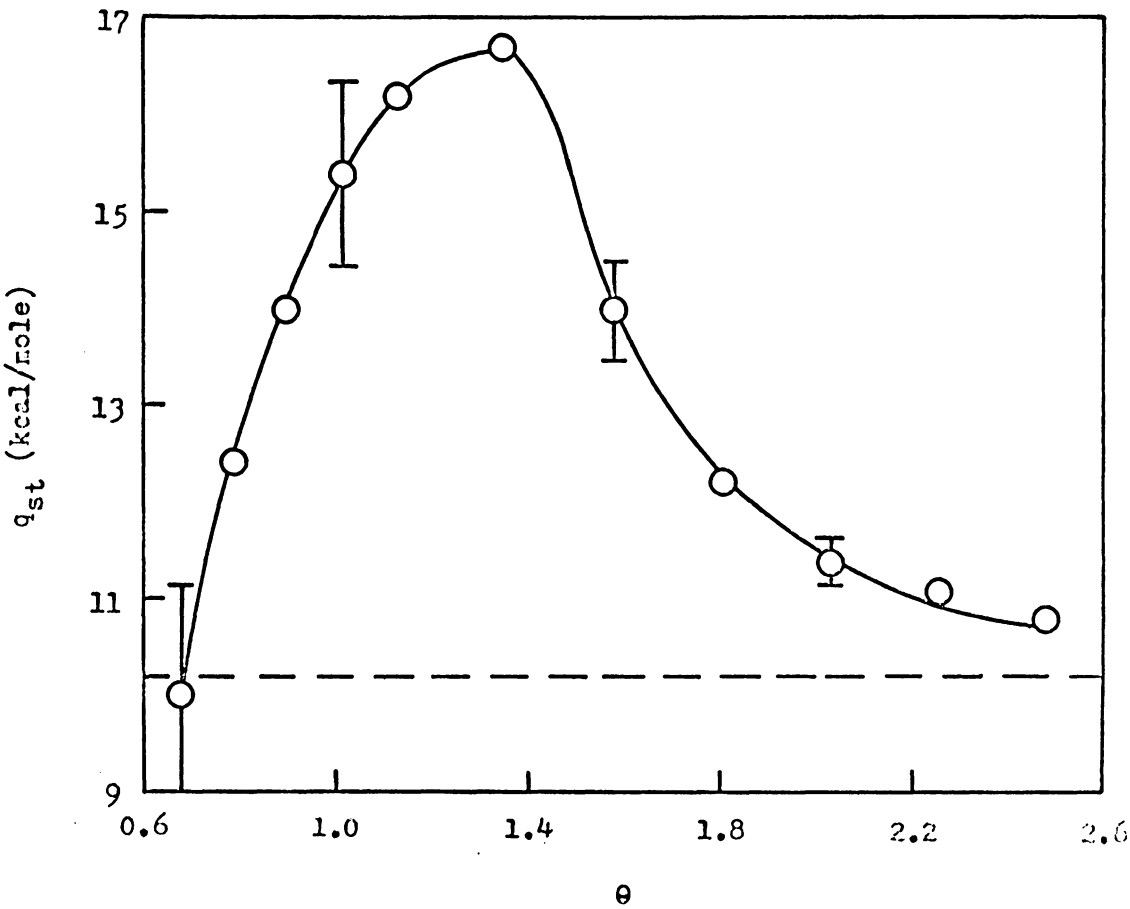

Figure 9. Isosteric Heat of Adsorption for Ethanol on Cab-O-Sil

ethanol is calculated to be about 26 A^2, which is significantly closer to the σ_L value of 21 A^2 for ethanol (see Table 4). At surface coverages greater than 1.4, the isosteric heat continues to decrease, and gradually approaches the heat of vaporization of ethanol.

The isosteric heat curves for benzene and cyclohexane on Cab-O-Sil are shown in Figure 10. The heats of vaporization of benzene and cyclohexane are almost identical, and are represented by the dashed line in Figure 10. Both heat curves appear to contain maxima at low coverages, but the errors in q_{st} in this region are very large. Additional experimental data at low coverage would be needed to determine whether these maxima are real. Hockey and Pethica (47) have attributed the maxima at low coverage in the heat curves for benzene on dehydroxylated silicas to cooperative adsorption into surface micropores.

The heat curve for cyclohexane decreases gradually with increasing coverage, and does not approach the heat of vaporization until well into the multilayer region. This result supports the previous conclusion that cyclohexane is not packed to normal density in the monolayer region. The isosteric heat curve obtained for benzene on Cab-O-Sil is anomalous in two respects. First, it lies below the heat curve for cyclohexane. It was expected to lie above the cyclohexane heat curve because of interactions of the π electrons of benzene with the hydroxyl groups on the Cab-O-Sil surface. Secondly, the benzene heat curve drops below the heat of vaporization. These two anomalies may be related to the fact that the Cab-O-Sil surface is only 25% hydroxylated, but they cannot be adequately explained without additional experimental investigation.

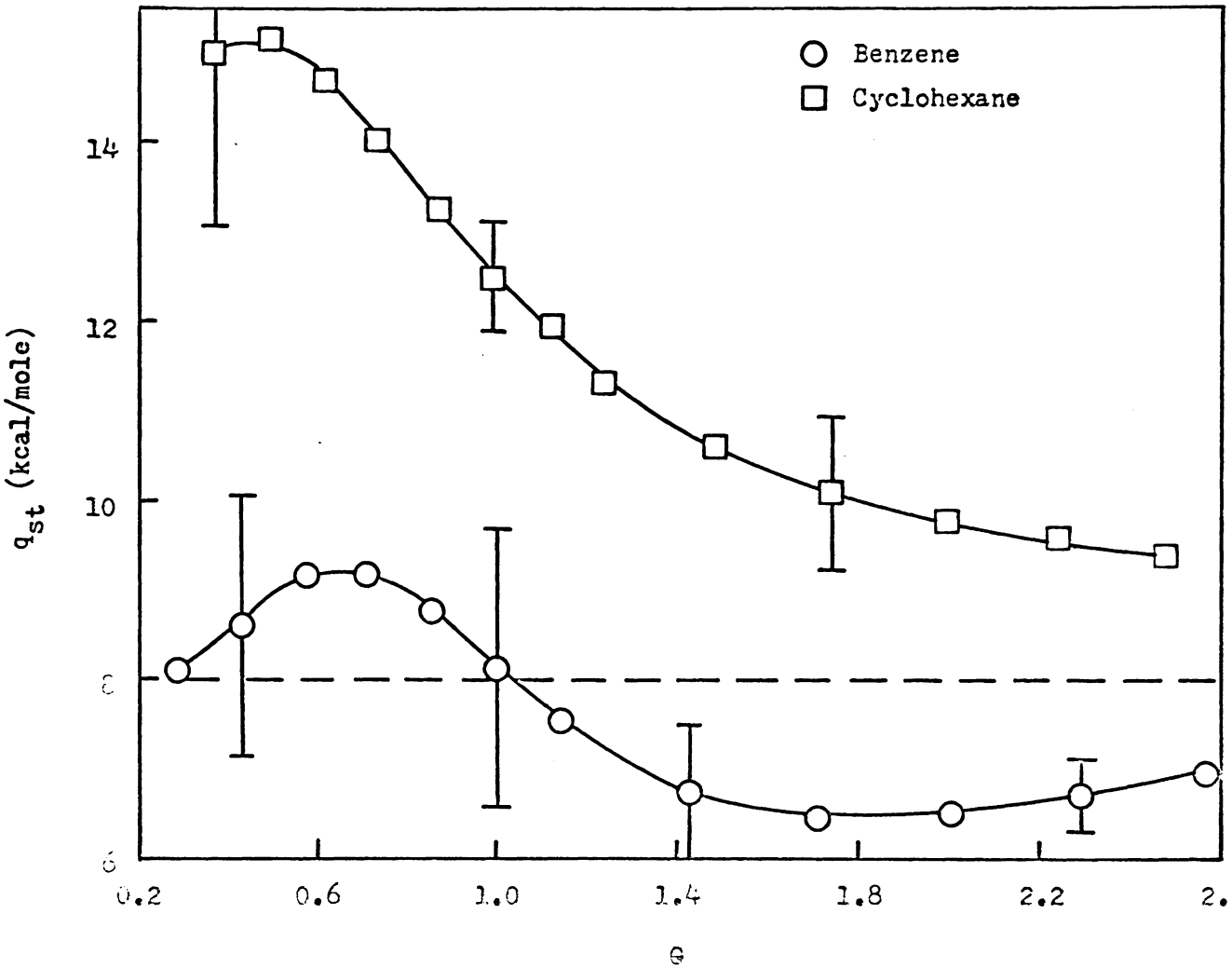

Figure 10. Isosteric Heats of Adsorption for Benzene and Cyclohexane on Cab-O-Sil

Graphon isotherms

The adsorption isotherms for benzene and cyclohexane on Graphon are shown in Figures 11 and 12, respectively. The isotherms have been plotted as N versus P. As for Cab-O-Sil, the error in N for the Graphon isotherms is about $\pm$ 0.3 x 10^{-6} mole/m^2. The amounts adsorbed decrease markedly with increasing temperature. Isotherms for both adsorbates are Type II, and are very similar to those obtained for ethanol on Cab-O-Sil. The initial sharp rises observed in the benzene and cyclohexane isotherms on Graphon indicate fairly strong interactions of benzene and cyclohexane with the high energy surface sites.

The adsorption isotherms (N versus P) for ethanol on Graphon, shown in Figure 13, also show the strong temperature dependence characteristic of gas/solid adsorption. The ethanol/Graphon isotherms are not Type II, but are intermediate between Types II and III. The initial portion of the isotherm is concave rather than convex, followed by a sharp rise in the isotherm as pressure increases. The initial concavity indicates a weak interaction of ethanol with the nonpolar Graphon surface. The same type of adsorption isotherm for ethanol on carbon surfaces has been observed by Berezin *et al.* (48) and by Berezkina *et al.* (49).

Figure 14 compares the 20°C isotherms for the three adsorbates on Graphon, plotted as N versus P/P^s. The amounts of benzene and cyclohexane adsorbed at low relative pressures are about the same, with the benzene isotherm running a little higher as relative pressure increases. These two isotherms are almost within experimental error of each other. The crossing of the benzene and cyclohexane isotherms at high relative pressure is probably not significant. In the high pressure region

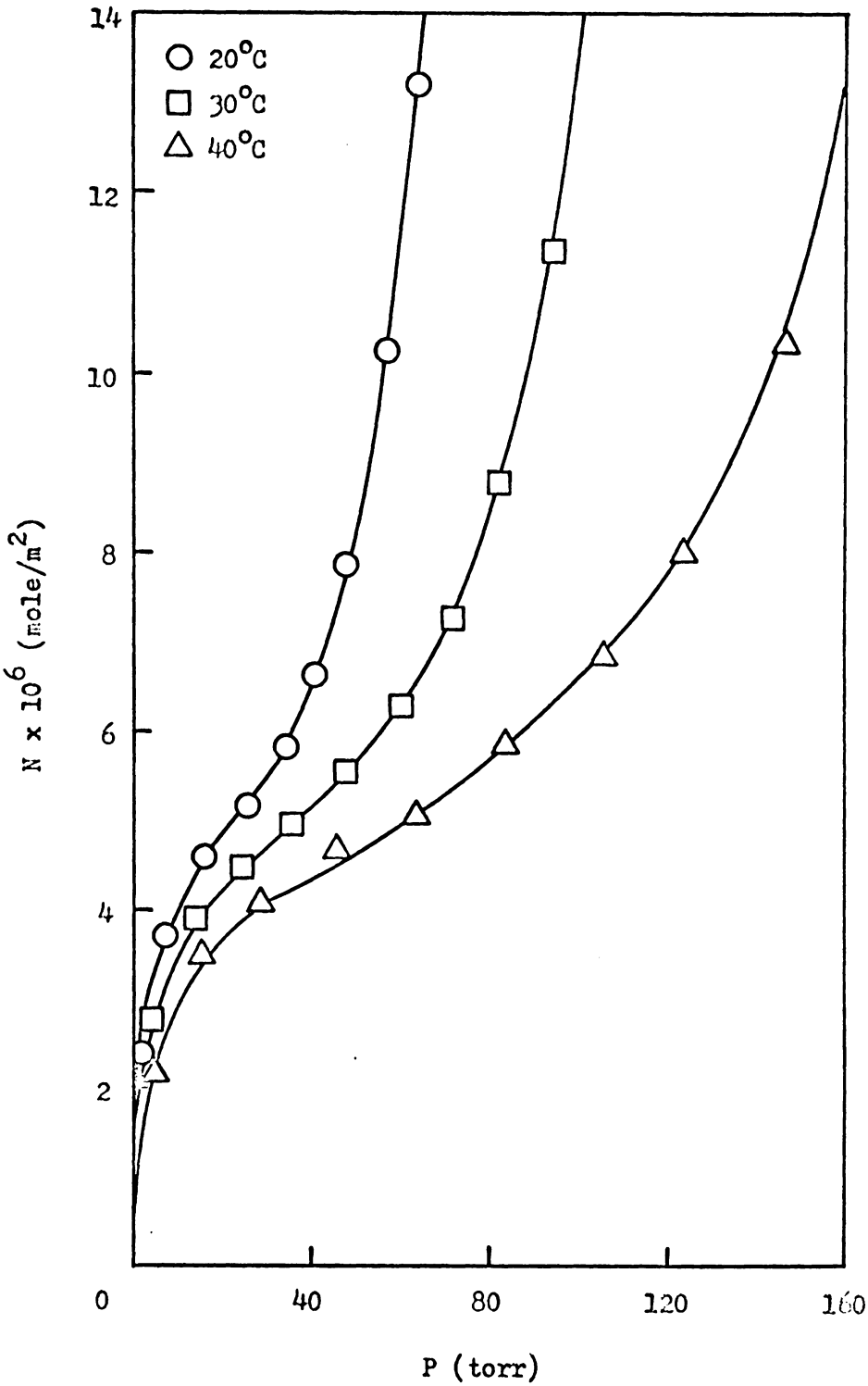

Figure 11. Benzene/Graphon Isotherms at 20, 30, and 40°C

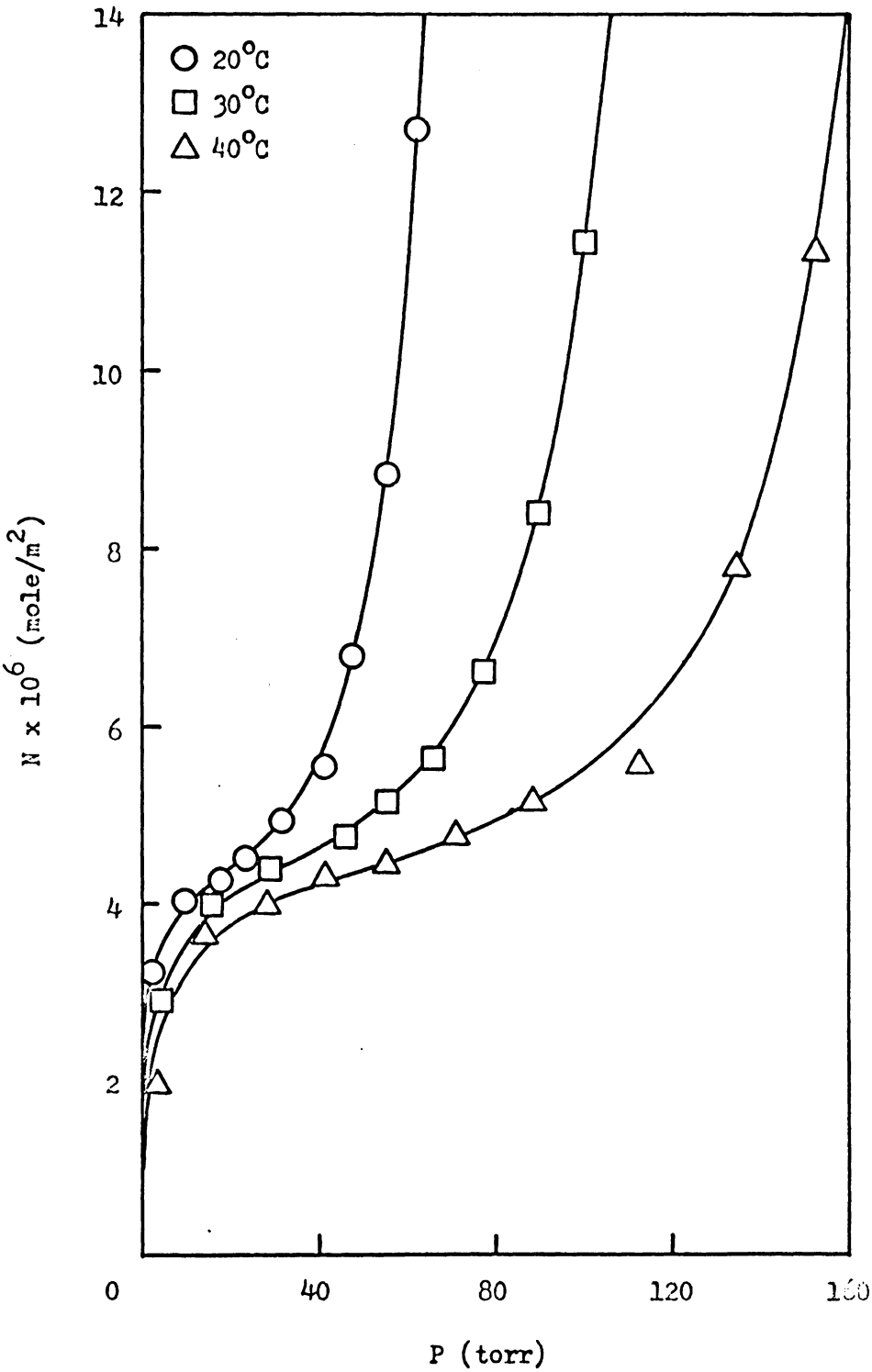

Figure 12. Cyclohexane/Graphon Isotherms at 20, 30, and 40°C

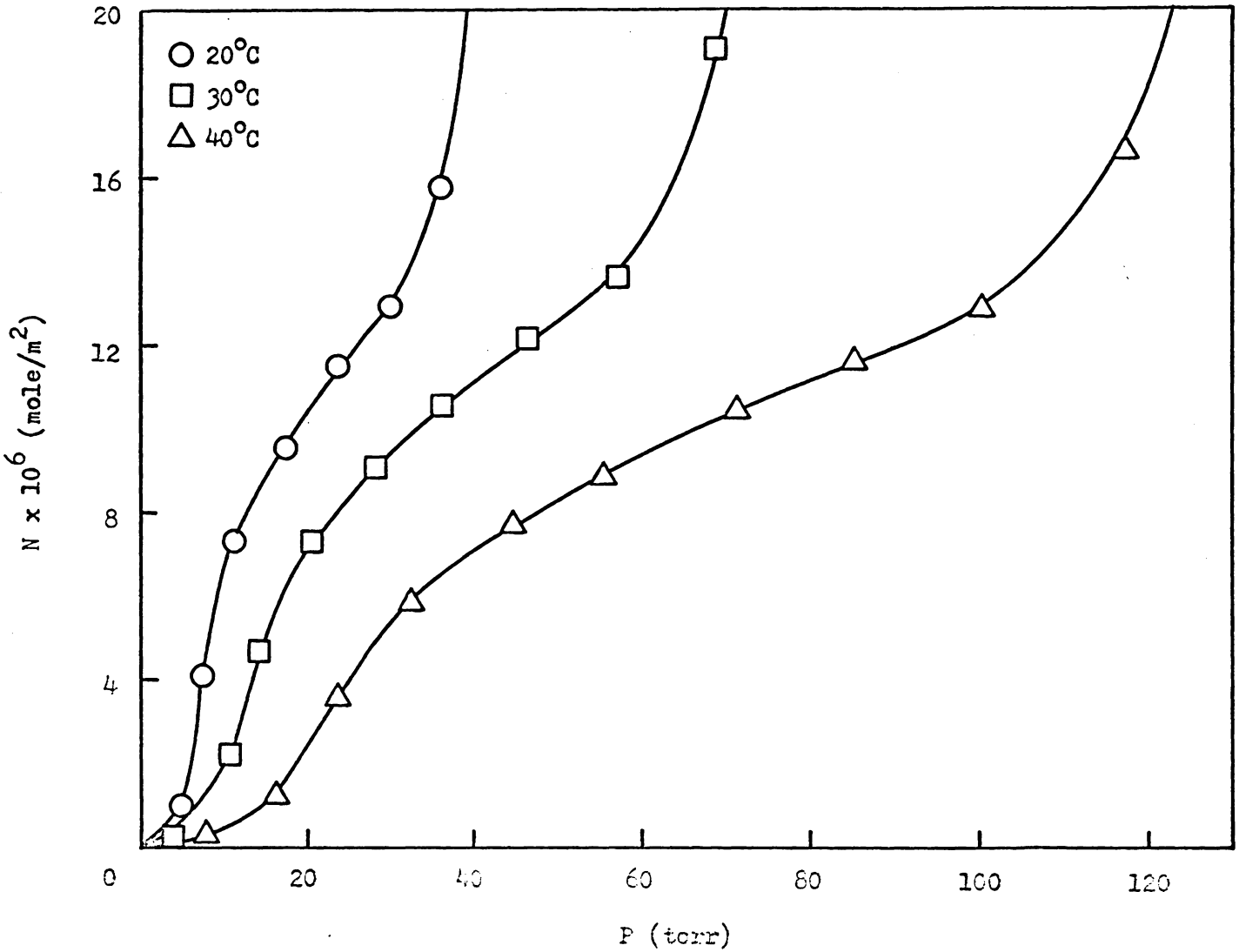

Figure 13. Ethanol/Graphon Isotherms at 20, 30, and 40°C

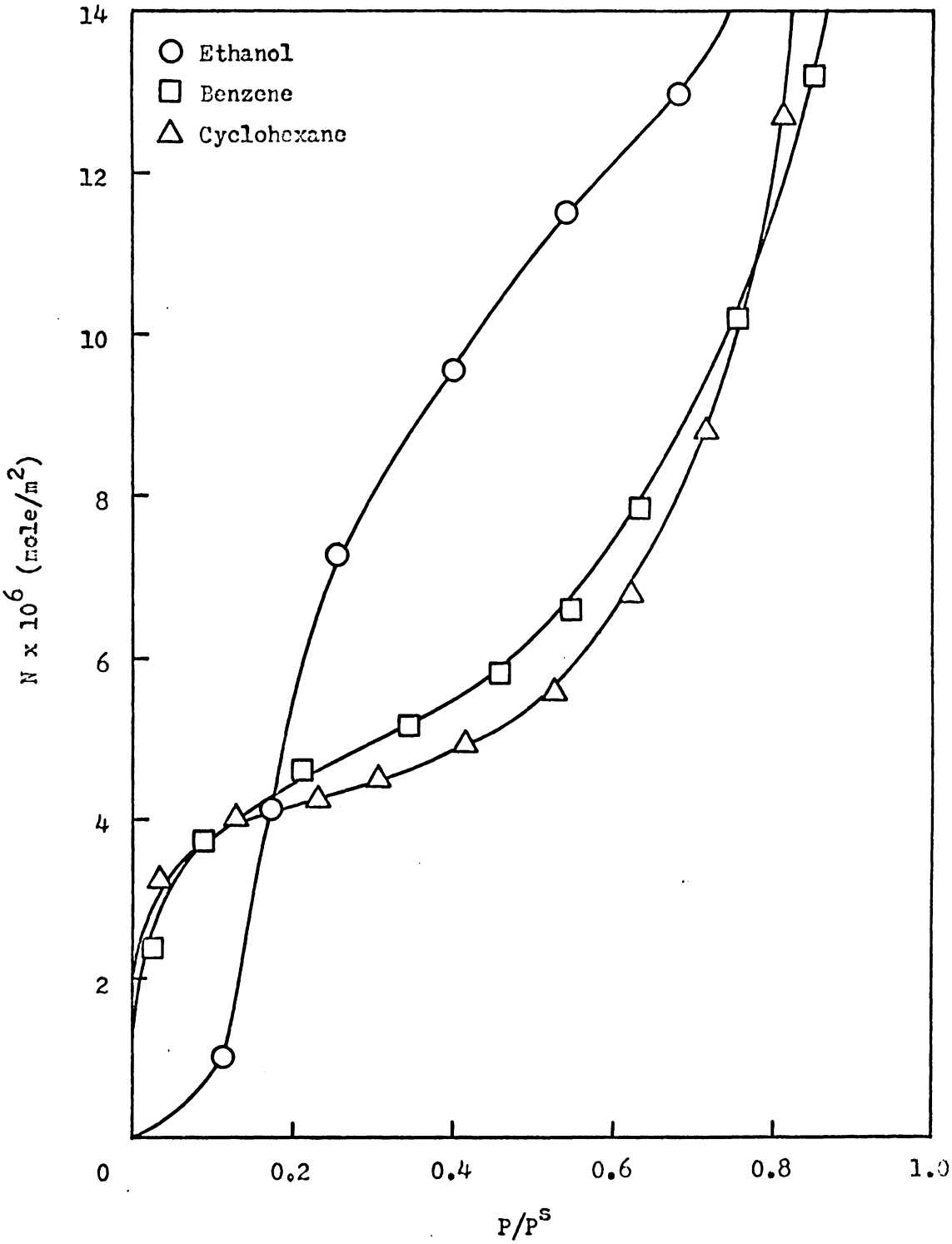

Figure 14. Pure Ethanol, Benzene, and Cyclohexane on Graphon at 20°C

equilibration of benzene with Graphon was not complete even after one hour; the latter few points on the benzene isotherm could, thus, be higher. The amount of ethanol adsorbed is lower than the amounts of benzene and cyclohexane adsorbed at low relative pressures, becoming higher as relative pressure increases. Similar trends in adsorption behavior were observed in the 30 and 40°C isotherms for the three adsorbates on Graphon.

The monolayer capacities and cross-sectional areas for benzene and cyclohexane on Graphon, determined from the BET model, are listed in Table 4. The BET equation did not fit the ethanol/Graphon isotherms. The n_m values listed in Table 4 are averages of the results obtained at the three adsorption temperatures. The values of n_m and σ for benzene and cyclohexane on Graphon are almost identical. The σ values are significantly closer to σ_L than the values obtained for these same two adsorbates on Cab-O-Sil. The experimental σ values agree well with values previously reported for benzene and cyclohexane on carbon surfaces (44).

Isosteric heats of adsorption as a function of surface coverage for benzene and cyclohexane on Graphon are shown in Figure 15. The isosteric heat data for the three adsorbates on Graphon are tabulated in Appendix II. The behavior of q_{st} at low coverage ($\theta < 0.75$) could not be ascertained since data was not obtained for this region. The heat curve for cyclohexane decreases sharply with increasing coverage, becoming almost equal to the heat of vaporization at monolayer coverage. The benzene heat curve shows similar behavior. The data were not precise enough to determine whether the slight maximum observed in the benzene heat curve

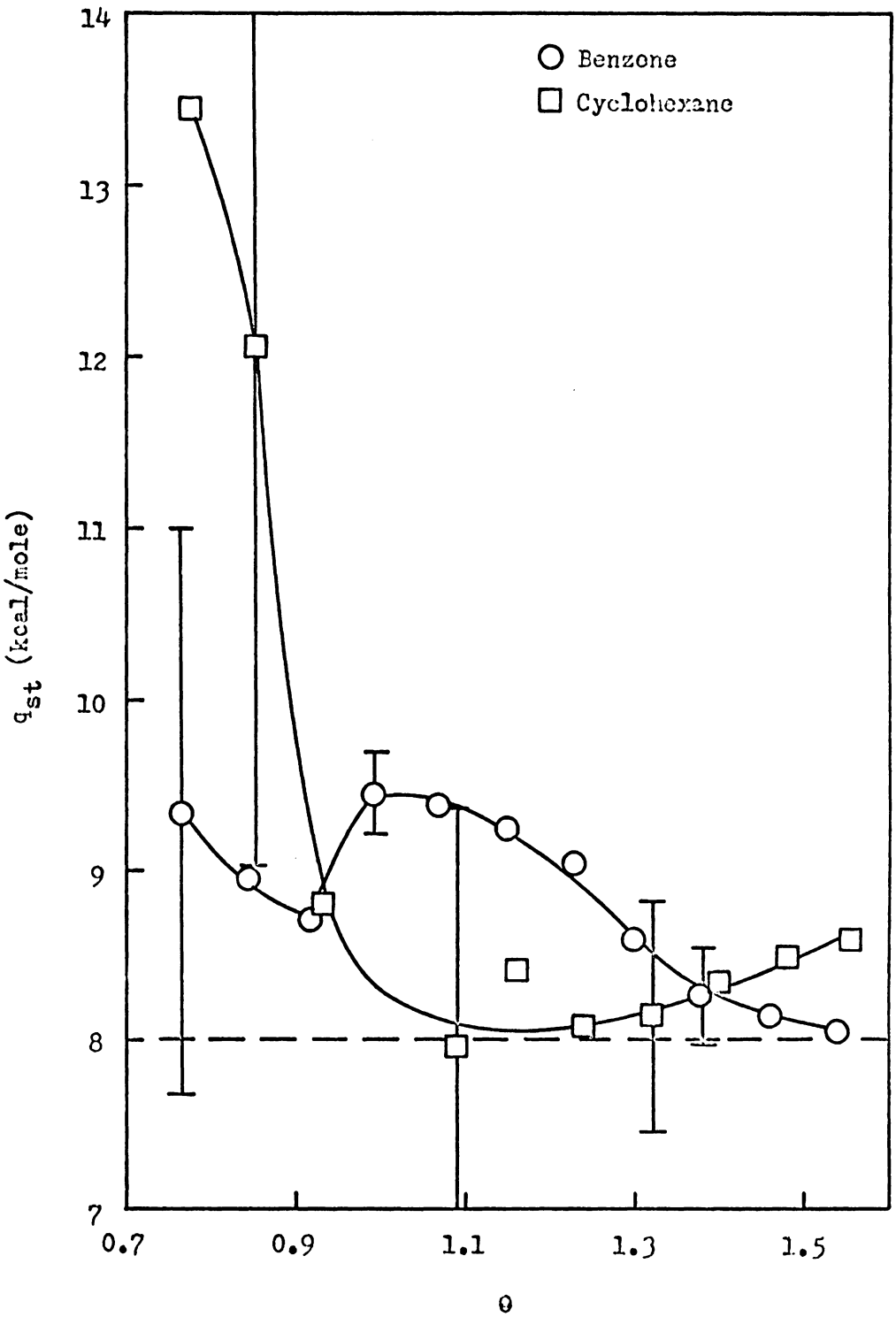

Figure 15. Isosteric Heats of Adsorption for Benzene and Cyclohexane on Graphon

is significant.

The isosteric heat plot for ethanol on Graphon is shown in Figure 16. Since the ethanol/Graphon isotherms did not fit the BET equation, an experimental n_m value could not be determined. The n_m value used to calculate surface coverage in Figure 16 was calculated from Equation (28) assuming an area of 23 A^2 for ethanol. At low coverage the sharp drop in q_{st} characteristic of adsorption onto a heterogeneous surface is observed. At an approximate surface coverage of 0.55 a maximum occurs, indicating lateral interactions between ethanol molecules on the Graphon surface. The isosteric heat decreases gradually past the maximum, indicating that there is no sharp division between the first ($\theta = 1$) and second ($\theta = 2$) adsorbed layers. The behavior of the isosteric heat as a function of coverage suggests that ethanol is oriented with the ethyl group lying on the surface, leaving the hydroxyl groups free to hydrogen bond. A similar type of orientation has been postulated by Innes and Rowley (8) for the methanol/charcoal system, and by Berezin et al. (48) for adsorption of ethanol on graphitized carbon black. Besides accounting for lateral interactions, hydrogen bonding could cause multilayer adsorption to begin before the first layer has been completed. Such adsorption behavior would account for the lack of a sharp drop in q_{st} past the maximum in Figure 16.

The nature of the adsorbed phase for ethanol on Graphon was further investigated by calculating the integral entropy of adsorption, S, which is defined as:

$$\left(\frac{\partial \ln P}{\partial T}\right)_{\pi} = \frac{S}{RT} \qquad (30)$$

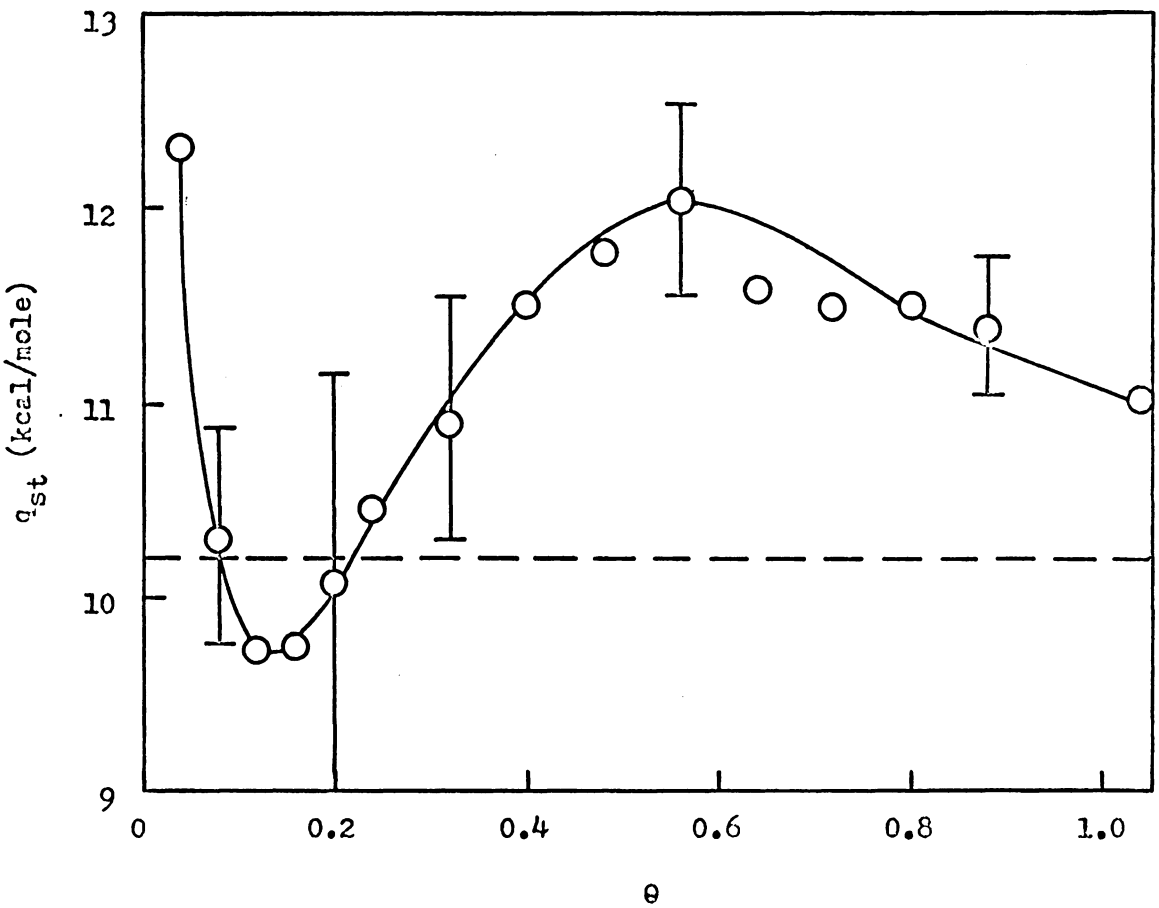

Figure 16. Isosteric Heat of Adsorption for Ethanol on Graphon

where π is the spreading pressure. Calculation of the integral entropy of adsorption requires very accurate values of spreading pressure. To obtain precise spreading pressures, adsorption data at low surface coverages must be available. Since adsorption of ethanol on Graphon was measured at much lower surface coverages for the 30 and 40°C isotherms than for the 20°C isotherm (see Figure 13), only the 30 and 40°C isotherms were used to calculate S. Details of the calculation have been discussed by Hill, Emmett, and Joyner (50). Figure 17 gives the entropy of adsorption relative to the liquid state as a function of surface coverage for ethanol on Graphon. The entropy values are tabulated in Appendix II. The entropy of the adsorbed phase is less than the entropy of liquid ethanol, as a consequence of the reduced number of translational and rotational degrees of freedom in the adsorbed phase. Figure 17 shows a minimum at about $\theta = 0.1$. A minimum at low coverage has also been observed for adsorption of nitrogen on graphite (51), and has been attributed to adsorption on the high energy surface sites. The entropy plot is consistent with the proposed structuring of ethanol on the Graphon surface, as discussed above. After the high energy sites have been occupied, the adsorbed phase becomes more random as ethanol molecules begin to adsorb with the ethyl group lying on the surface. As the amount of adsorbed ethanol increases, hydrogen bonding interactions between adsorbed molecules cause the adsorbed phase to become more ordered. For physical adsorption systems, the entropy usually goes through a minimum at $\theta = 1$ (50, 51). The fact that no sharp change is observed in the entropy plot at monolayer coverage indicates a lack of a sharp division between the first and second adsorbed layers. The entropy

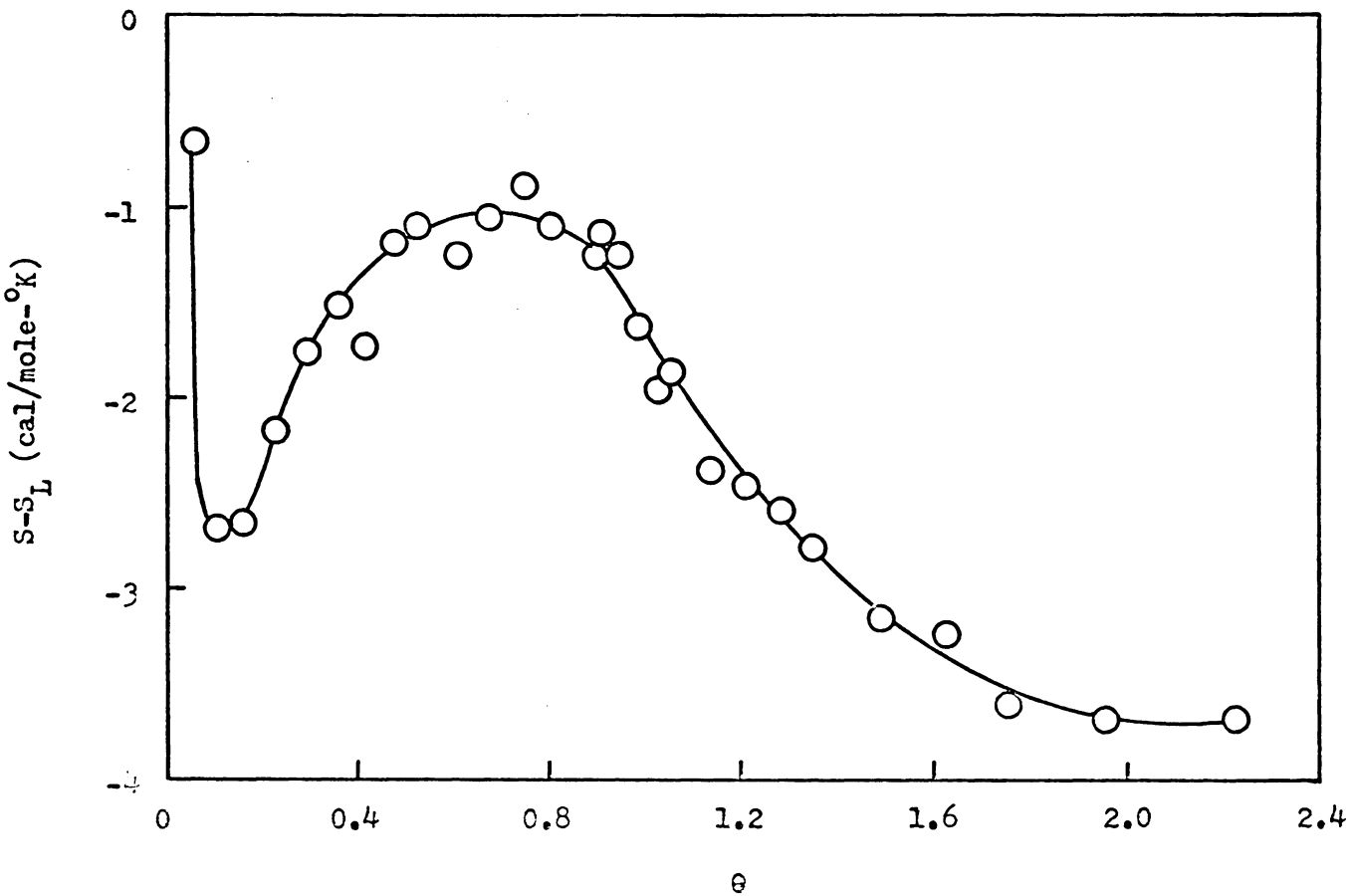

Figure 17. Integral Entropy of Adsorption for Ethanol on Graphon

continues to decrease into the second adsorbed layer. This type of behavior would be expected if hydrogen bonding interactions occur between ethanol molecules in the first and second adsorbed layers.

Binary Vapor Adsorption Isotherms

The adsorption isotherms that were obtained for the binary vapor mixtures are presented graphically in the following sections. The approximate error in the amounts of the components adsorbed is $\pm$ 0.3 x 10^{-6} mole/m^2. The experimental data and a sample calculation of binary vapor adsorption are given in Appendix III. The binary vapor adsorption isotherms are discussed in terms of the adsorbate-adsorbent interactions that were observed in the pure vapor isotherms. Since each binary vapor isotherm was measured at only one value of the total pressure, heats of adsorption for the components in the mixtures could not be calculated.

Cab-O-Sil isotherms

The binary vapor adsorption isotherms for ethanol-cyclohexane, ethanol-benzene, and benzene-cyclohexane vapor mixtures on Cab-O-Sil at 20, 30, and 40°C are shown in Figures 18 through 26. The isotherms have been plotted as N, the number of moles of each component adsorbed per square meter of adsorbent, versus vapor phase composition, y_i. The corresponding pure component isotherms, represented by the dashed curves, have been included on these graphs for comparison purposes. Although this method of representing binary vapor adsorption data has not been used previously, it illustrates some interesting features.

The adsorption isotherms for ethanol-cyclohexane mixtures on Cab-O-Sil, shown in Figures 18-20, indicate that ethanol is the

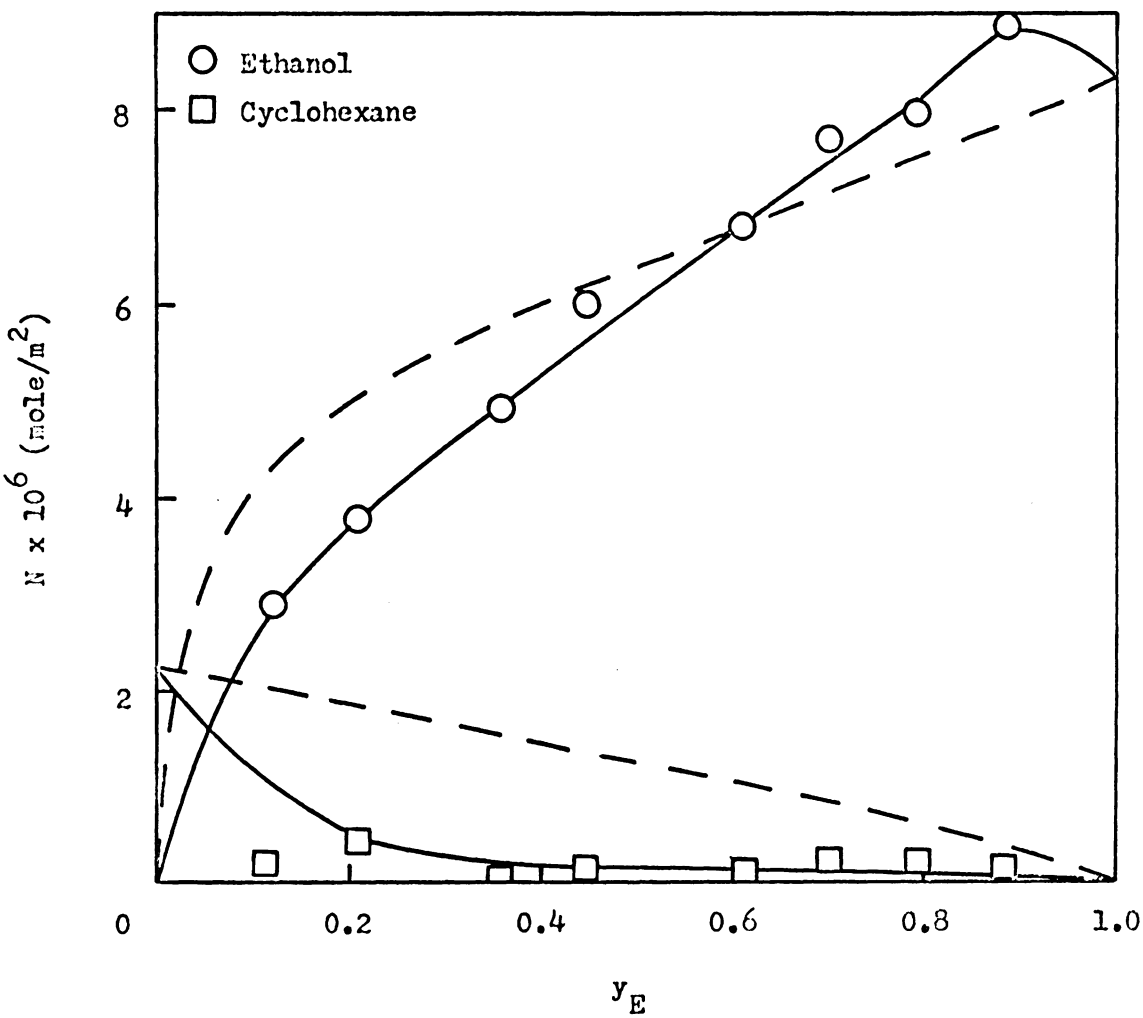

Figure 18. Ethanol-Cyclohexane/Cab-O-Sil Isotherm at 20°C

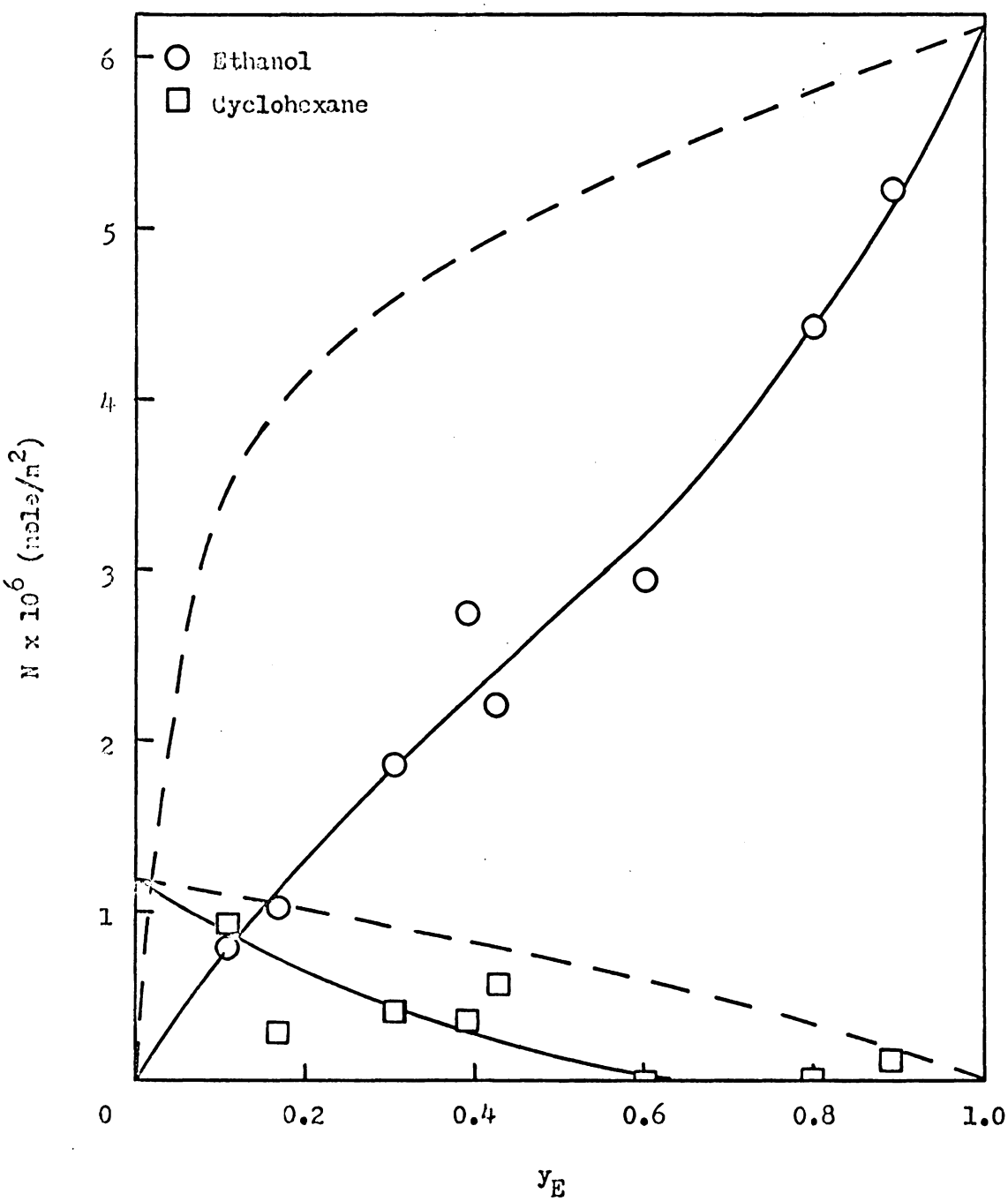

Figure 19. Ethanol-Cyclohexane/Cab-O-Sil Isotherm at 30°C

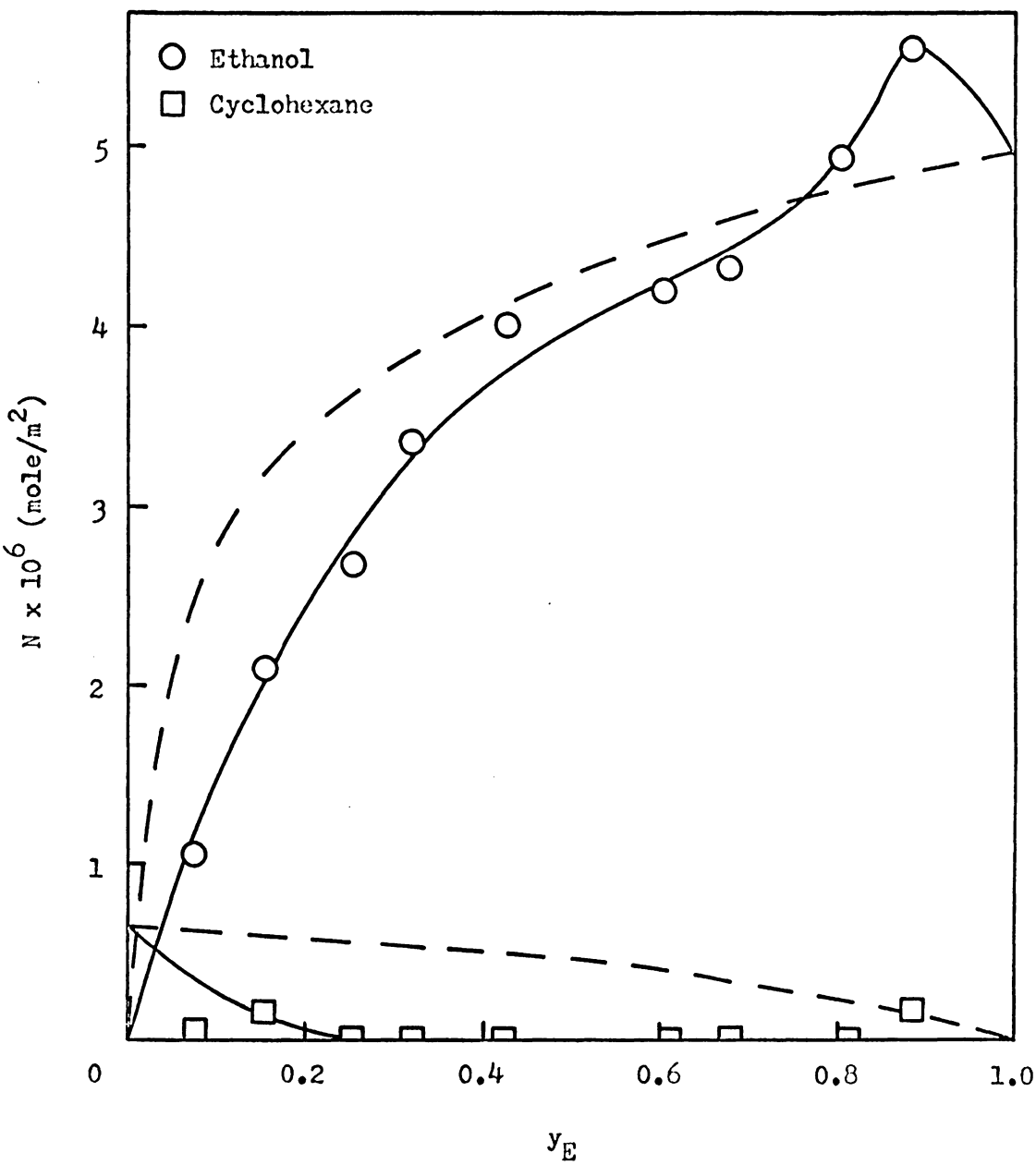

Figure 20. Ethanol-Cyclohexane/Cab-O-Sil Isotherm at 40°C

dominant component in the adsorbed phase. Adsorption of cyclohexane may be appreciable only at low vapor mole fractions of ethanol. The amounts of cyclohexane adsorbed from the mixtures are much less than from the pure state. Such behavior is also observed for ethanol, with two exceptions. In the 20 and 40°C isotherms, enhancement of adsorption of ethanol over the pure state is observed at high ethanol mole fractions. This phenomenon cannot be adequately explained without further data.

The ethanol-benzene/Cab-O-Sil isotherms, shown in Figures 21-23, indicate that ethanol again dominates the adsorbed phase, but not to the extent that it does when mixed with cyclohexane. Adsorption of both ethanol and benzene from the mixtures is generally less than from the pure states. However, at 40°C enhancement of adsorption of ethanol and benzene is observed at high and low ethanol mole fractions, respectively.

For adsorption of benzene-cyclohexane mixtures onto Cab-O-Sil, shown in Figures 24-26, there are appreciable amounts of both components adsorbed over the entire mole fraction range. Unlike the other two mixtures, neither component is capable of dominating the Cab-O-Sil surface. For benzene-cyclohexane mixtures at all three temperatures, adsorption of both components is greater from the mixtures than from the pure states, in contrast to the general behavior observed for the other two mixtures. This phenomenon could not be explained.

The relative amounts of adsorption of a species from mixtures and from the pure state has not been widely discussed. Myers (28) has observed that for systems showing fairly strong adsorbate-adsorbent interactions, adsorption from mixtures is generally less than from the pure state. This behavior has been attributed to competition of the

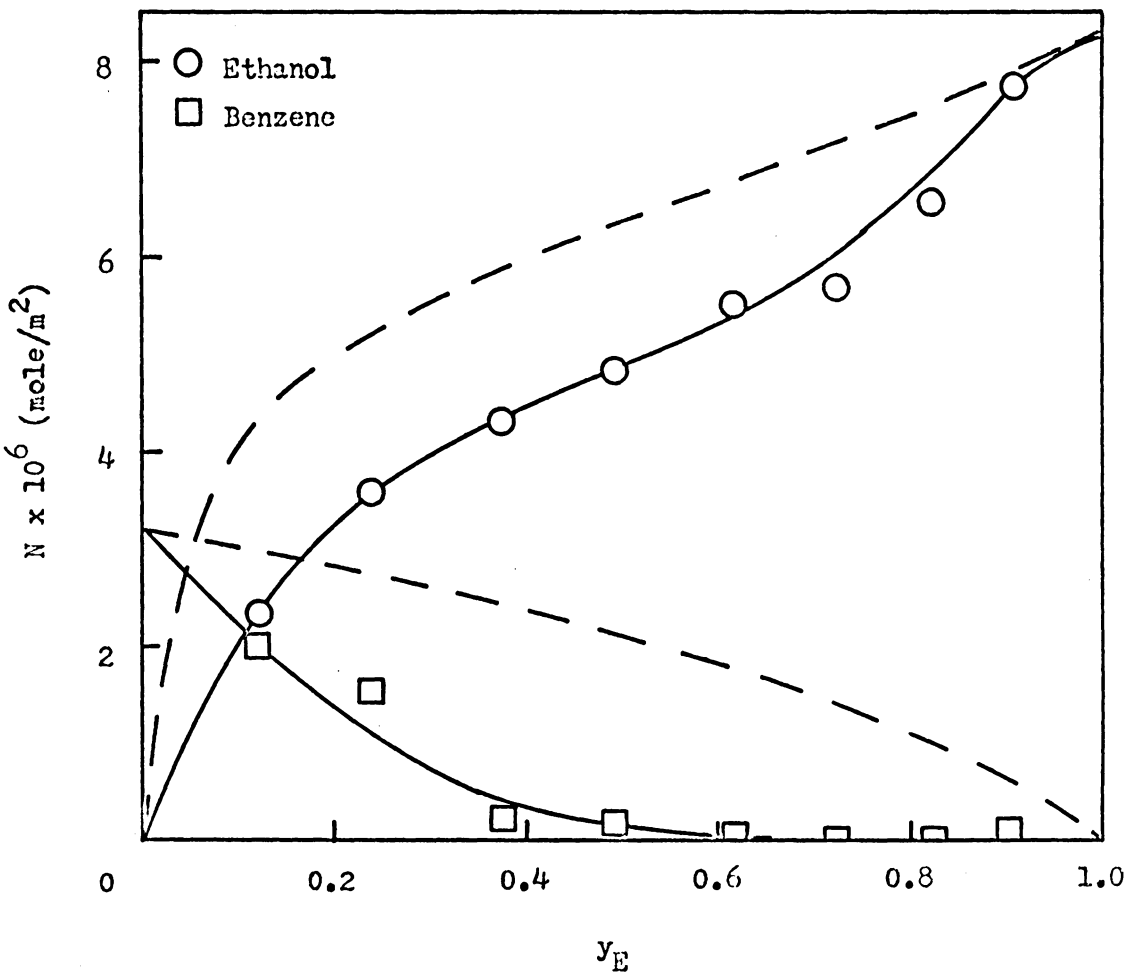

Figure 21. Ethanol-Benzene/Cab-O-Sil Isotherm at 20°C

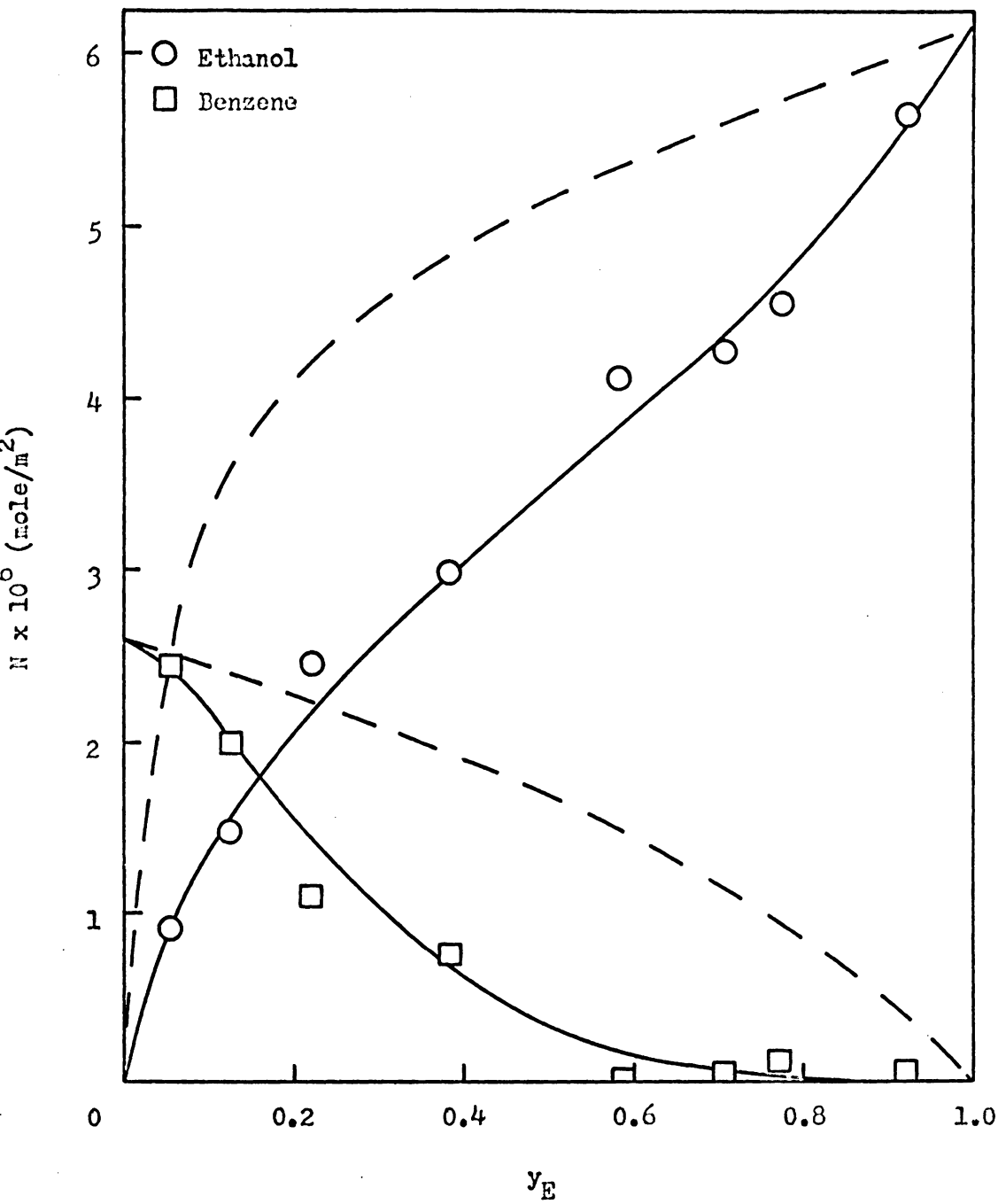

Figure 22. Ethanol-Benzene/Cab-O-Sil Isotherm at 30°C

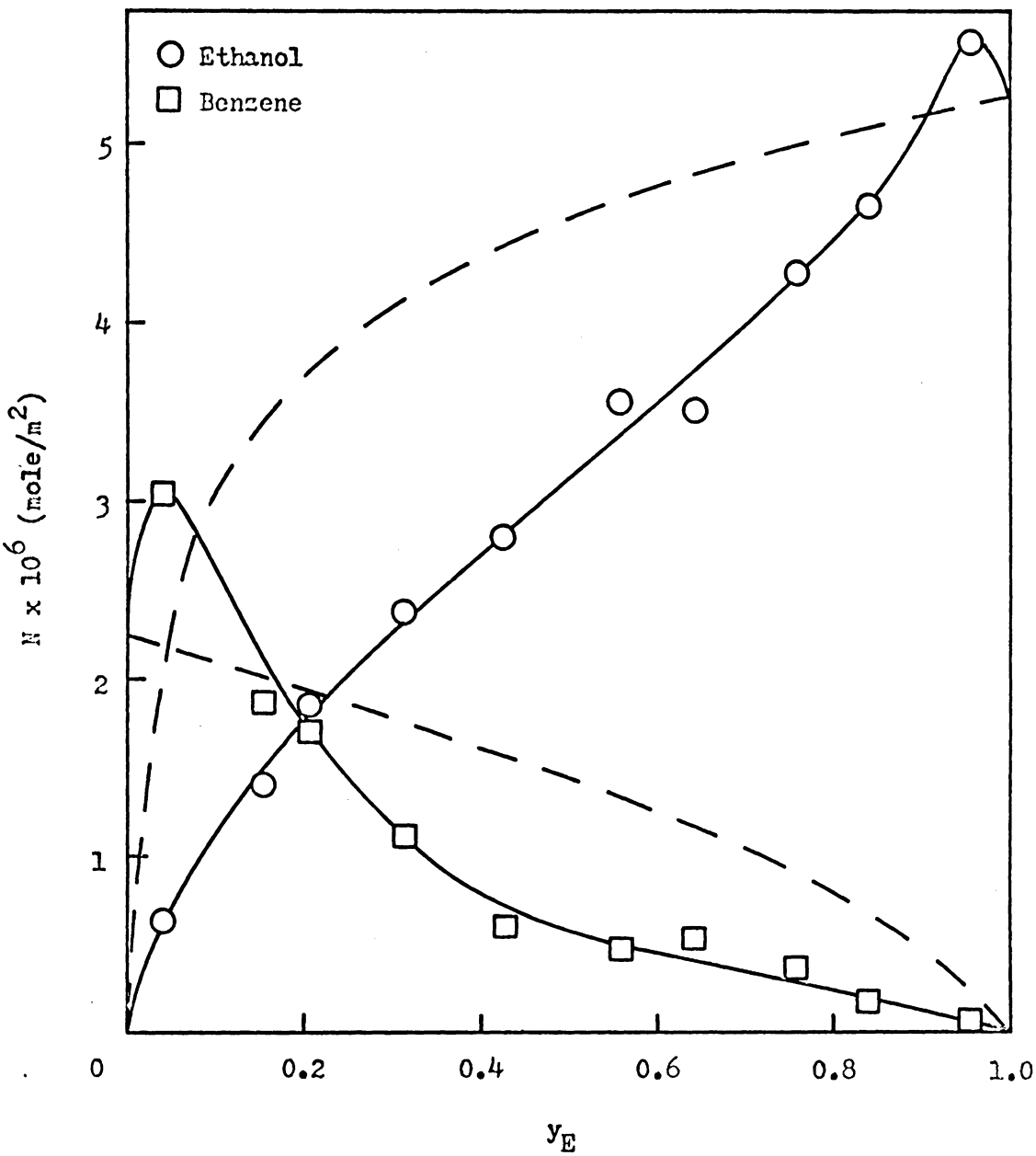

Figure 23. Ethanol-Benzene/Cab-O-Sil Isotherm at 40°C

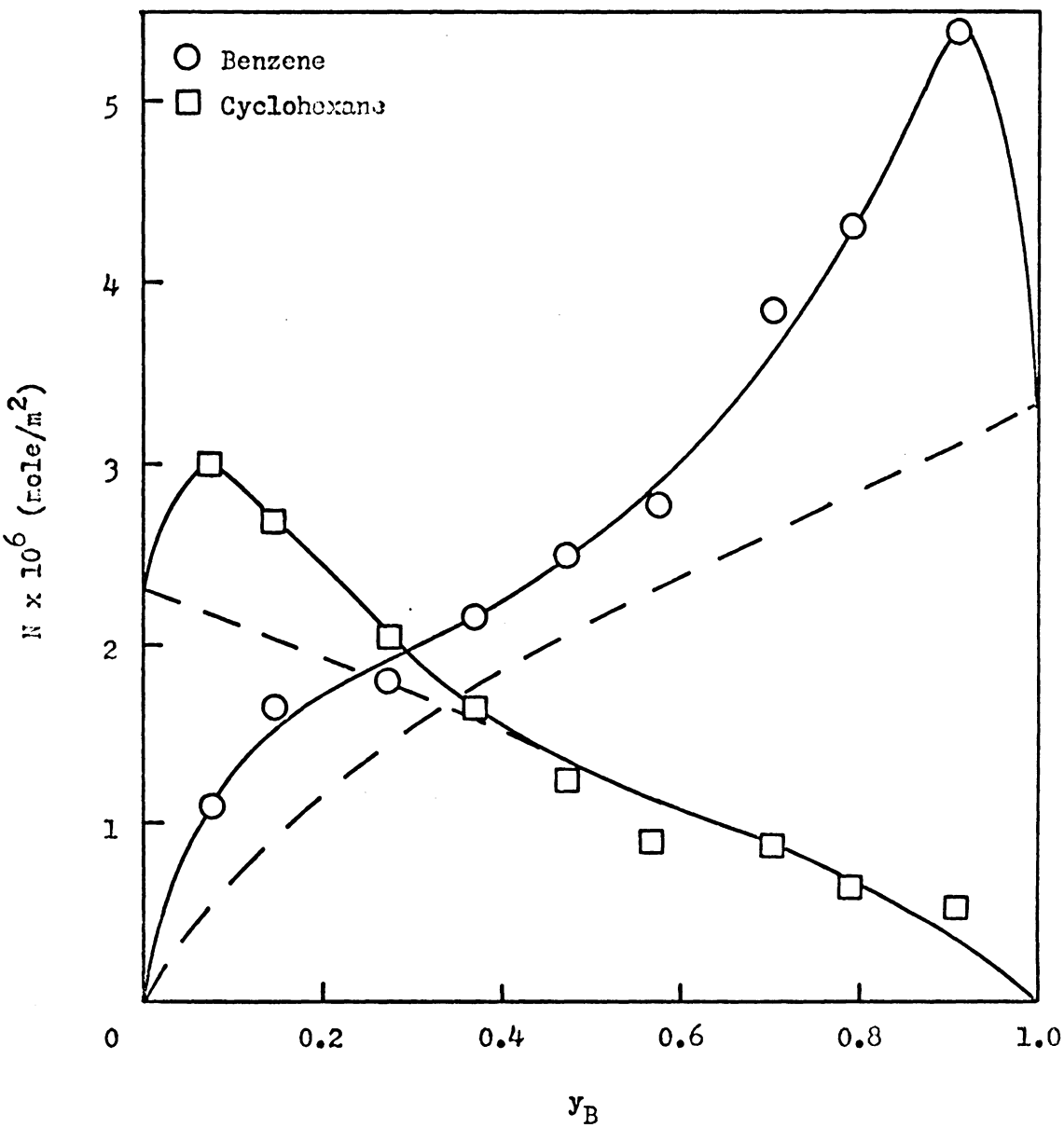

Figure 24. Benzene-Cyclohexane/Cab-O-Sil Isotherm at 20°C

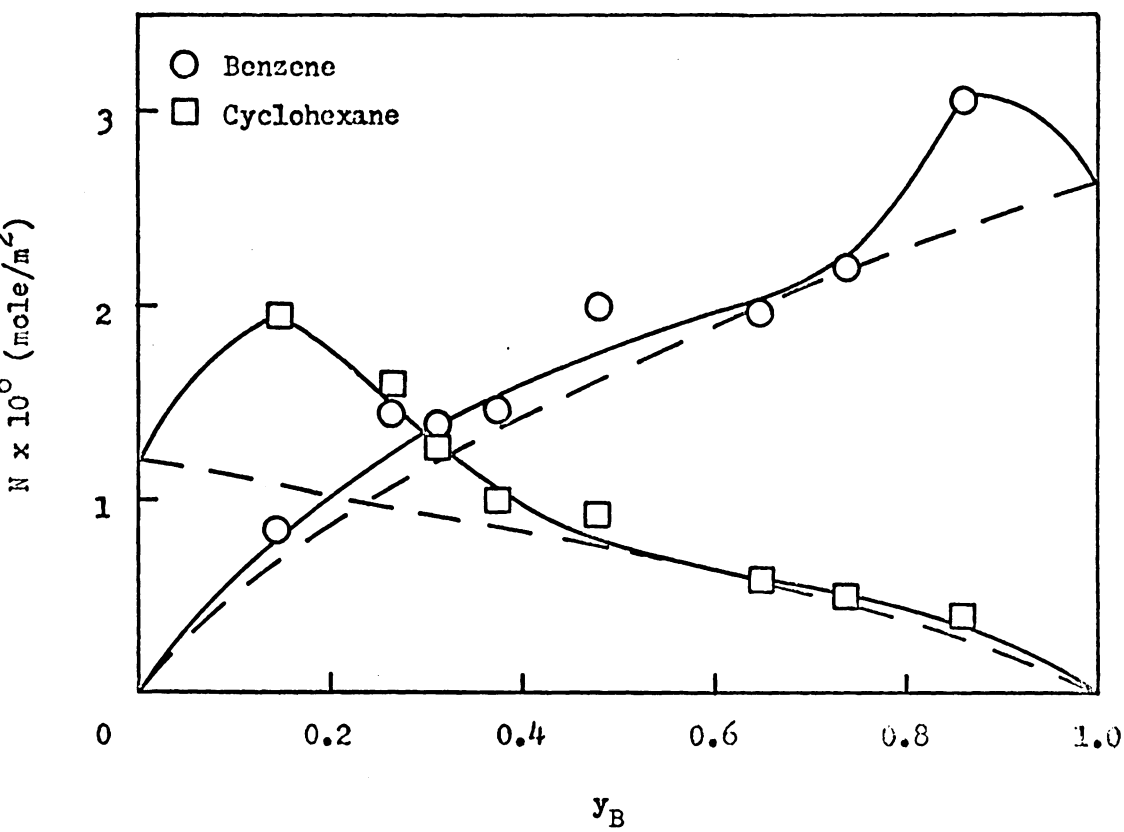

Figure 25. Benzene-Cyclohexane/Cab-O-Sil Isotherm at 30°C

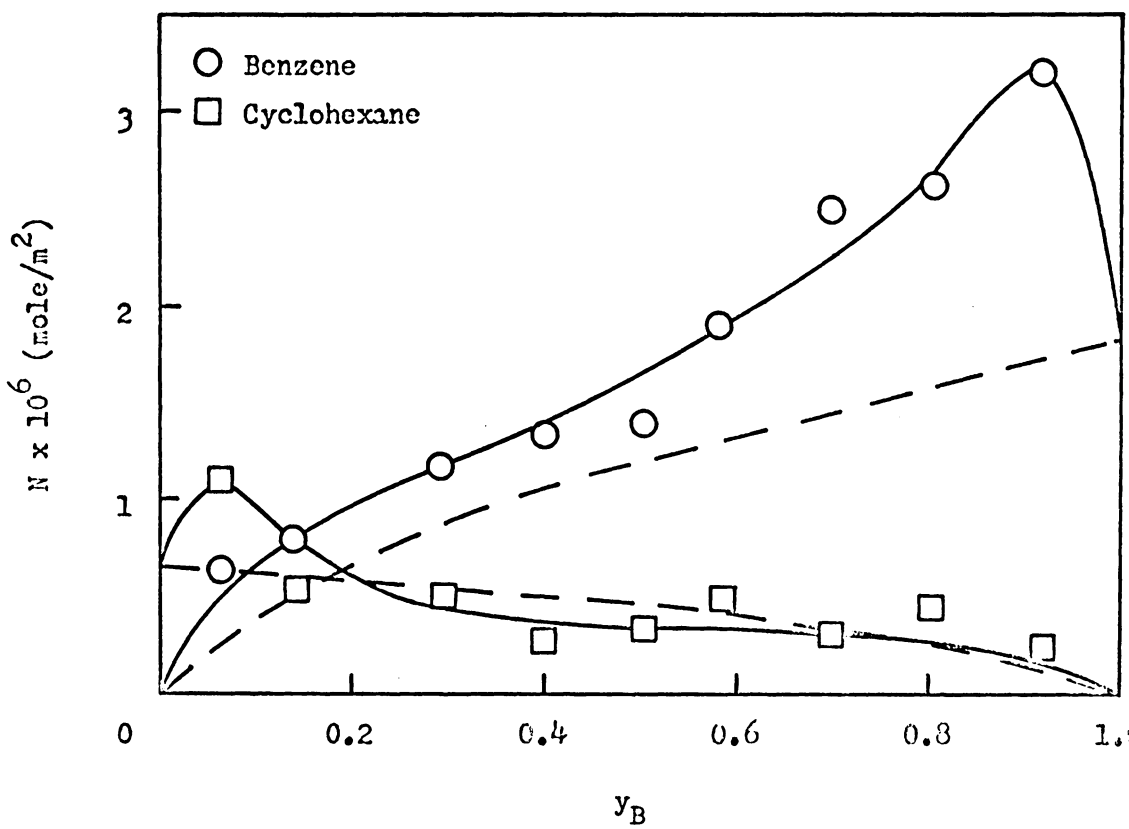

Figure 26. Benzene-Cyclohexane/Cab-O-Sil Isotherm at 40°C

components for surface sites. An enhancement of adsorption over the pure state has been observed by Pavlyuchenko (11) for chloroform-acetone vapor mixtures onto carbon. Bering, Serpinskii, and Surinova (30) have postulated that for the chloroform-acetone/carbon system, in which adsorbate-adsorbent interactions are fairly weak, the enhancement is caused by attractive forces between the two components in the adsorbed phase. The pronounced enhancements in adsorption from the mixtures observed for the benzene-cyclohexane/Cab-O-Sil systems, and the slight enhancements observed in some of the other isotherms, are difficult to rationalize. Without data on heats of adsorption of the components in the mixtures, this unexpected behavior cannot be explained.

Examination of Figures 18-26 indicates that the temperature dependence of adsorption of the components is the same as for pure vapor adsorption; that is, the amount of a component adsorbed decreases with increasing temperature. The 40°C ethanol-benzene/Cab-O-Sil isotherm cannot be compared to the other two isotherms, since the former was measured at a total pressure of 40 torr and the latter at 30 torr. The only exception occurred for the ethanol-cyclohexane/Cab-O-Sil system. For these isotherms, the amount of ethanol adsorbed followed the trend 20°C > 40°C > 30°C. This anomalous temperature dependence could be due to the fact that the Cab-O-Sil sample used to measure the 30°C isotherm was different from the sample used for the other two isotherms. Possible differences in the two Cab-O-Sil samples will be discussed further in another section.

Although Figures 18-26 give some indication of selective adsorption, selectivity is best illustrated by adsorbate-vapor composition diagrams.

The 20°C isotherms for the three mixtures have been replotted in Figure 27 as adsorbed phase composition, x, versus vapor phase composition, y. The asterisks in Figure 27 denote the component of each mixture whose mole fractions have been plotted. If no selective adsorption were occurring in these systems, the compositions of the adsorbed and vapor phases would be equal, and the isotherms would lie along the dashed line in Figure 27. If the component whose compositions are being plotted is selectively adsorbed from a mixture, the isotherm will lie above the dashed line. The further the isotherm lies from the dashed line, the greater the selectivity. The trends in selectivity observed for the three mixtures on Cab-O-Sil can be explained qualitatively on the basis of adsorbate-adsorbent interactions. Since ethanol is capable of polar interactions with the Cab-O-Sil surface, it is selectively adsorbed from ethanol-cyclohexane and ethanol-benzene mixtures. The selective adsorption of benzene from benzene-cyclohexane mixtures may be attributed to interactions between the π electrons of benzene and the hydroxyl groups of the Cab-O-Sil surface. Selective adsorption of benzene from benzene-cyclohexane mixtures on Cab-O-Sil is consistent with the observations of Lewis *et al.* (4). For mixtures of components having nearly equal vapor pressures, the more unsaturated component is selectively adsorbed on silica. The selectivity observed for the benzene-cyclohexane mixtures is much less pronounced than for the other two mixtures, since the strengths of the adsorbate-adsorbent interactions in the benzene-cyclohexane/Cab-O-Sil system are more nearly equal than in the systems containing ethanol. The 30 and 40°C composition diagrams for the three mixtures on Cab-O-Sil show the same trends in selectivity.

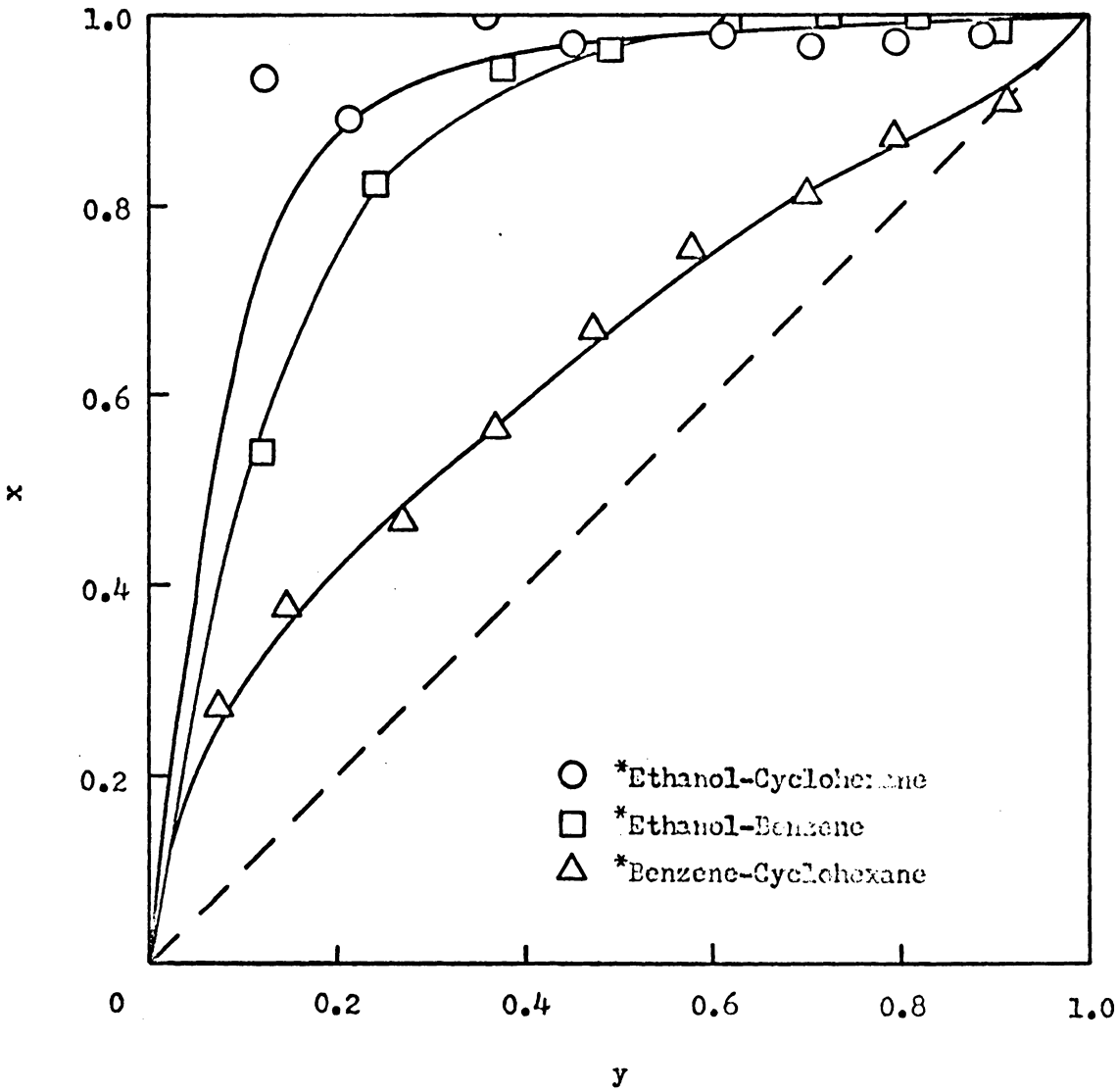

Figure 27. Composition Diagrams for the Three Mixtures on Cab-O-Sil at 20°C

The variation of selectivity with temperature for each mixture on Cab-O-Sil is illustrated in Figures 28-30. For ethanol-cyclohexane mixtures (Figure 28), selectivity follows the trend $40^{\circ}C > 20^{\circ}C > 30^{\circ}C$. The composition diagrams for ethanol-benzene mixtures (Figure 29) indicate that selectivity increases with increasing temperature. For benzene-cyclohexane mixtures (Figure 30), the greatest selectivity is observed at $40^{\circ}C$; selectivities at 20 and $30^{\circ}C$ are almost identical. As was pointed out by Bering, Serpinskii, and Surinova (19), selectivity can either increase or decrease with temperature, depending on the relative magnitudes of the heats of adsorption of the components in the mixture.

The dashed lines in Figures 28-30 represent the $30^{\circ}C$ solution adsorption isotherms obtained by Matayo and Wightman (52). In contrast to adsorption from the vapor phase, no temperature dependence was observed in the solution adsorption isotherms over a temperature range from 25 to $35^{\circ}C$. Comparing the solution isotherms to the $30^{\circ}C$ vapor phase isotherms, it is observed that selectivity is greater from solution than from the vapor phase for ethanol-cyclohexane and benzene-cyclohexane mixtures on Cab-O-Sil. For ethanol-benzene mixtures, selectivity is greater from solution for ethanol mole fractions < 0.5. Comparisons between adsorption from solution and from the vapor phase are extremely rare. Kiselev and Pavlova (53) have found that selectivity is greater from solution for adsorption of benzene-hexane mixtures on silica gel. This is the first reported systematic study of adsorption from the vapor phase and from solution.

Graphon isotherms

The adsorption isotherms for benzene-cyclohexane vapor mixtures onto

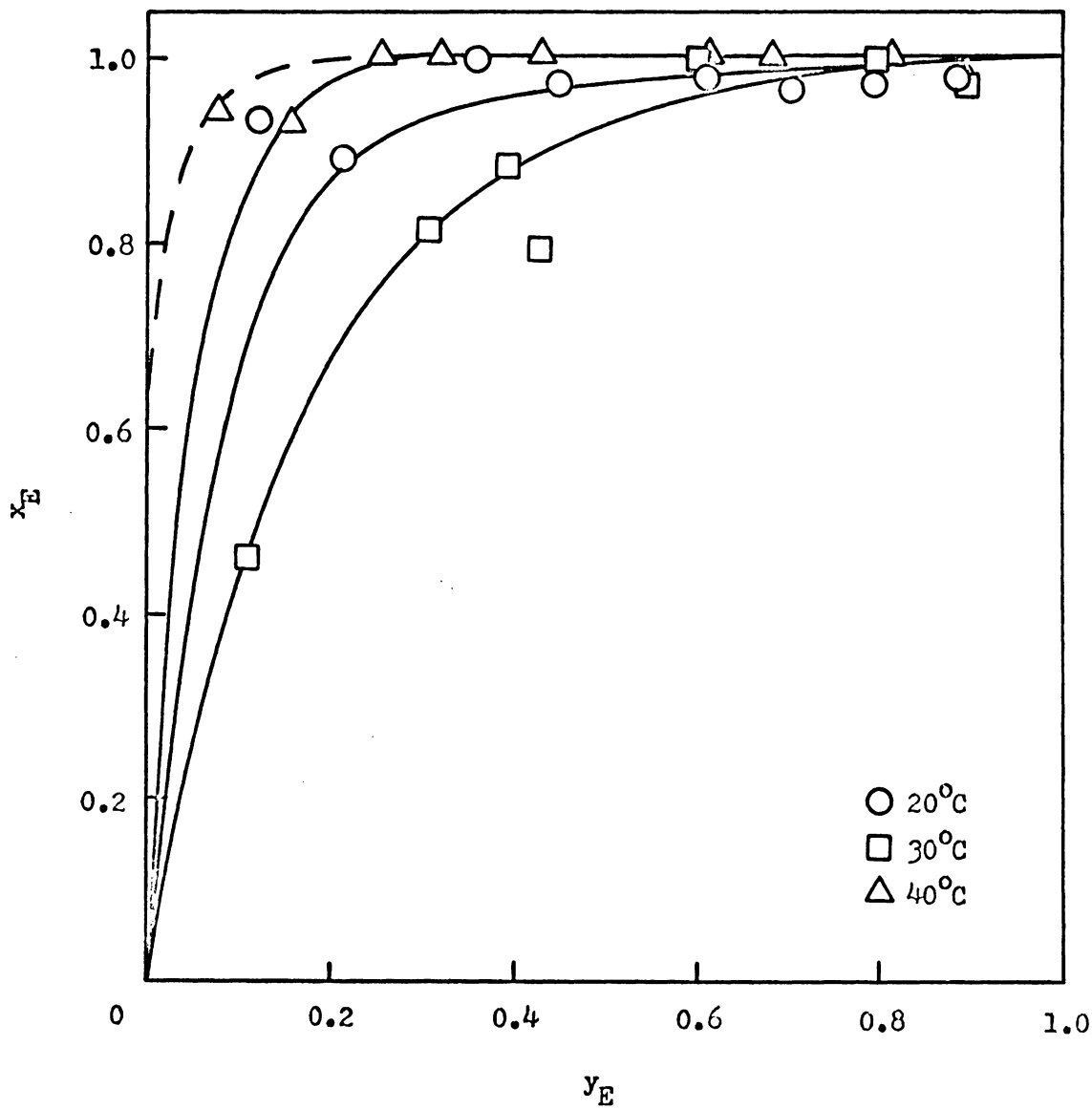

Figure 28. Composition Diagrams for Ethanol-Cyclohexane Mixtures on Cab-O-Sil at 20, 30, and 40°C

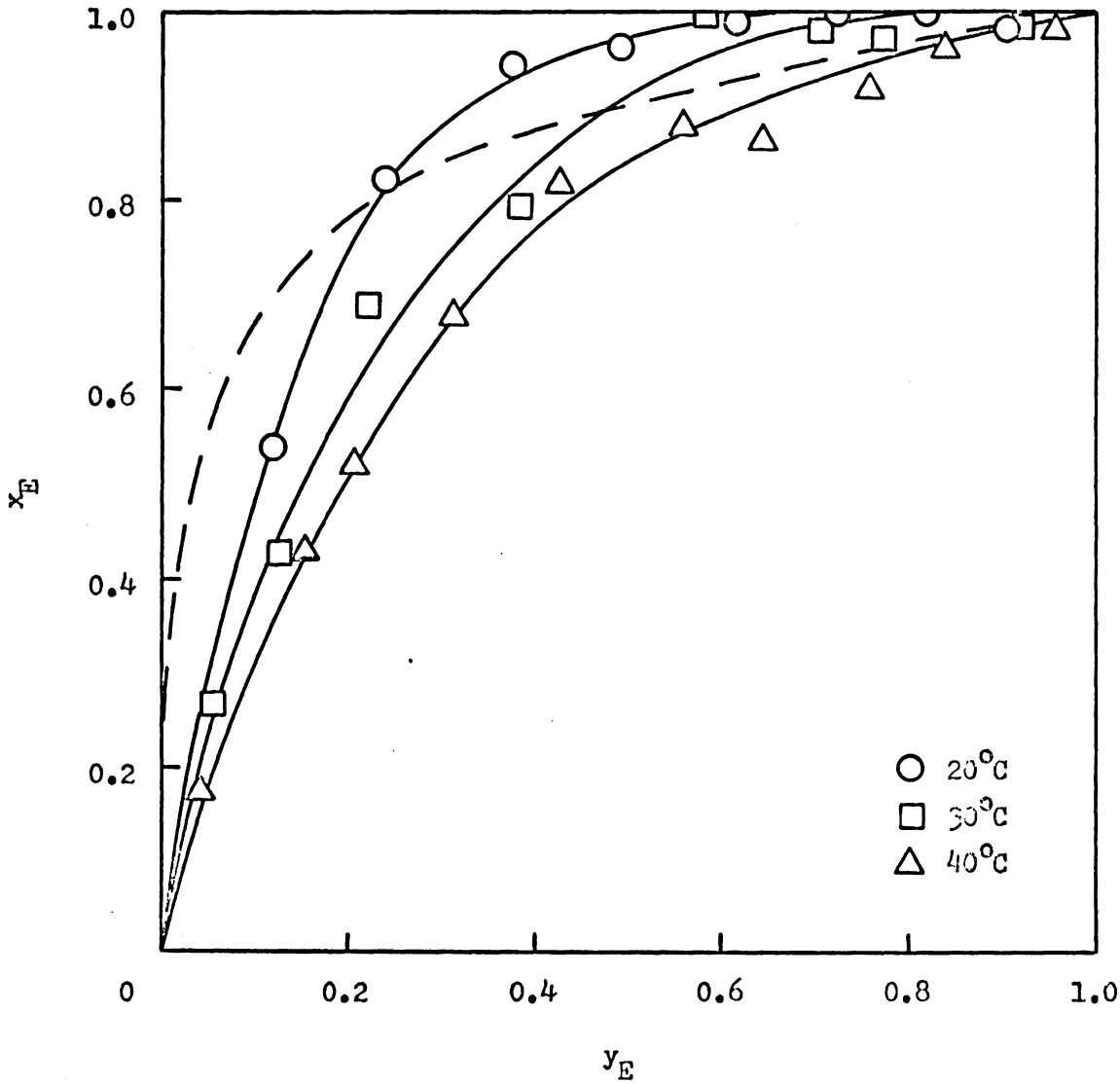

Figure 29. Composition Diagrams for Ethanol-Benzene Mixtures on Cab-O-Sil at 20, 30, and 40°C

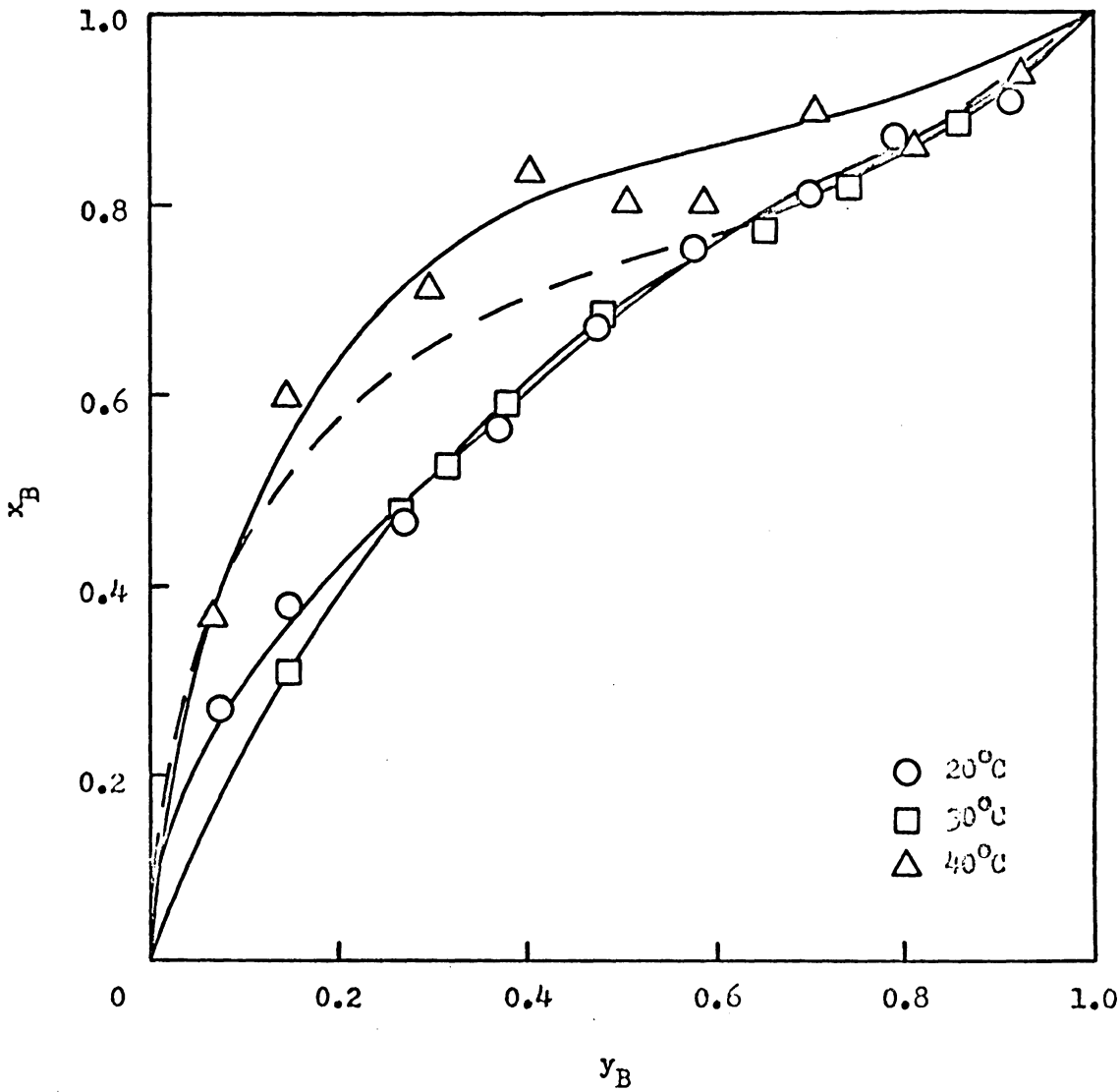

Figure 30. Composition Diagrams for Benzene-Cyclohexane Mixtures on Cab-O-Sil at 20, 30, and 40°C

Graphon at 20, 30, and 40°C are shown in Figures 31-33. Fairly large amounts of both components are adsorbed over the entire vapor composition range. It is apparent that the Graphon surface has little preference for either component. The adsorption behavior of the benzene-cyclohexane mixtures, thus, reflects the similar adsorption behavior observed for these two adsorbates in the pure vapor isotherms. Over most of the vapor composition range adsorption of both components from the mixtures is less than from the pure states. However, adsorption of benzene from the mixtures becomes greater than from the pure state at high benzene mole fractions. Similar behavior is observed for cyclohexane.

The adsorption isotherms at 20, 30, and 40°C for benzene-ethanol vapor mixtures on Graphon are shown in Figures 34-36. The amount of ethanol adsorbed from the mixtures is very small at high benzene mole fractions, becoming extremely large at low benzene mole fractions. For all three isotherms, adsorption of ethanol from the mixtures is generally much less than from the pure state. It is not known whether the slight enhancement in adsorption of ethanol in the 40°C isotherm at high benzene concentrations is significant, since the two curves are within experimental error of each other. The adsorption behavior of benzene is very interesting. At all three temperatures, adsorption of benzene from the mixtures is greater than from the pure state at intermediate to high benzene mole fractions. The range of compositions for which enhancement of benzene adsorption occurs varies with temperature. At lower benzene mole fractions, adsorption of benzene from the mixtures is much less than from the pure state at 20°C, and approaches the amount adsorbed from the pure state as the temperature increases. Moreover, at 20°C the benzene

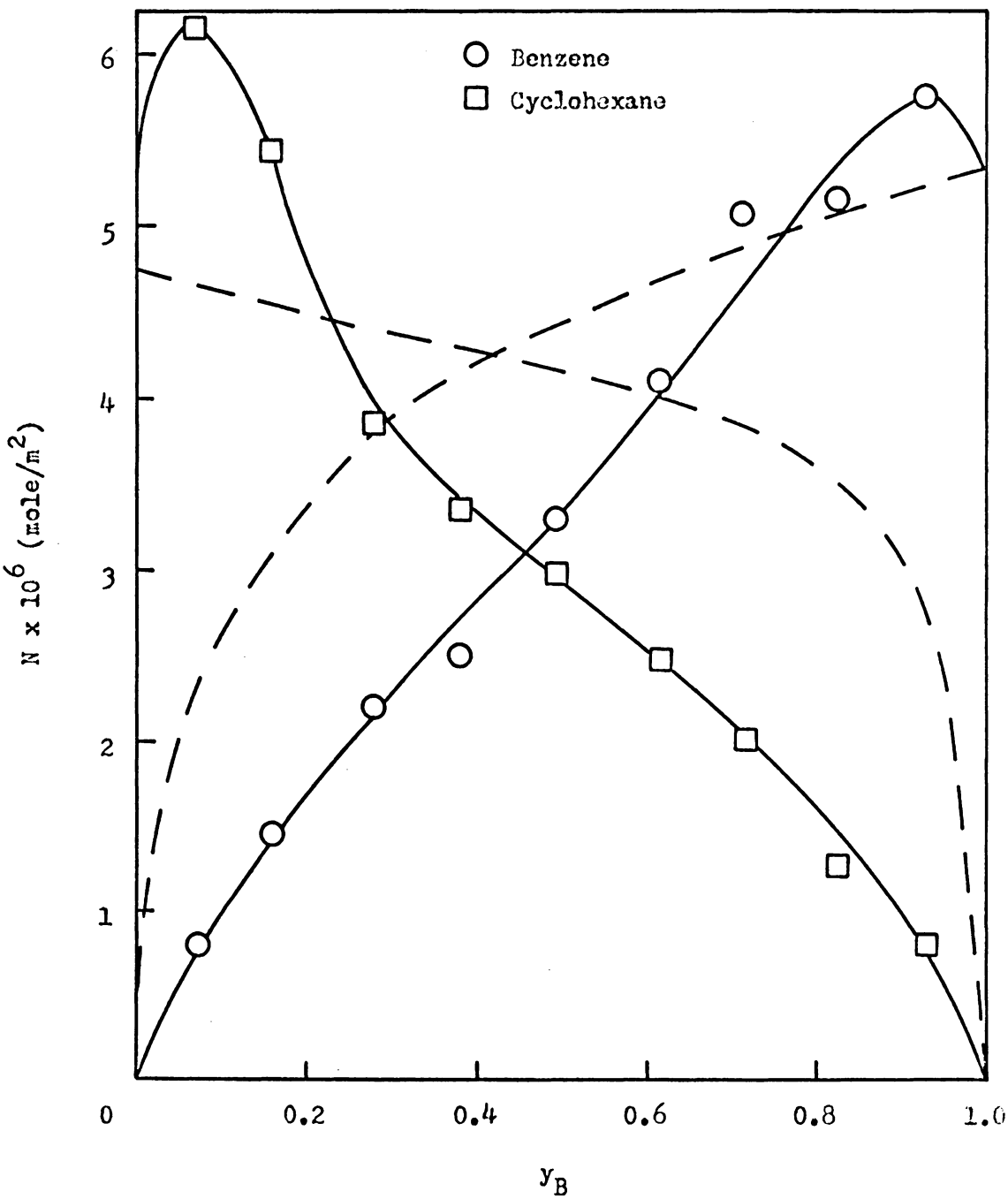

Figure 31. Benzene-Cyclohexane/Graphon Isotherm at 20°C

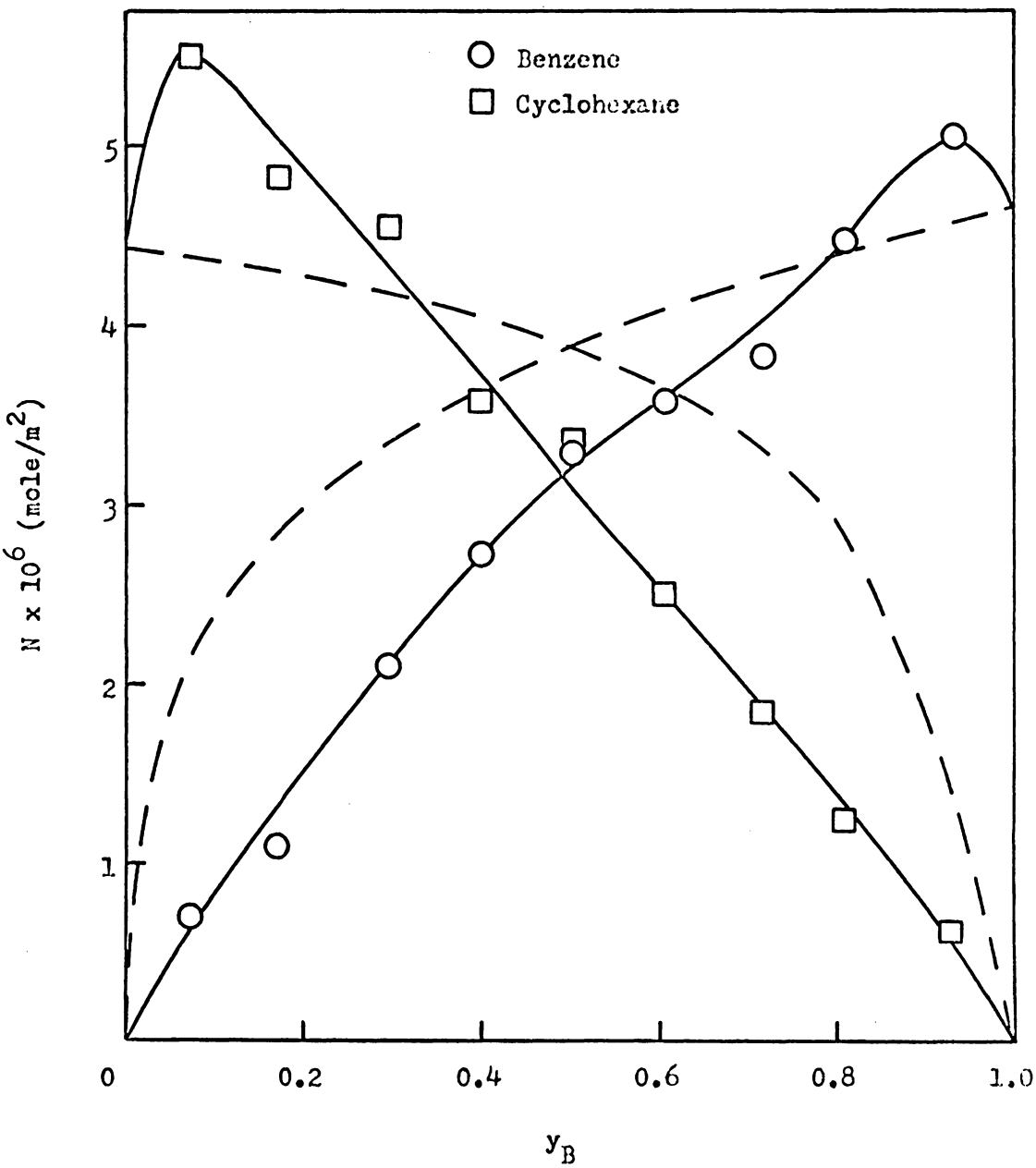

Figure 32. Benzene-Cyclohexane/Graphon Isotherm at 30°C

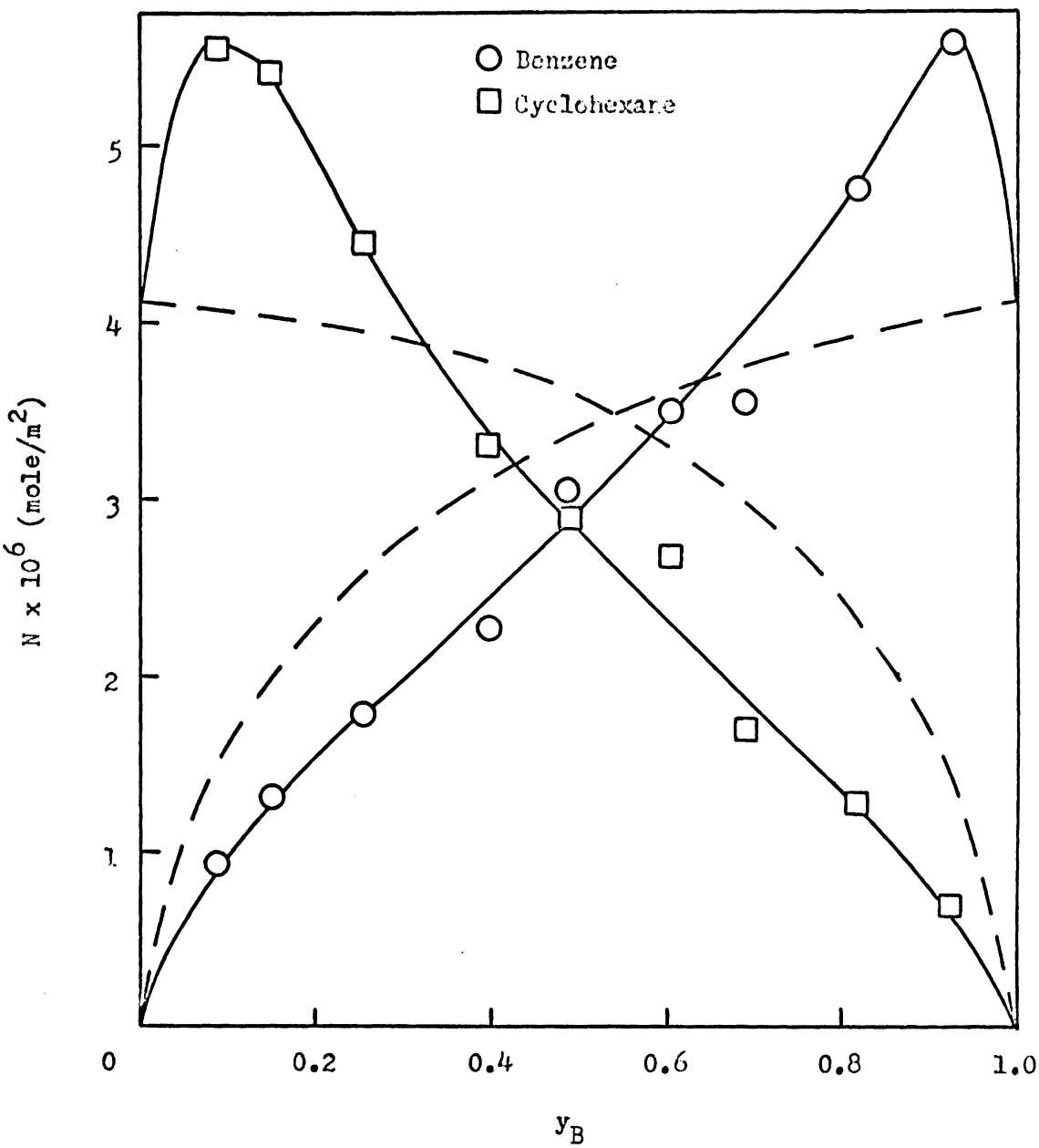

Figure 33. Benzene-Cyclohexane/Graphon Isotherm at 40°C

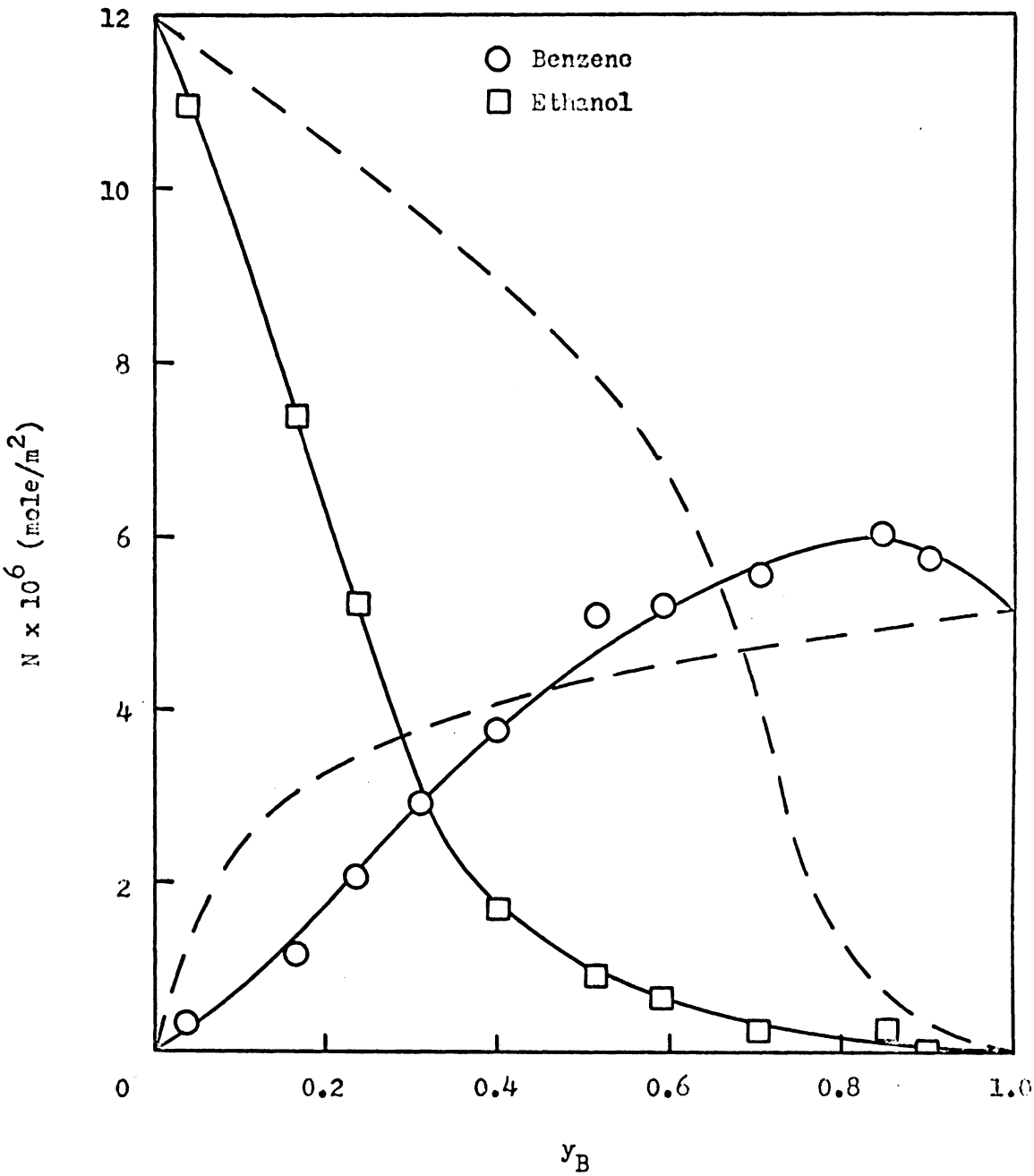

Figure 34. Benzene-Ethanol/Graphon Isotherm at 20°C

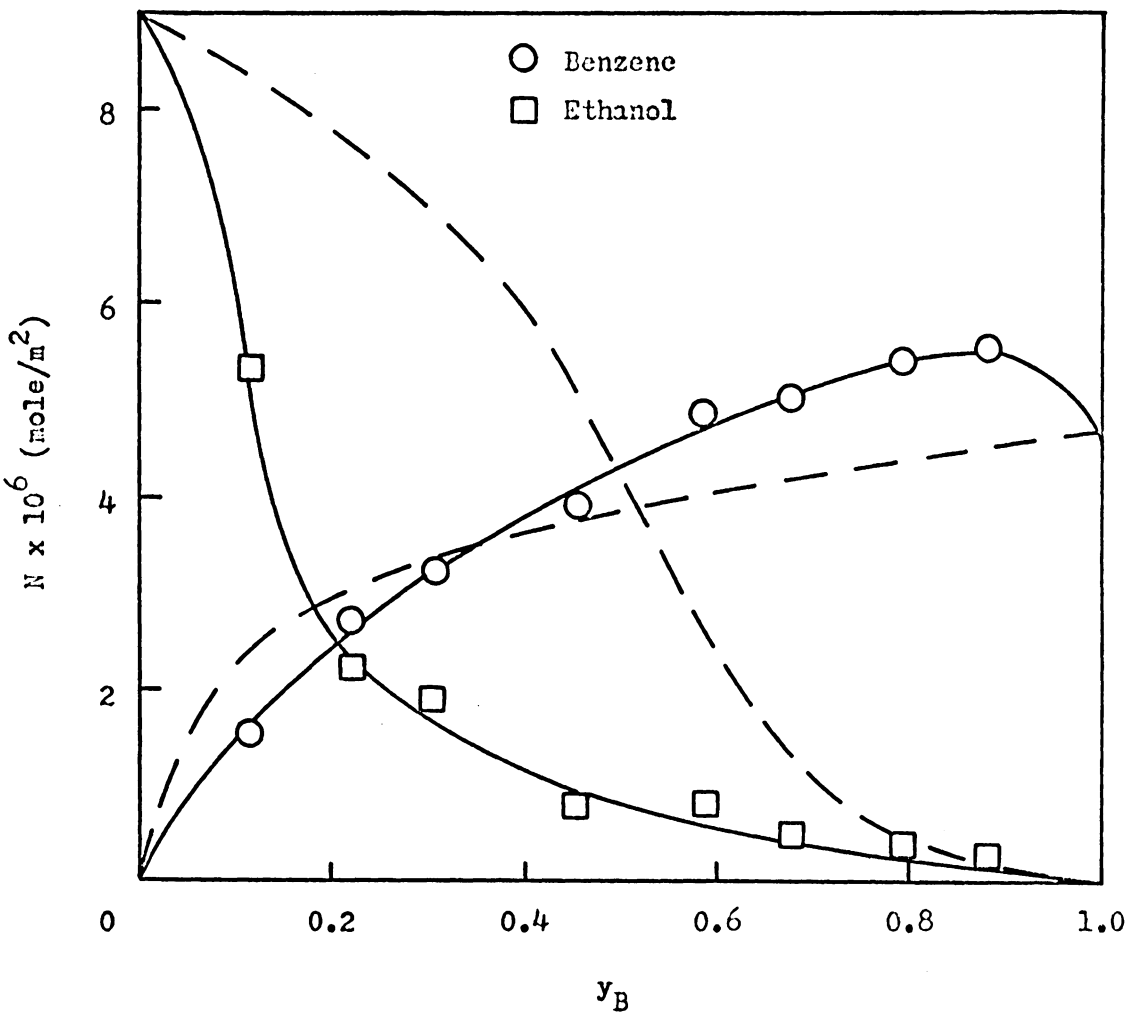

Figure 35. Benzene-Ethanol/Graphon Isotherm at 30°C

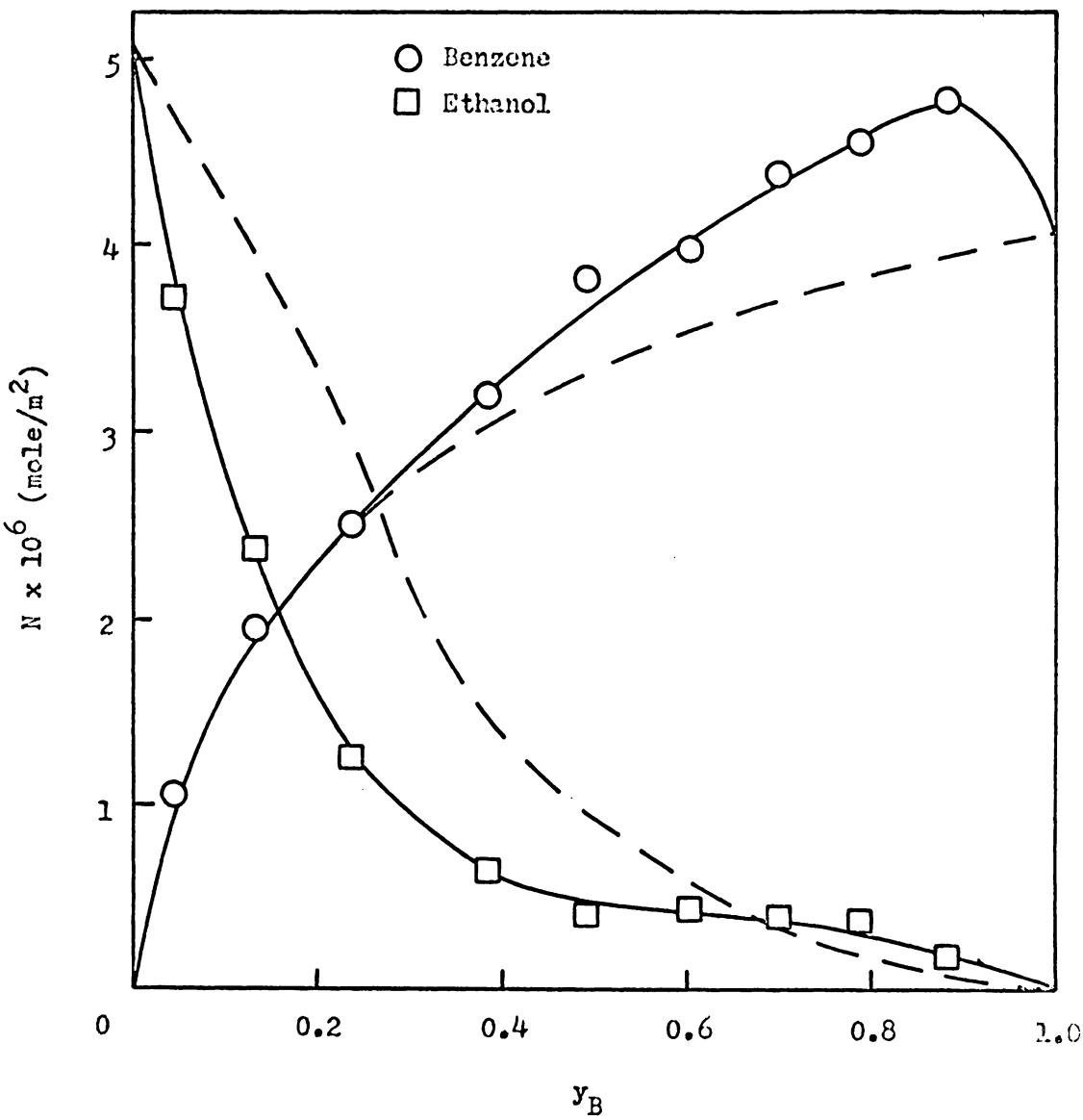

Figure 36. Benzene-Ethanol/Graphon Isotherm at 40°C

isotherm is initially concave, indicating a weak interaction of benzene with the Graphon surface when large amounts of ethanol are present.

The behavior of the heat and entropy of adsorption for pure ethanol on Graphon suggested that hydrogen bonding interactions in the adsorbed phase are important. Assuming that the same types of interactions are occurring in adsorption from the mixtures, the behavior of the benzene-ethanol/Graphon isotherms may be rationalized. The large decrease in the amount of ethanol adsorbed when benzene is present could be due to benzene disrupting the hydrogen bonding interactions between adsorbed ethanol molecules. The enhancement in adsorption of benzene occurring at high benzene mole fractions could be caused by attractions between benzene molecules and the hydroxyl groups of adsorbed ethanol molecules. This type of interaction would tend to diminish with increasing ethanol concentration, since hydrogen bonding interactions between ethanol molecules would be more favorable. Shen and Smith (20) and Kiselev (54) have postulated a strong interaction for the π electrons of benzene with hydroxylated surfaces.

The adsorption isotherms obtained for cyclohexane-ethanol vapor mixtures on Graphon are shown in Figures 37-39. These isotherms are very similar to those obtained for benzene-ethanol mixtures, again reflecting the similar adsorption behavior of benzene and cyclohexane on Graphon. The amount of ethanol adsorbed, small at high cyclohexane mole fractions, becomes extremely large as the concentration of ethanol in the vapor phase increases. Adsorption of ethanol from the mixtures is much less than from the pure state; this behavior is probably due to cyclohexane interrupting the hydrogen bonding interactions between ethanol molecules.

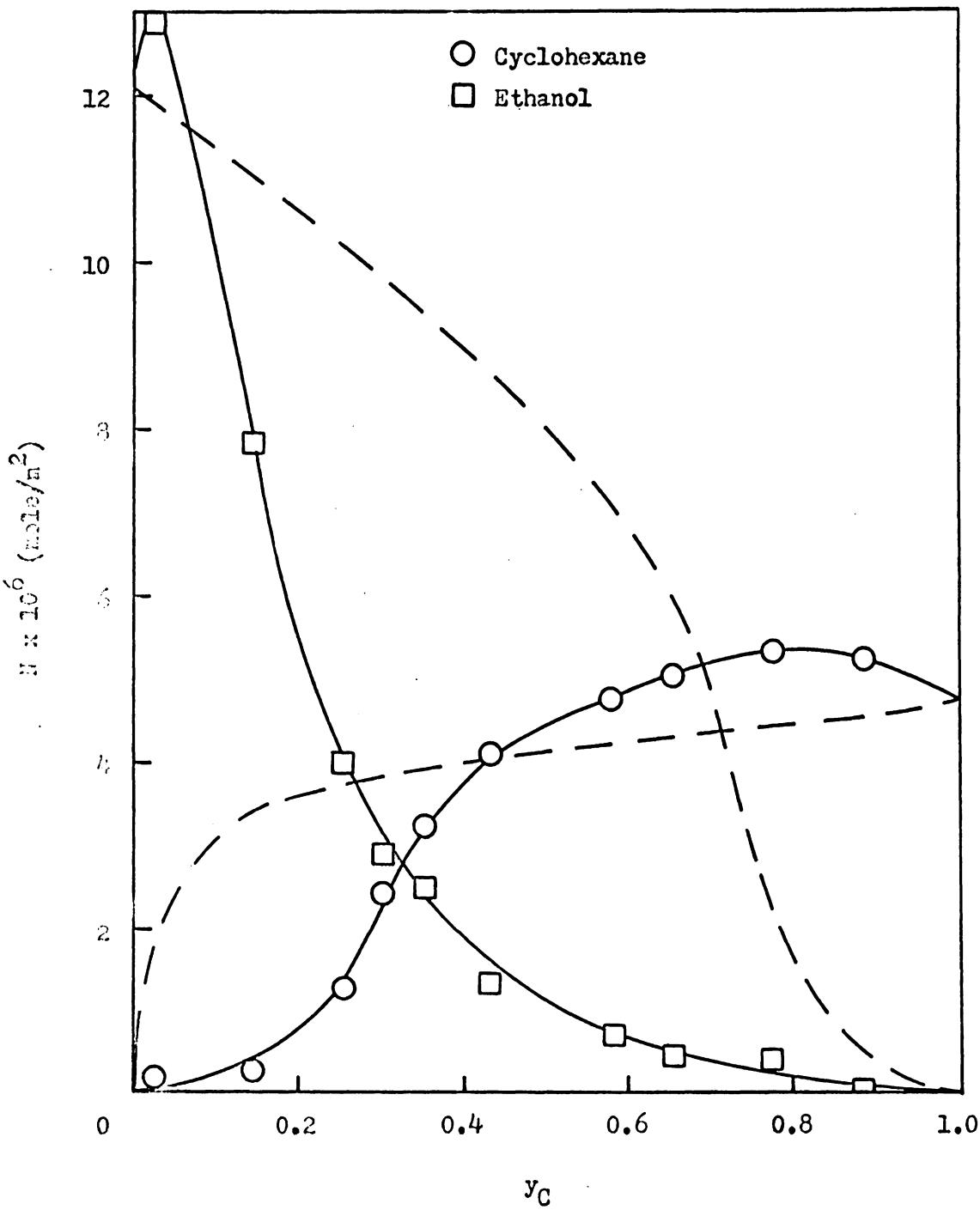

Figure 37. Cyclohexane-Ethanol/Graphon Isotherm at 20°C

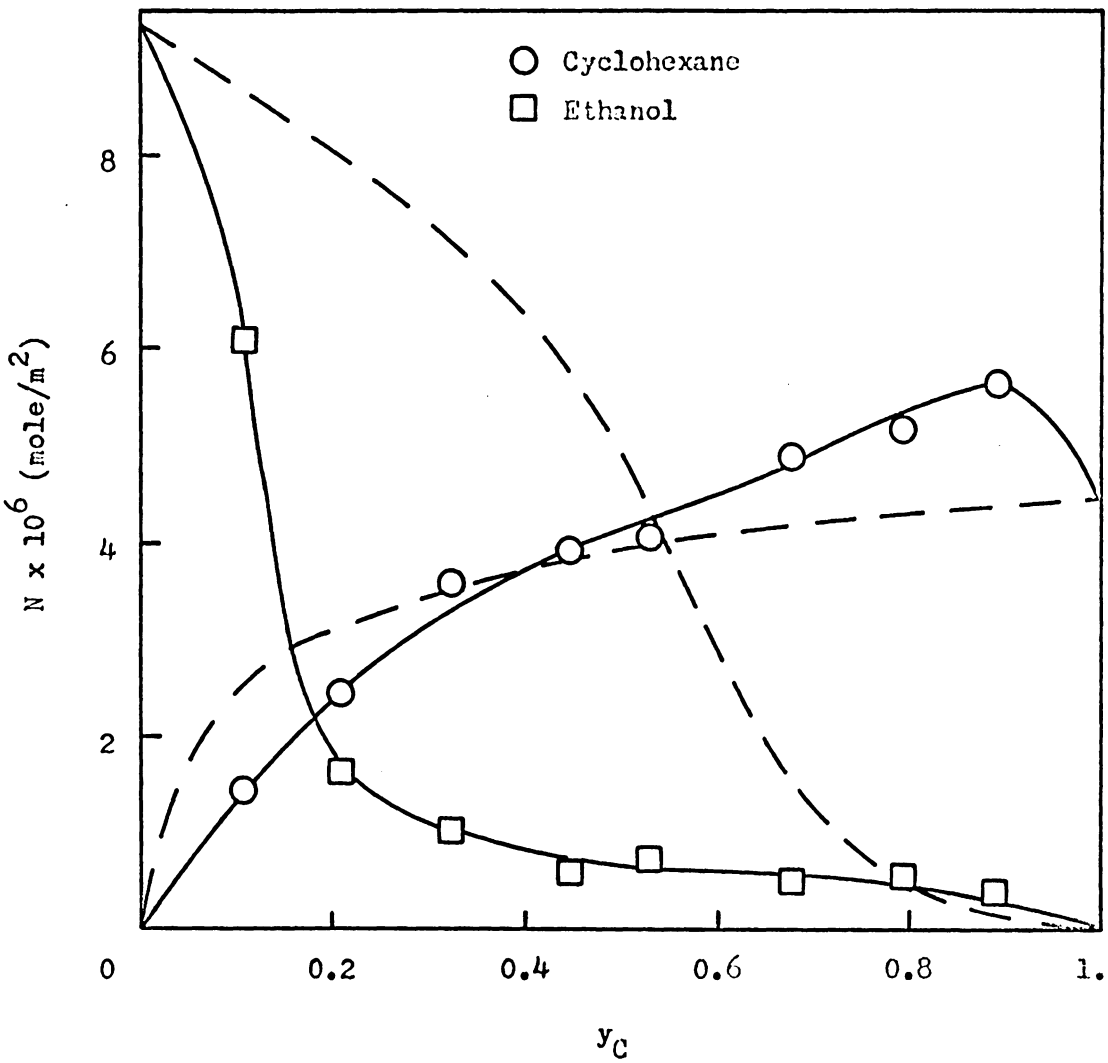

Figure 38. Cyclohexane-Ethanol/Graphon Isotherm at 30°C

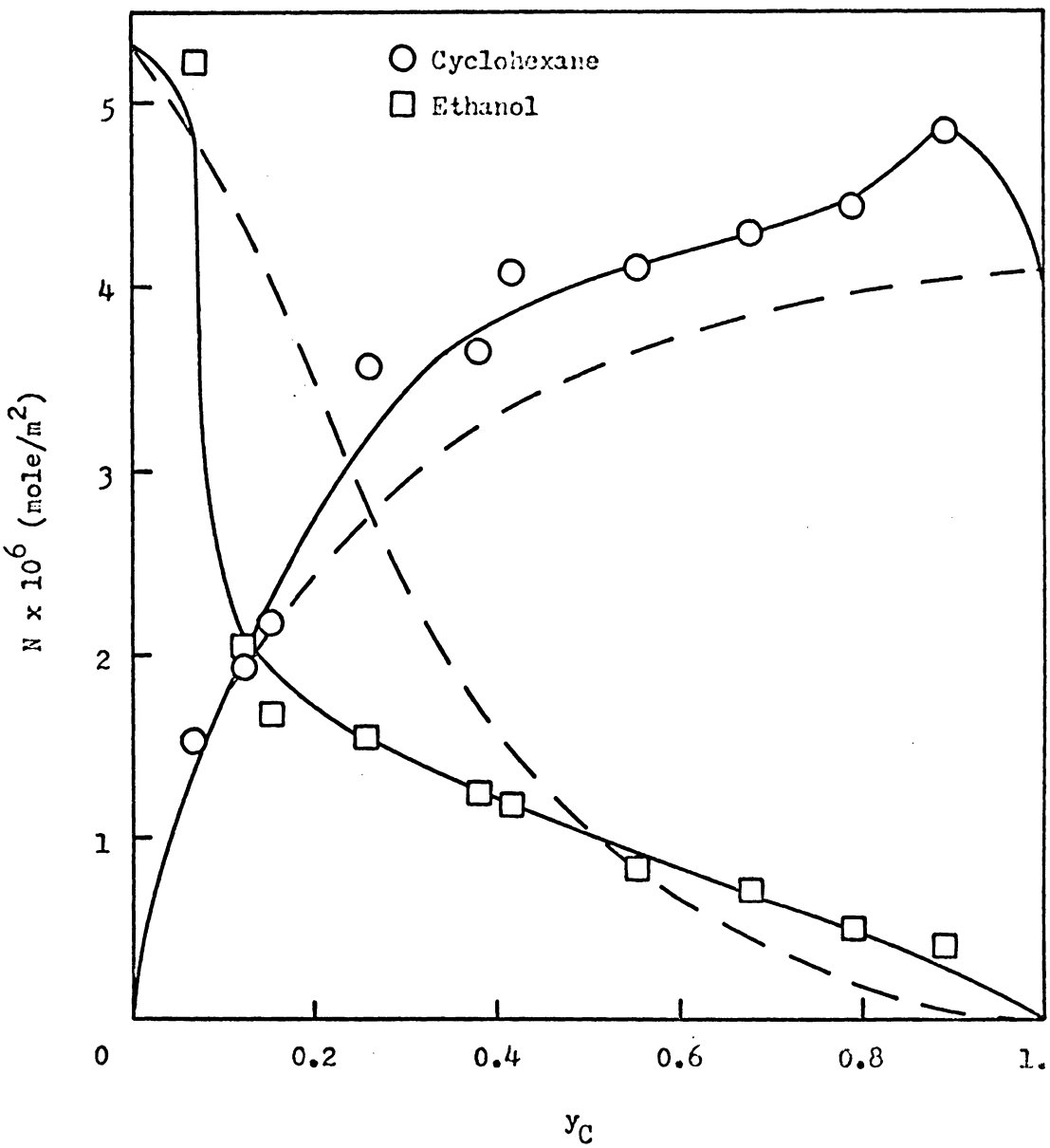

Figure 39. Cyclohexane-Ethanol/Graphon Isotherm at 40°C

Enhancement in adsorption of cyclohexane occurs throughout a good portion of the composition range. Similar to the benzene-ethanol system, the 20°C cyclohexane-ethanol isotherm illustrates that the amount of cyclohexane adsorbed from the mixtures at low cyclohexane mole fractions is much less than from the pure state. Moreover, the cyclohexane isotherm is initially concave at this temperature. As adsorption temperature increases, adsorption of cyclohexane from the mixtures at low cyclohexane mole fractions approaches the amount adsorbed from the pure state.

To illustrate the selectivity occurring in the Graphon systems, the 20°C isotherms for the three mixtures have been replotted in Figure 40 as adsorbed phase composition versus vapor phase composition. The asterisks in Figure 40 denote the component of each mixture whose mole fractions have been plotted. The isotherms would lie along the dashed line if no selective adsorption were occurring. The most striking feature of these composition diagrams is that an adsorption azeotrope occurs for each mixture. For cyclohexane-ethanol/Graphon, a very slight selective adsorption of ethanol occurs for cyclohexane mole fractions < 0.25, whereas a pronounced selective adsorption of cyclohexane occurs at higher mole fractions. For benzene-ethanol/Graphon, the adsorption azeotrope occurs at a benzene mole fraction of 0.2. The selectivities observed for the cyclohexane-ethanol and benzene-ethanol mixtures are almost identical, reflecting the similar adsorption behavior of benzene and cyclohexane on Graphon. Almost no selectivity is observed for benzene-cyclohexane mixtures on Graphon. A slight selective adsorption of benzene occurs at benzene mole fractions < 0.6; at higher mole

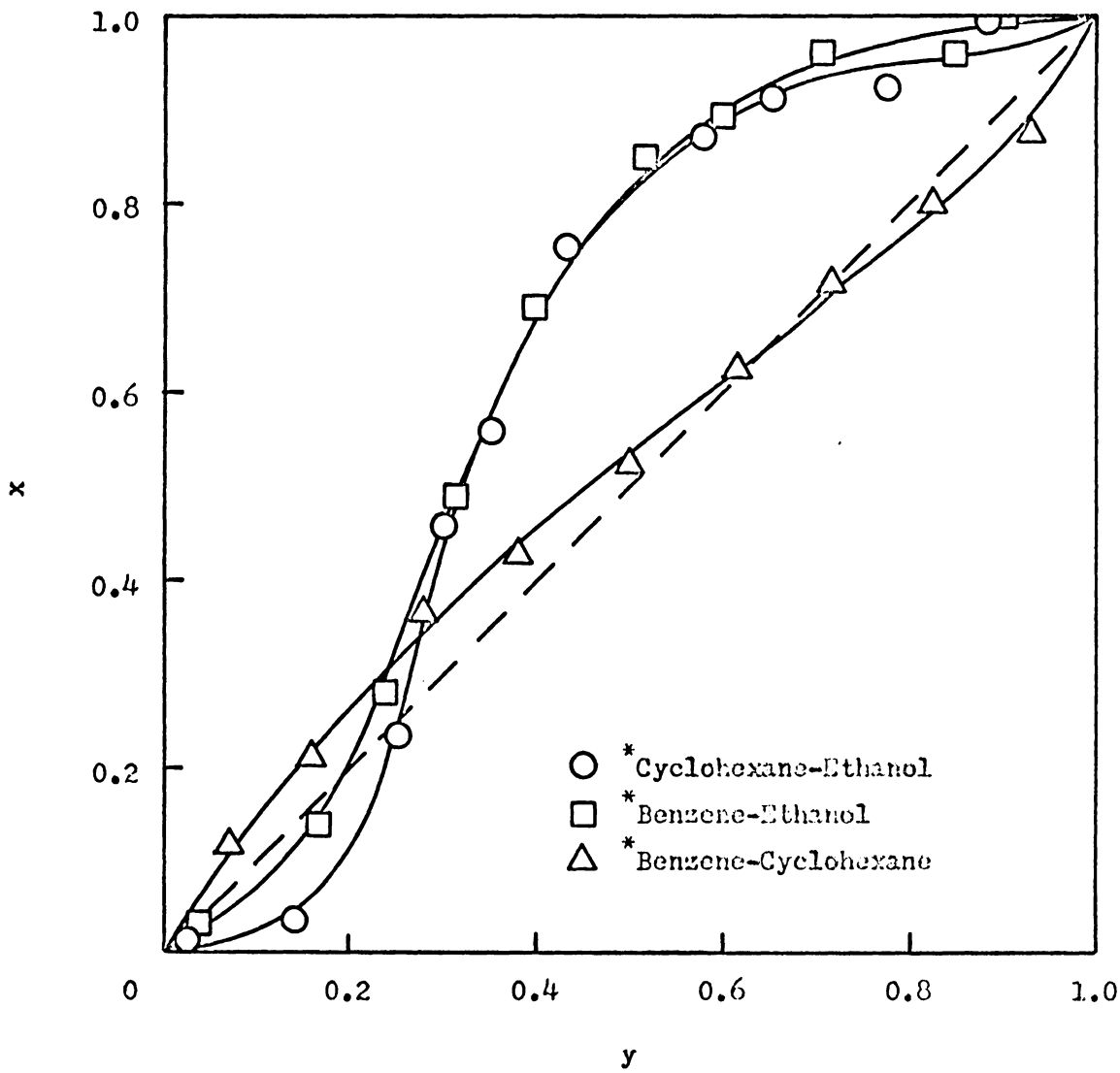

Figure 40. Composition Diagrams for the Three Mixtures on Graphon at 20°C

fractions cyclohexane is selectively adsorbed. This result is in accord with observations made by Lewis et al. (4). For mixtures whose components have similar vapor pressures but different degrees of unsaturation, carbon surfaces show little preference for either component.

Figure 41 compares the composition diagrams for benzene-cyclohexane mixtures on Graphon at 20, 30, and 40°C. An adsorption azeotrope occurs in all three isotherms; the azeotropic composition is different for each temperature. The selectivity does not vary greatly with temperature. The dashed line in Figure 41 represents the 30°C solution adsorption isotherm obtained by Matayo and Wightman (52). No azeotrope is observed in the solution isotherm; selective adsorption of benzene occurs at all solution compositions.

The composition diagrams at 20, 30, and 40°C for benzene-ethanol mixtures on Graphon are shown in Figure 42. No adsorption azeotropes occur in the 30 and 40°C isotherms, and selective adsorption of benzene occurs over the entire composition range. Selectivity generally increases with decreasing temperature. The 30°C solution adsorption isotherm is similar to the corresponding binary vapor adsorption isotherm at low benzene mole fractions. At benzene mole fractions > 0.2, selectivity is greater from solution than from the vapor phase.

The composition diagrams for cyclohexane-ethanol mixtures on Graphon at the three temperatures are shown in Figure 43. Similar to the benzene-ethanol/Graphon system, no adsorption azeotropes occur at 30 and 40°C. At these two temperatures selective adsorption of cyclohexane is observed over the entire composition range. The temperature dependence of the selectivity varies greatly with composition. The 30°C solution

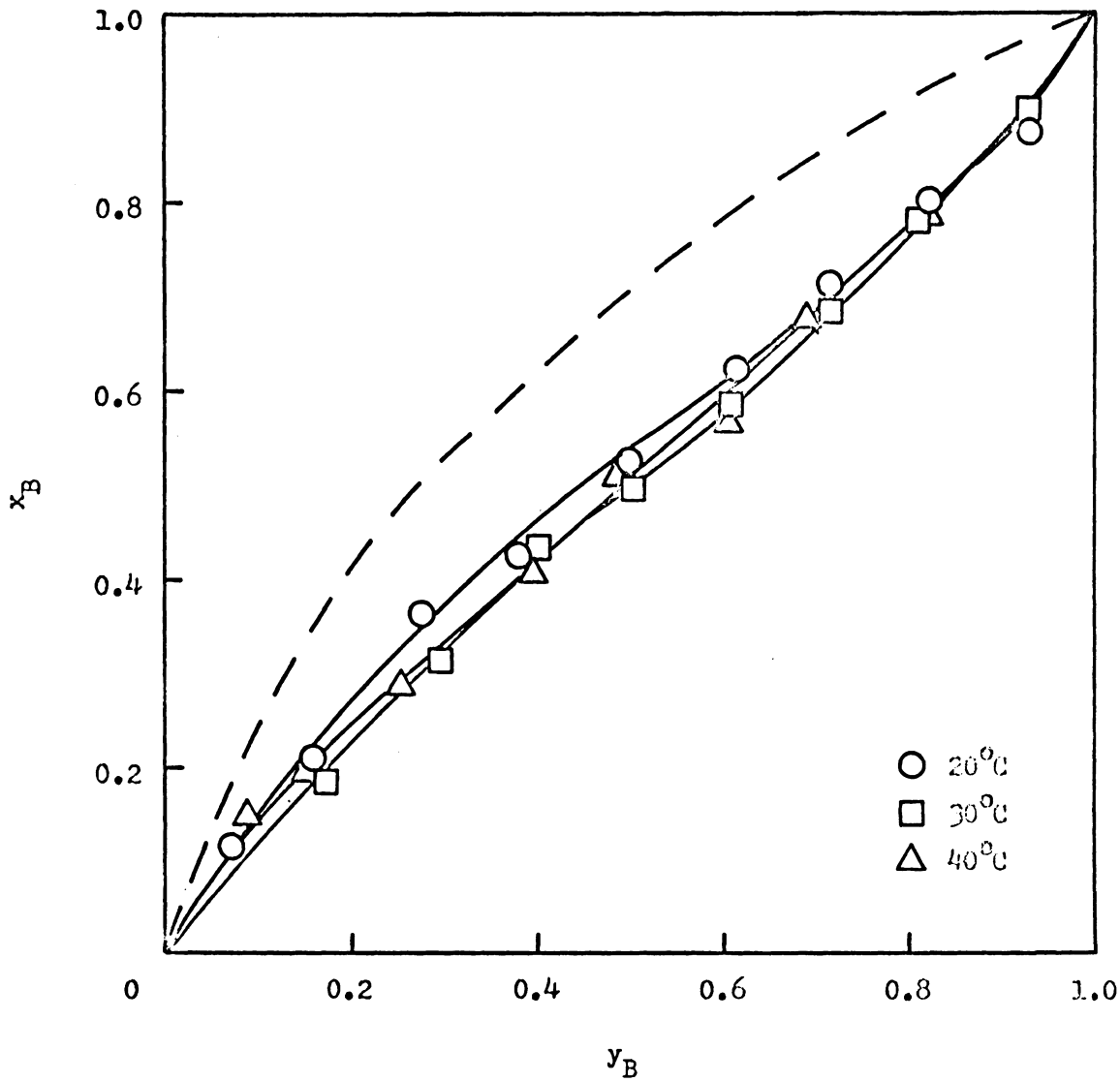

Figure 41. Composition Diagrams for Benzene-Cyclohexane Mixtures on Graphon at 20, 30, and 40°C

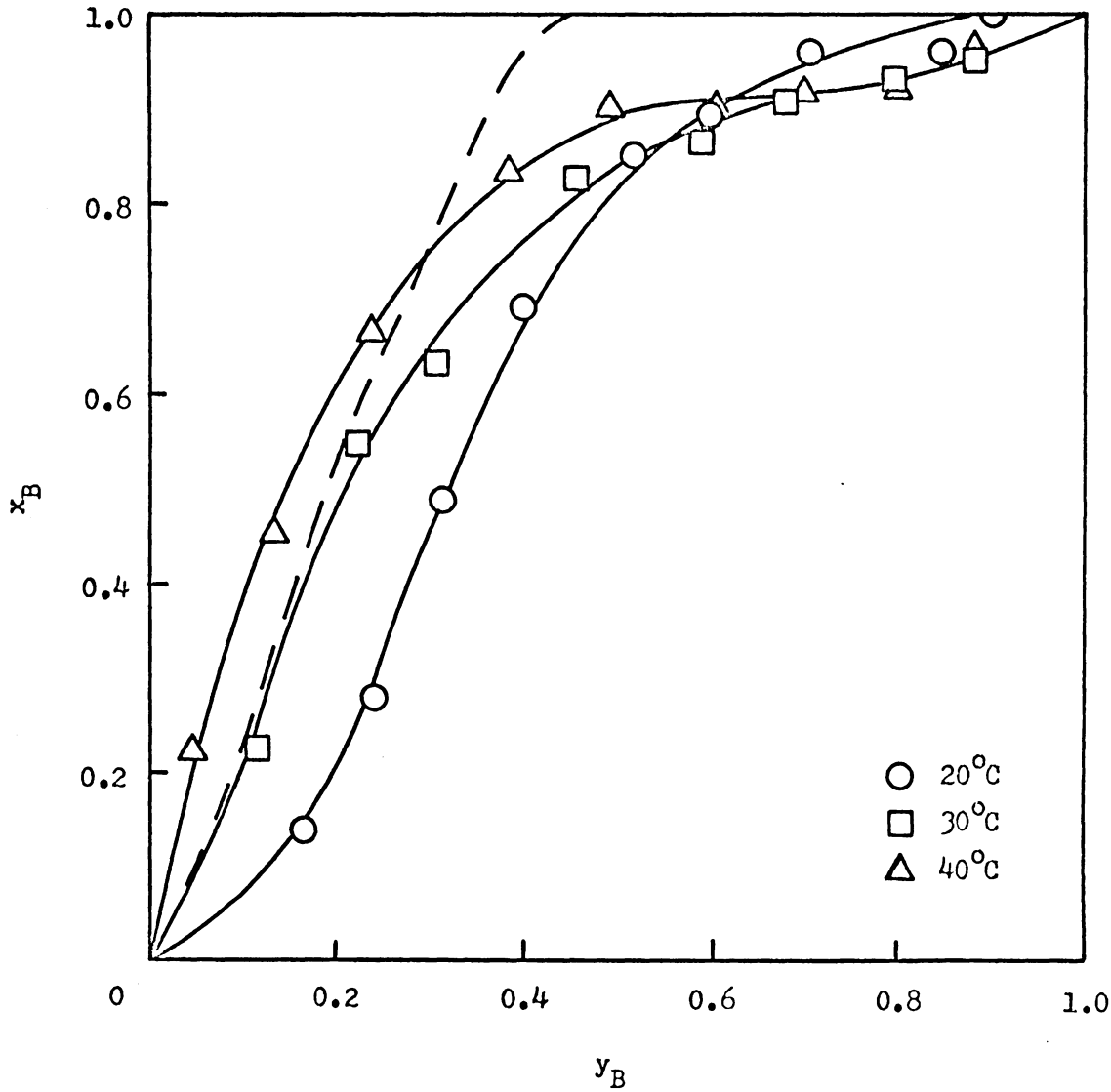

Figure 42. Composition Diagrams for Benzene-Ethanol Mixtures on Graphon at 20, 30, and 40°C

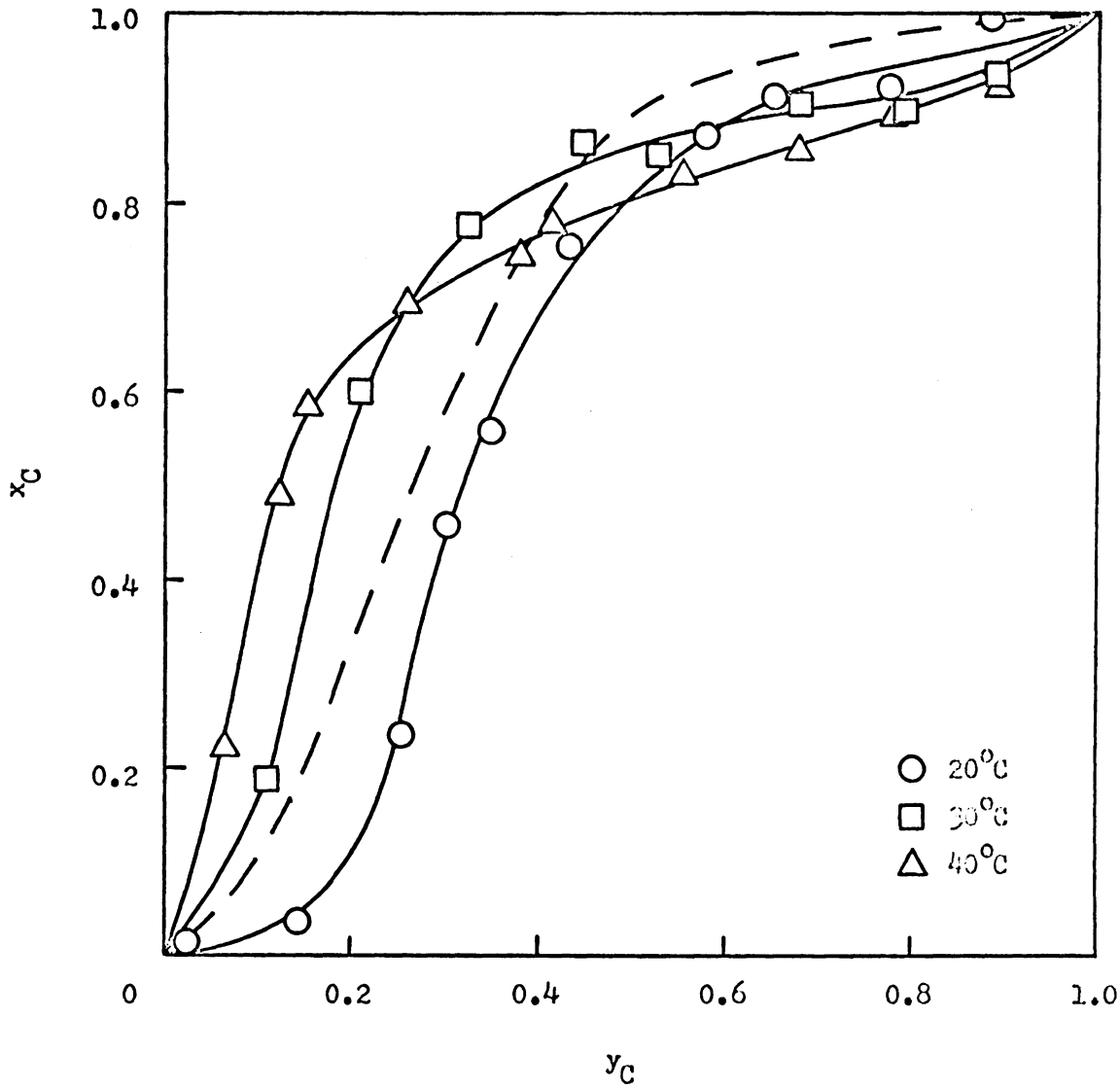

Figure 43. Composition Diagrams for Cyclohexane-Ethanol Mixtures on Graphon at 20, 30, and 40°C

adsorption isotherm falls below the corresponding binary vapor isotherm for cyclohexane mole fractions < 0.4. At higher mole fractions, selectivity from solution is slightly greater than from the vapor phase. A close examination of Figure 43 reveals that an adsorption azeotrope may exist in the solution isotherm at very low cyclohexane mole fractions.

Figure 41 illustrates that while very little selective adsorption of either component occurs from benzene-cyclohexane vapor mixtures on Graphon, there is a pronounced selective adsorption of benzene from solution. Comparison of Figures 42 and 43 shows that the selectivities in the 30°C benzene-ethanol and cyclohexane-ethanol vapor phase isotherms are very similar. In contrast, selective adsorption from solution is much higher for benzene-ethanol mixtures than for cyclohexane-ethanol mixtures. Figure 42 indicates than in adsorption from solution, benzene excludes ethanol from the adsorbed phase at benzene mole fractions > 0.4. The strong interaction of benzene with Graphon in adsorption from solution might be due to adsorption of benzene into surface pores. This type of phenomenon would also account for the very slow equilibration of benzene vapor with Graphon at high pressures, as was pointed out in the section on pure vapor adsorption.

For all of the Cab-O-Sil and Graphon systems studied, it has been observed that the selectivity in adsorption from solution is generally higher than from the vapor phase. Since all three binary solutions show positive deviations from Raoult's Law, there would be a driving force for the two components of a given solution to separate from each other upon introduction of a solid surface. No such driving force would be present in adsorption from binary vapor mixtures. At the low pressures

studied, intermolecular interactions between components in the vapor phase would be negligible.

Models

Since data for adsorption of binary vapor mixtures onto solids are scarce, the various models proposed for calculating binary vapor adsorption isotherms have not been adequately tested. The ideal adsorbed solution model (27, 28) has been fairly successful in predicting binary vapor adsorption equilibria from pure component adsorption data. The success of this model may be attributed to the fact that it was rigorously derived from thermodynamics with a minimum number of assumptions. This section will, therefore, be primarily devoted to comparisons between the experimental binary vapor adsorption isotherms and the isotherms calculated from the experimental pure vapor isotherms using the ideal adsorbed solution model. Such comparisons are also useful in interpreting some of the binary vapor adsorption data that was presented in the previous section.

The models proposed by Kidnay and Myers (31) and by Fernbacher and Wenzel (32) are simplifications of the ideal adsorbed solution model. They are much easier to use since spreading pressure curves for the pure components need not be calculated. But these methods are valid only if the pure component isotherms meet certain requirements, as was discussed in Section II. None of the pure vapor isotherms obtained in this work fulfilled the conditions necessary for the Kidnay and Myers model. The requirements for the Fernbacher and Wenzel model were fulfilled only for adsorption of benzene and cyclohexane on Graphon. Since spreading

pressure curves for benzene and cyclohexane on Graphon were needed for other calculations, the benzene-cyclohexane/Graphon isotherms were calculated from the ideal adsorbed solution model. Use of the Fernbacher and Wenzel model on this system has not been included, since it gives virtually the same results as the ideal adsorbed solution model.

Use of the ideal adsorbed solution model first requires knowledge of spreading pressure as a function of equilibrium gas phase pressure for each of the components in the mixture. Spreading pressure curves were obtained from the pure vapor isotherms by use of the Gibbs adsorption equation:

$$\frac{\pi}{RT} = \int_0^P \frac{N}{P}\, dP \qquad (15)$$

Except at very low pressures, the integration was performed numerically using the Trapezoidal Rule. Since the integrand in Equation (15) is undefined when P = 0, it was necessary to use an analytic equation to integrate in the low pressure region. The simplest expression is Henry's Law:

$$N = kP \qquad (30)$$

The necessity of using Henry's Law was the major source of error in the spreading pressure curves, since the integrand in Equation (15) becomes very large as P approaches zero. The validity of the approximation could not be ascertained because data was not measured at low pressures. The calculated spreading pressures for all of the pure vapor isotherms are tabulated in Appendix IV.

The spreading pressure curves obtained for ethanol, benzene, and cyclohexane on Cab-O-Sil at 20°C are shown in Figure 44. The 30 and 40°C spreading pressure curves are similar in appearance. According to the ideal adsorbed solution model, the composition, x_1, of a mixture having a particular value of spreading pressure is calculated from the pressures of the pure components having this same spreading pressure:

$$x_1 = \frac{P-P_2^*}{P_1^*-P_2^*} \qquad (16b)$$

Examination of Figure 44 shows that this procedure cannot be used for calculating adsorption of ethanol-cyclohexane or ethanol-benzene vapor mixtures onto Cab-O-Sil. For example, for ethanol-benzene mixtures on Cab-O-Sil at a total pressure of 30 torr, the spreading pressures of interest lie between the spreading pressure of benzene at 30 torr ($\pi/RT = 5 \times 10^{-6}$ mole/m^2) and the spreading pressure of ethanol at 30 torr ($\pi/RT = 20 \times 10^{-6}$ mole/m^2). Figure 44 illustrates that for $\pi/RT > 11 \times 10^{-6}$ mole/m^2, P_B^* is not defined. The modification of the ideal adsorbed solution model developed by Sircar and Myers (22) applies to such cases, and was, therefore, used to calculate the adsorption isotherms for ethanol-benzene and ethanol-cyclohexane vapor mixtures on Cab-O-Sil.

In the Sircar and Myers model, the isotherms are calculated from the following equations:

$$\frac{1}{P} = \frac{y_1}{P_1^*} \exp\left[\frac{\pi_r(\pi_1^s-\pi^s)}{N_1^* RT}\right] + \frac{y_2}{P_2^*} \exp\left[\frac{\pi_r(\pi_2^s-\pi^s)}{N_2^* RT}\right] \qquad (19)$$

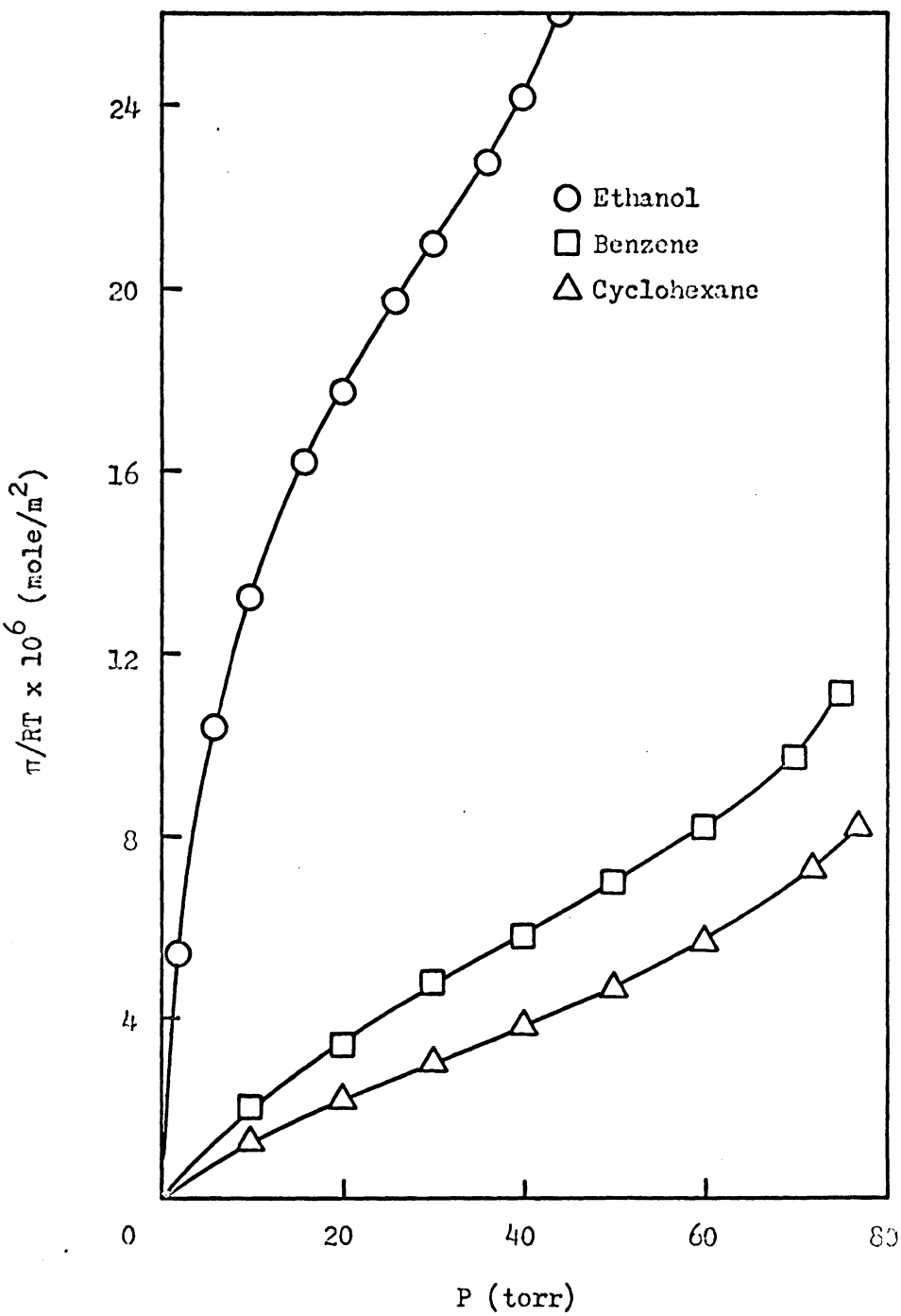

Figure 44. Spreading Pressure Curves for the Pure Adsorbates on Cab-O-Sil at 20°C

$$x_1 = \frac{Py_1}{P_1^*} \exp\left[\frac{\pi_r(\pi_1^s - \pi^s)}{N_1^* RT}\right] \qquad (20)$$

where

$$\pi_r = \frac{\pi}{\pi^s} = \frac{\pi_i^*}{\pi_i^s} \qquad (21)$$

The spreading pressure of pure component i at saturation, π_i^s, was obtained by integrating Equation (15) to saturation vapor pressure. The reduced spreading pressure, π_r, was then calculated from Equation (21). N_i^*, the amount of pure component i adsorbed at P_i^*, was obtained from the pure vapor adsorption isotherms. The spreading pressure of the mixture at saturation, π^s, which is a function of vapor phase composition y_i, was obtained from:

$$\frac{\pi^s - \pi_2^s}{RT} = \int_0^{a_1} \frac{n_1}{(1-x_1')a_1} da_1 \qquad (22)$$

where n_1 is the number of moles of component 1 adsorbed from solution, x_1' is the composition of the solution, and a_1 is the activity of the solution having composition x_1'. The solution adsorption data obtained by Matayo and Wightman (52) for ethanol-cyclohexane and ethanol-benzene mixtures on Cab-O-Sil at 30°C were used in Equation (22). Since no temperature dependence was observed for the solution adsorption isotherms, the 30°C data was used to calculate the binary vapor isotherms at all three temperatures. Activities of ethanol-cyclohexane solutions at 20

and 30°C and of ethanol-benzene solutions at 40°C are available in the literature (55). The activities of ethanol-cyclohexane solutions at 40°C were calculated from the 20 and 30°C activities by assuming that the heat of mixing is constant over the temperature range involved; that is, ln a_i versus 1/T is linear. Similarly, activities for ethanol-benzene solutions at 20 and 30°C were calculated from experimental activities at 40 and 50°C. The integration in Equation (22) was then performed numerically using the Trapezoidal Rule. Values of π^S as a function of y_i for each system are given in Appendix IV.

Since the experimental binary vapor adsorption isotherms were measured at constant total pressure, for each vapor phase composition y_i it was necessary to solve Equation (19) for π_r by successive approximations. These values of π_r, along with the corresponding values of P_i^* and N_i^*, were then used to calculate the adsorbed phase compositions x_i from Equation (20).

The isotherms calculated from the Sircar and Myers model for ethanol-cyclohexane and ethanol-benzene vapor mixtures on Cab-O-Sil are shown in Figures 45-50. Agreement between experimental and calculated isotherms is good for ethanol-cyclohexane mixtures at 20 and 40°C, and for ethanol-benzene mixtures at 20°C. For the other three isotherms, agreement is poor. It is interesting that the isotherms which show poor agreement with the model were all obtained on the first Cab-O-Sil sample. Since it is unreasonable for the model to be accurate at some temperatures and not at others, the comparisons imply that the surfaces of the two Cab-O-Sil samples used in the adsorption measurements were different. It is possible that chemisorption of ethanol occurred on the first Cab-O-Sil

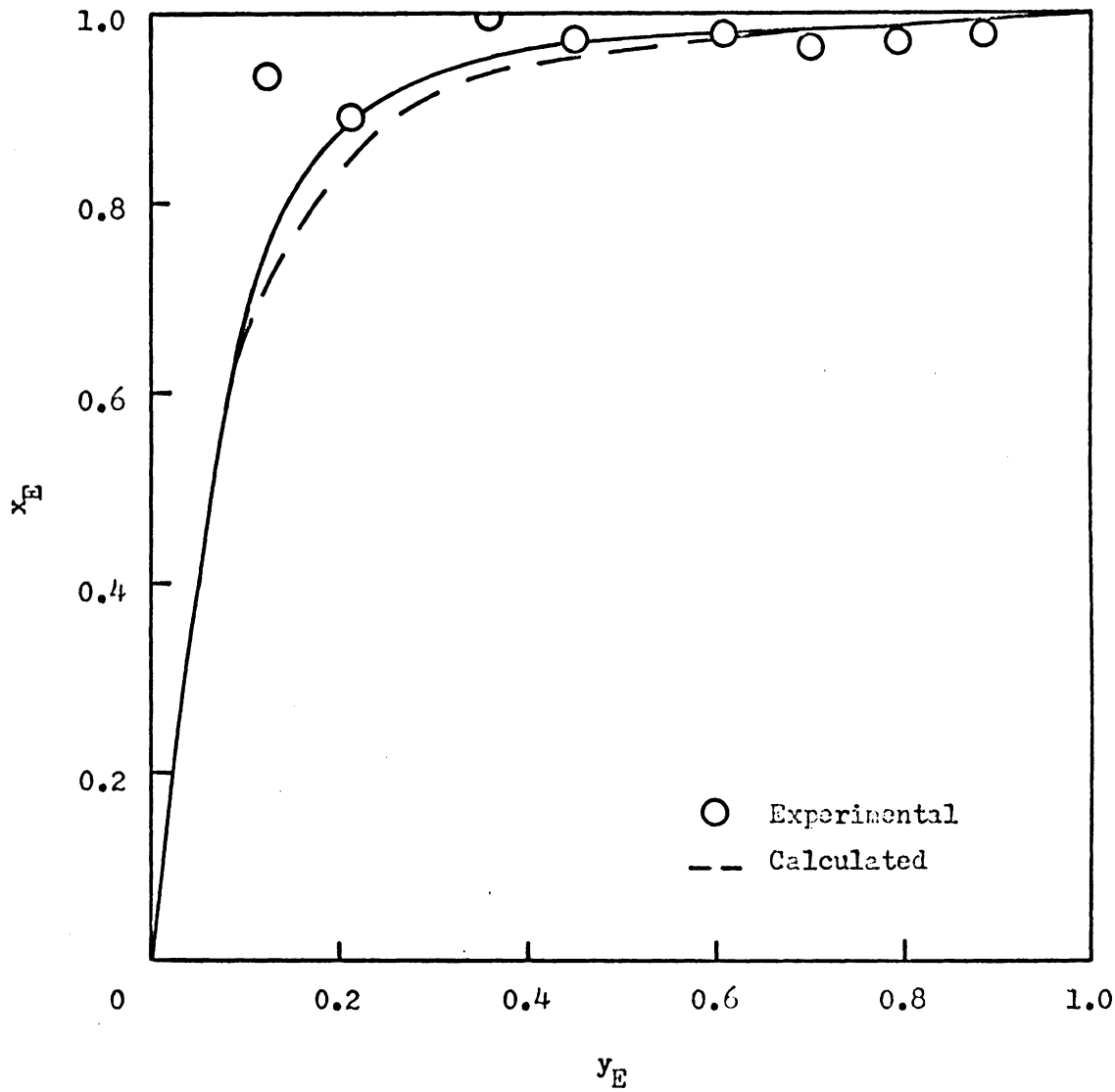

Figure 45. Calculated Ethanol-Cyclohexane/Cab-O-Sil Isotherm at 20°C

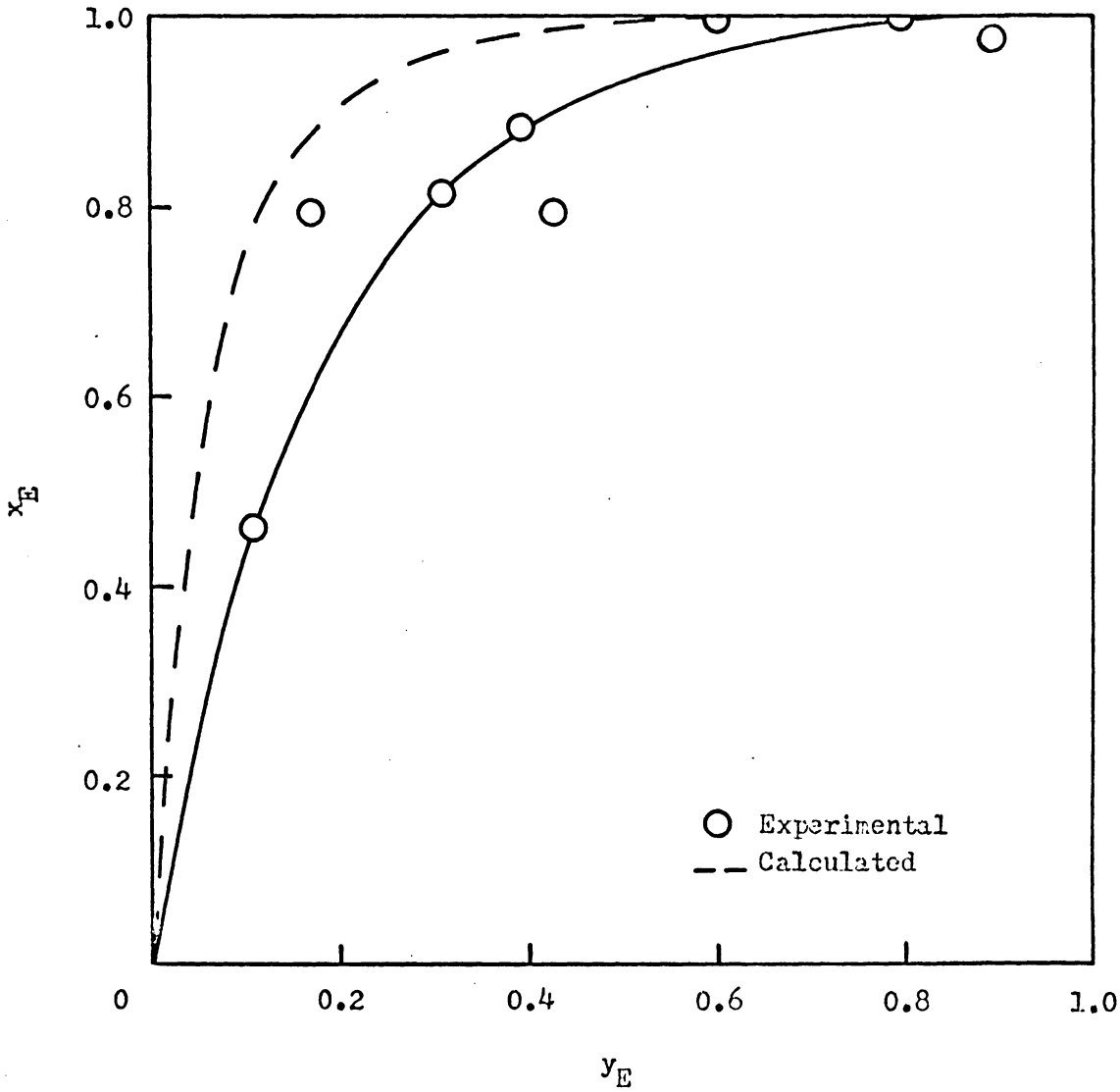

Figure 46. Calculated Ethanol-Cyclohexane/Cab-O-Sil Isotherm at 30°C

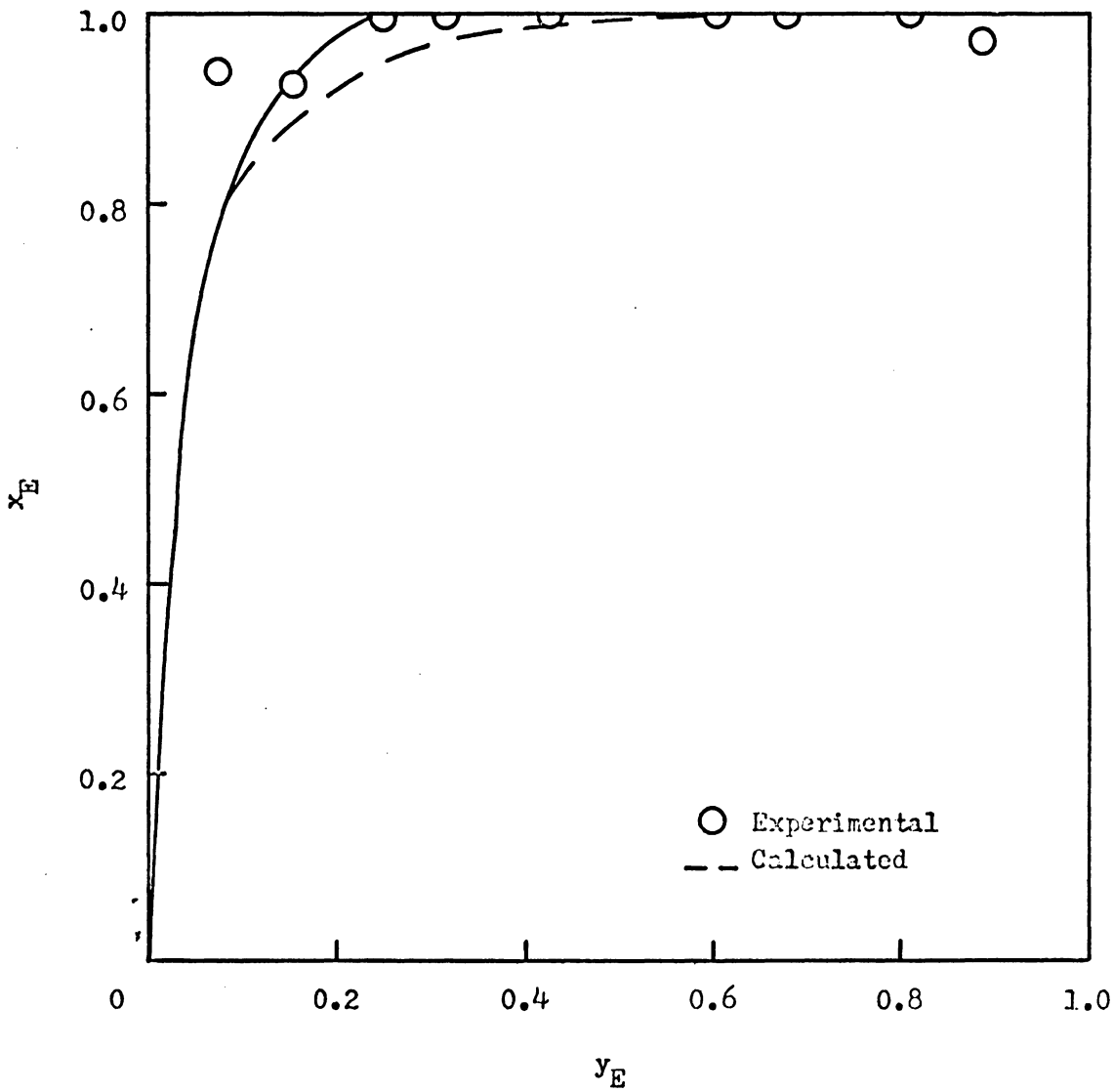

Figure 47. Calculated Ethanol-Cyclohexane/Cab-O-Sil Isotherm at 40°C

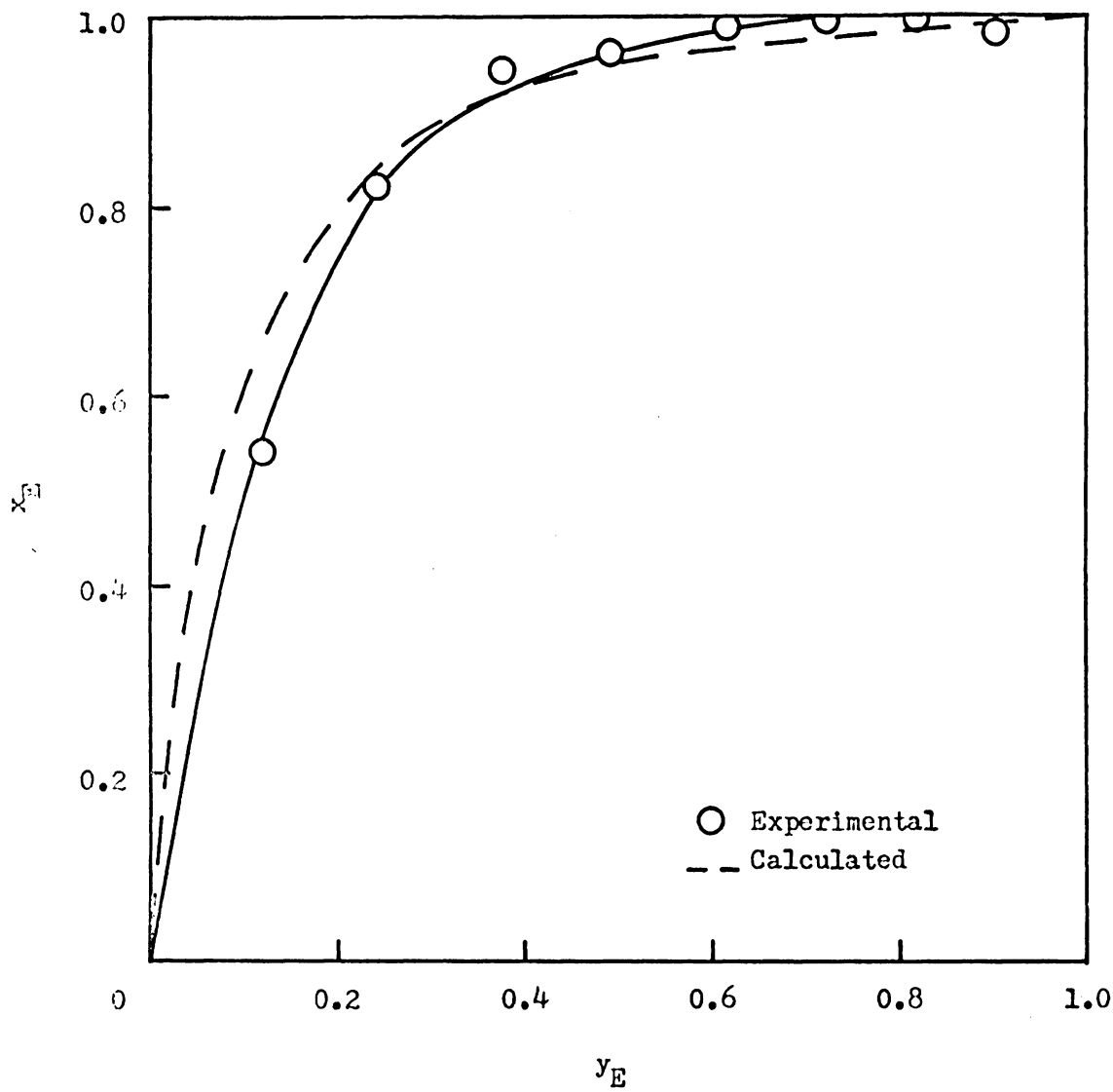

Figure 46. Calculated Ethanol-Benzene/Cab-O-Sil Isotherm at 20°C

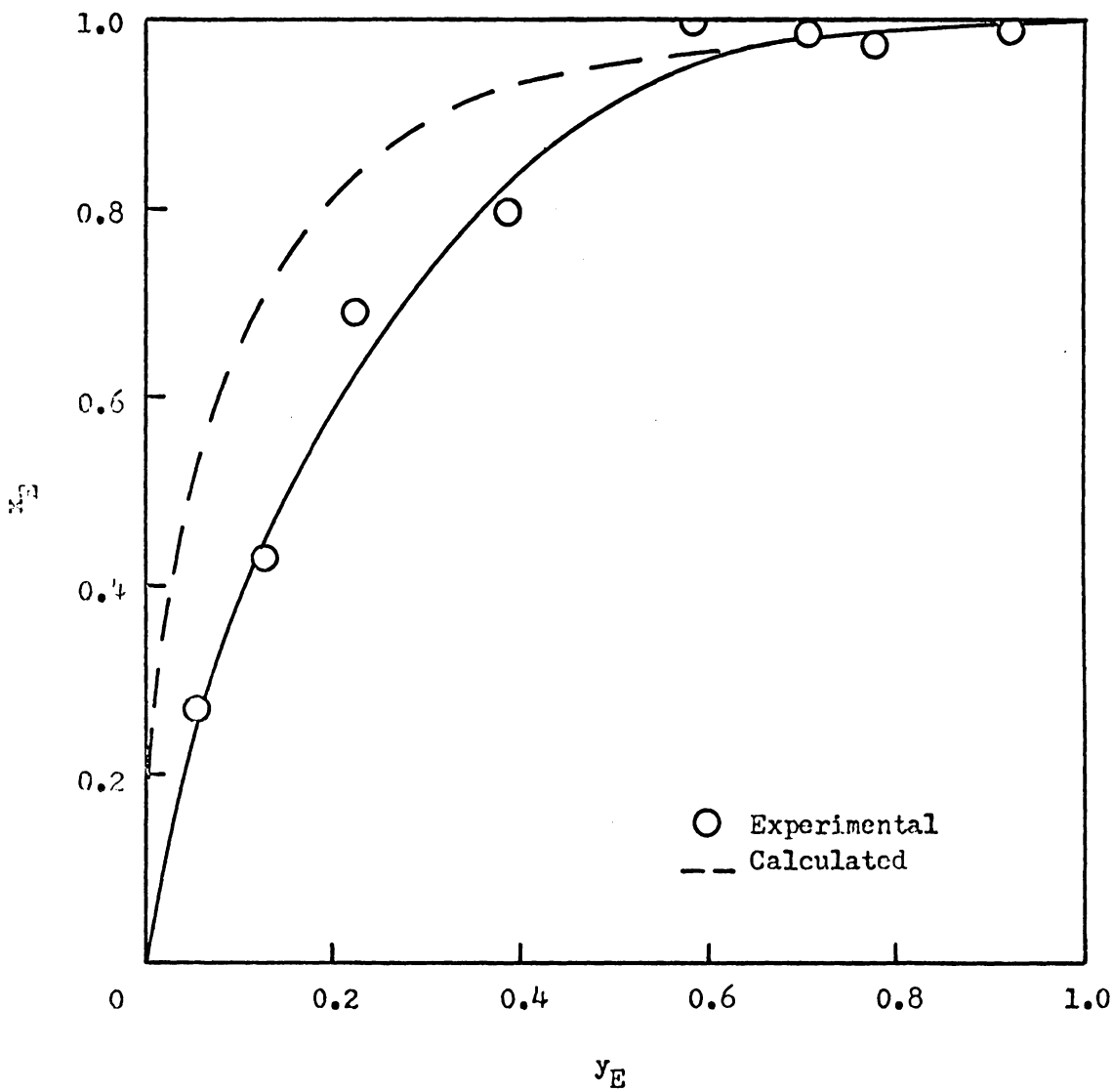

Figure 49. Calculated Ethanol-Benzene/Cab-O-Sil Isotherm at 30°C

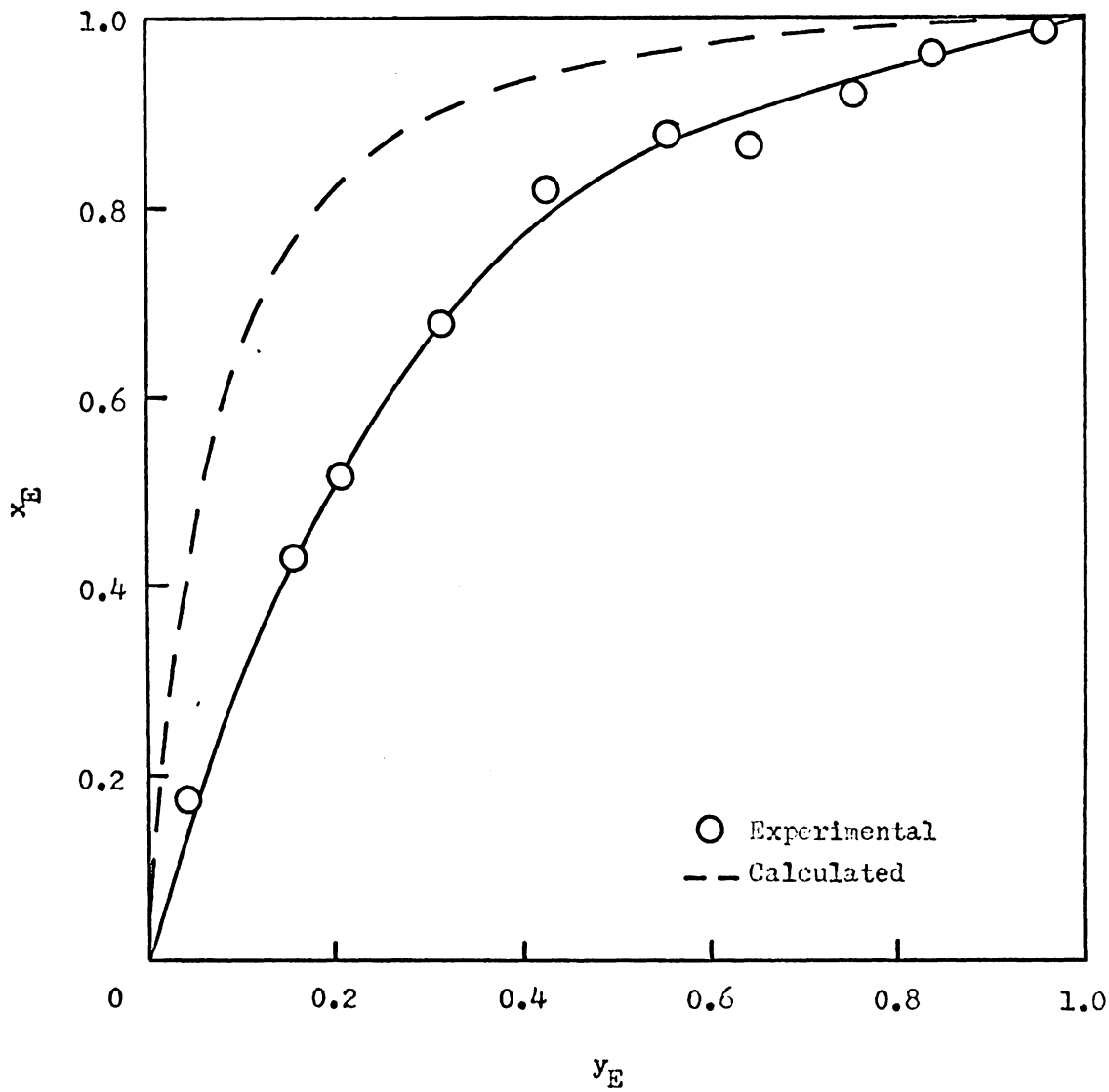

Figure 50. Calculated Ethanol-Benzene/Cab-O-Sil Isotherm at 40°C

sample. If so, selective adsorption of ethanol on such a surface would be lower than on a bare Cab-O-Sil surface. Chemisorption of methanol on silica surfaces has been observed previously (56, 57).

The agreement between calculated and experimental isotherms observed for ethanol-cyclohexane and ethanol-benzene mixtures on the second Cab-O-Sil sample implies that these two mixtures form ideal adsorbed solutions on the Cab-O-Sil surface. In contrast, these same mixtures form extremely nonideal liquid solutions. It has been observed (30) that for a system involving fairly strong adsorbate-adsorbent interactions, the adsorbed solution is more ideal than the corresponding liquid solution. This behavior was attributed to the decreased importance of intermolecular interactions between molecules in the adsorbed state. While adding benzene or cyclohexane to liquid ethanol disrupts the intermolecular interactions, addition of these same substances to an adsorbed film of ethanol has little effect, since ethanol is interacting primarily with the surface.

The benzene-cyclohexane/Cab-O-Sil isotherms were calculated from the ideal adsorbed solution model of Myers and Prausnitz (27, 28). From the spreading pressure curves and Equation (16b), the adsorbed phase compositions were determined. The corresponding vapor phase compositions were then calculated from:

$$y_i = \frac{P_i^* x_i}{P} \qquad (14)$$

The calculated benzene-cyclohexane/Cab-O-Sil isotherms are shown in Figures 51-53. The agreement between experimental and calculated

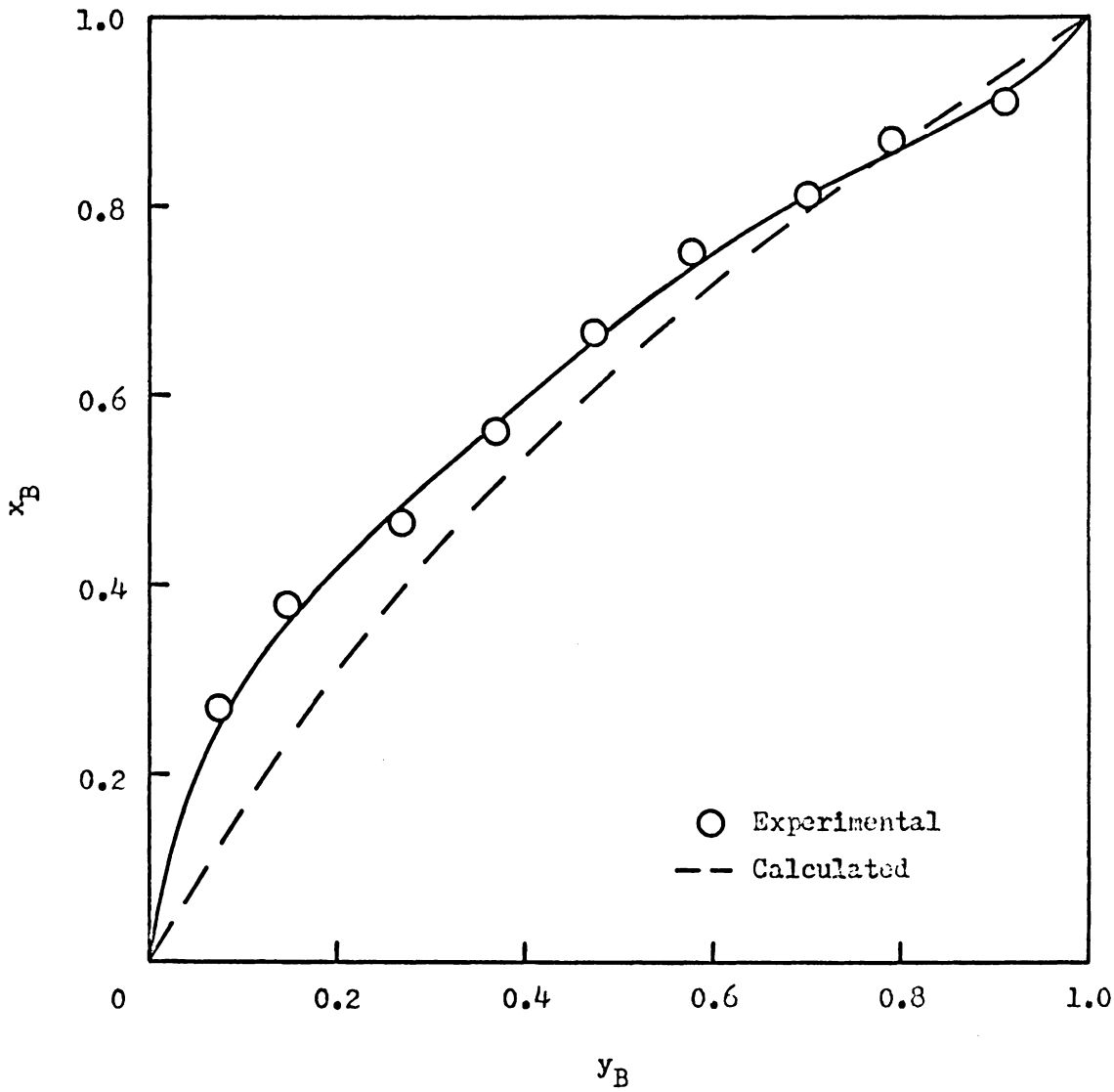

Figure 51. Calculated Benzene-Cyclohexane/Cab-O-Sil Isotherm at 20°C

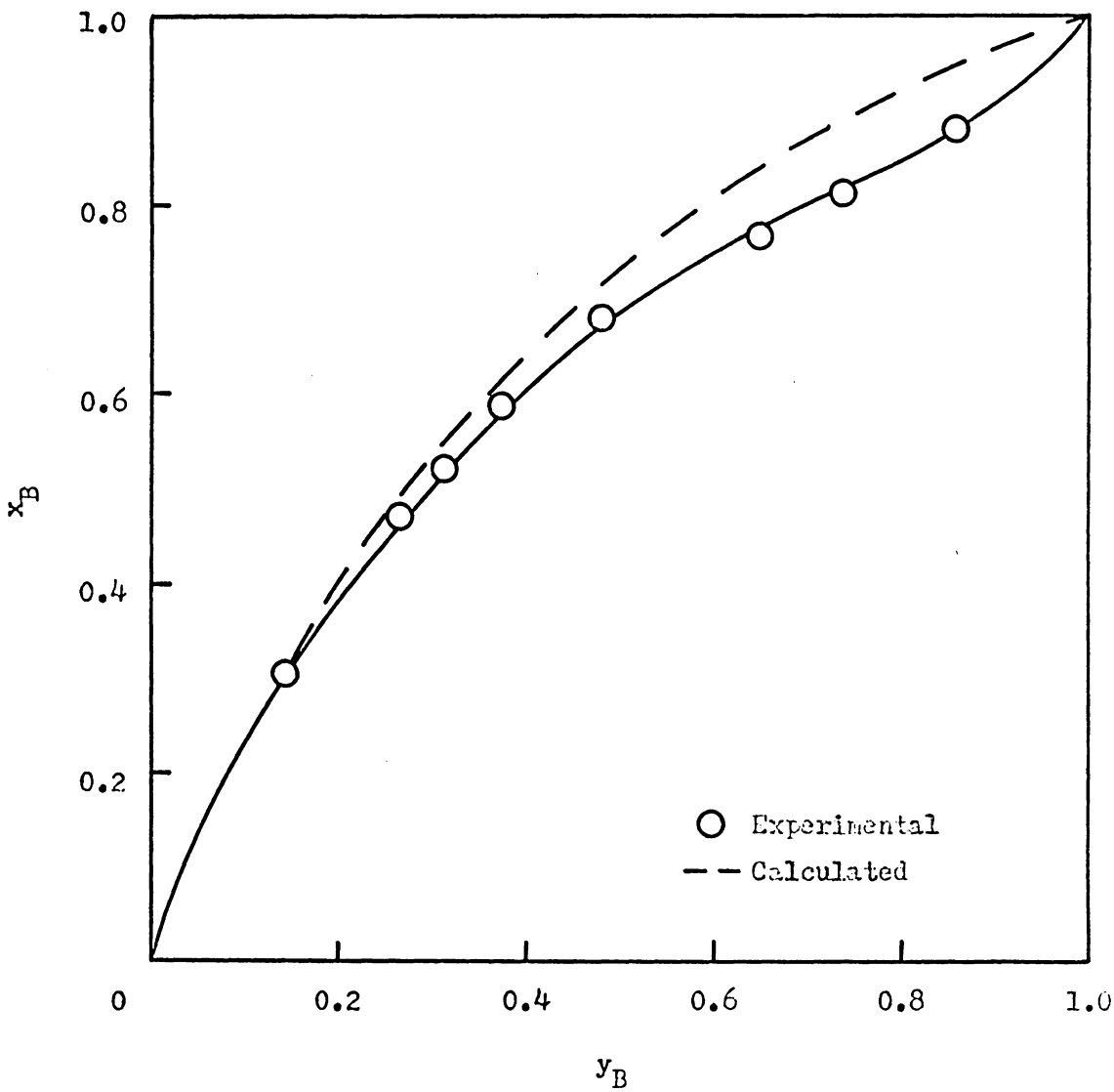

Figure 52. Calculated Benzene-Cyclohexane/Cab-O-Sil Isotherm at 30°C

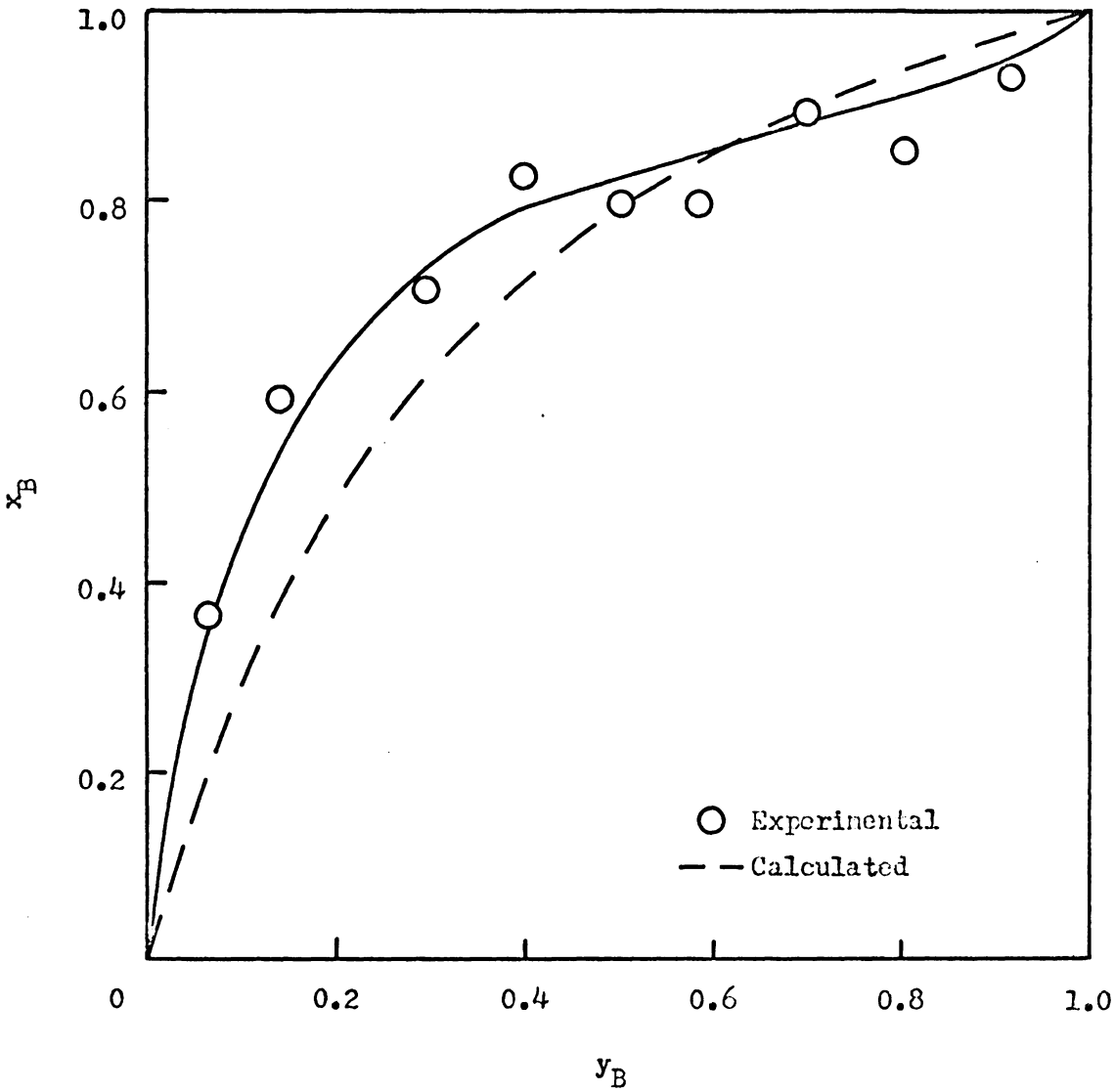

Figure 53. Calculated Benzene-Cyclohexane/Cab-O-Sil Isotherm at 40°C

isotherms is good, indicating that benzene and cyclohexane form a slightly nonideal adsorbed solution on the Cab-O-Sil surface. From a practical point of view, the discrepancies between experimental and calculated isotherms are not great enough to be important. The nonideal behavior observed for this system could not be explained.

The adsorption isotherms for the three mixtures on Graphon at 20°C all contain azeotropes, as shown above (Figure 40). The existence of an adsorption azeotrope implies that the adsorbed solution is very nonideal; therefore, the ideal adsorbed solution model would not be expected to give accurate predictions for the Graphon systems. However, application of the model to these systems illustrates some points which warrant discussion.

The spreading pressure curves for ethanol, benzene, and cyclohexane on Graphon at 20°C are shown in Figure 54. The curves for benzene and cyclohexane are almost identical; this same behavior is also observed at 30 and 40°C. Therefore, the ideal adsorbed solution model predicts almost no selective adsorption for benzene-cyclohexane mixtures on Graphon, as shown in Figures 55-57. Kidnay and Myers (31) have pointed out that for adsorbates having nearly equal values of P_i^*, very small nonidealities in the adsorbed solution can produce an azeotrope. Analogous behavior occurs for liquid solutions whose components have nearly equal vapor pressures (58). It may be concluded that benzene and cyclohexane form a slightly nonideal adsorbed solution on the Graphon surface. Although the ideal adsorbed solution model is not quantitatively correct, it does predict that separations of benzene-cyclohexane vapor mixtures by adsorption onto Graphon are not feasible.

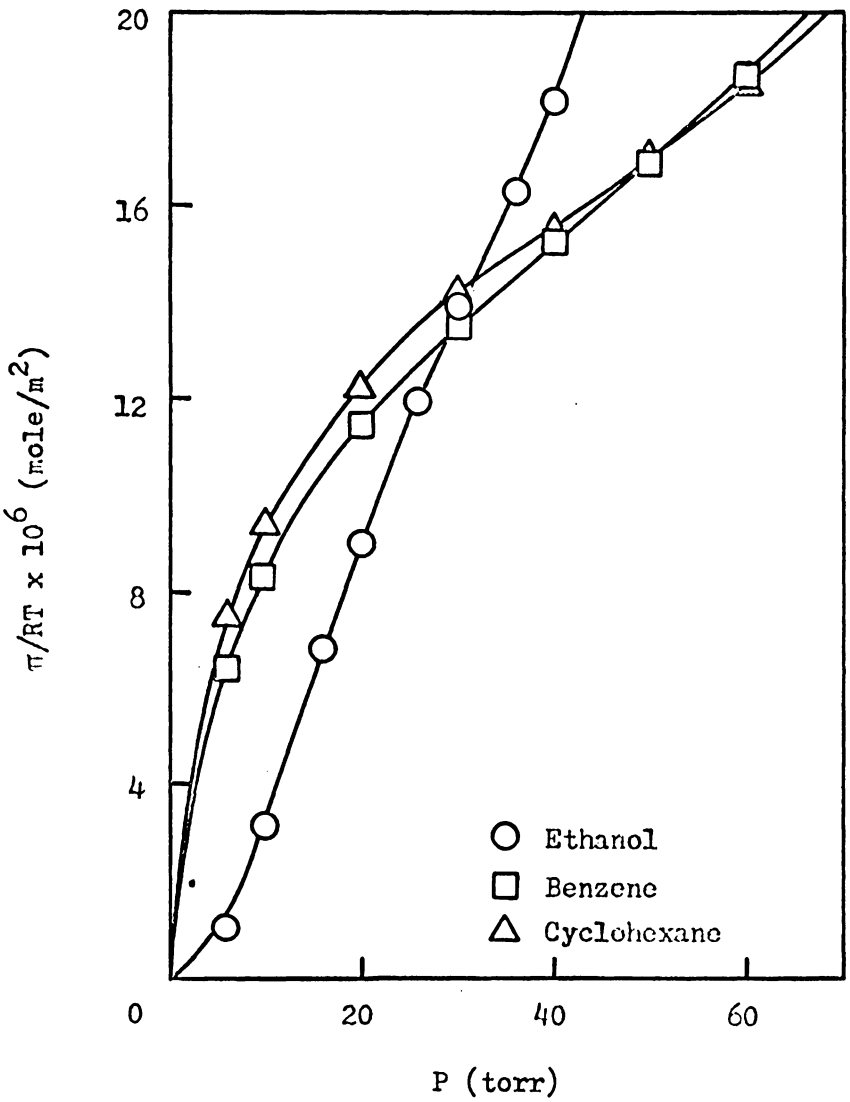

Figure 54. Spreading Pressure Curves for the Pure Adsorbates on Graphon at 20°C

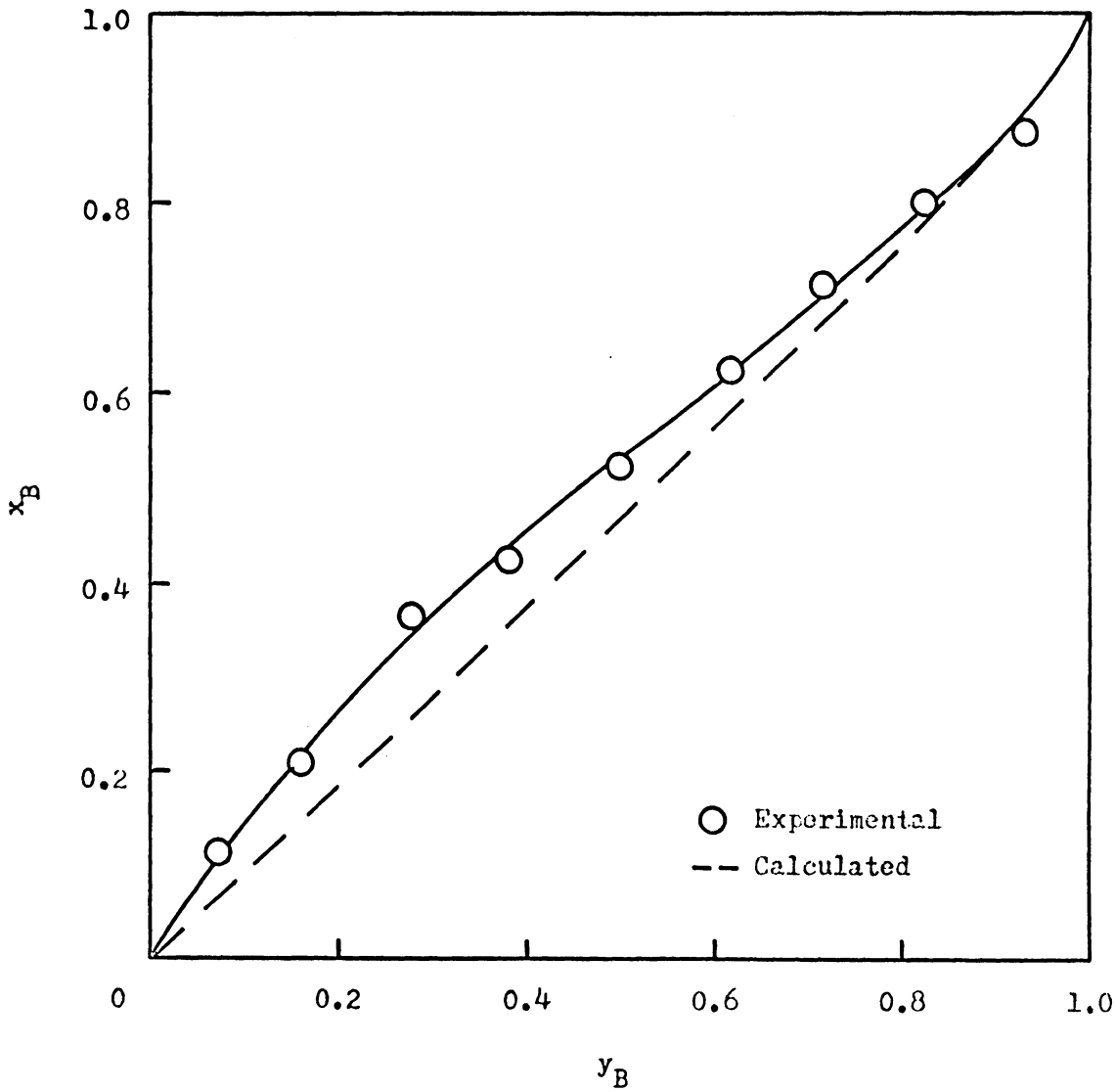

Figure 55. Calculated Benzene-Cyclohexane/Graphon Isotherm at 20°C

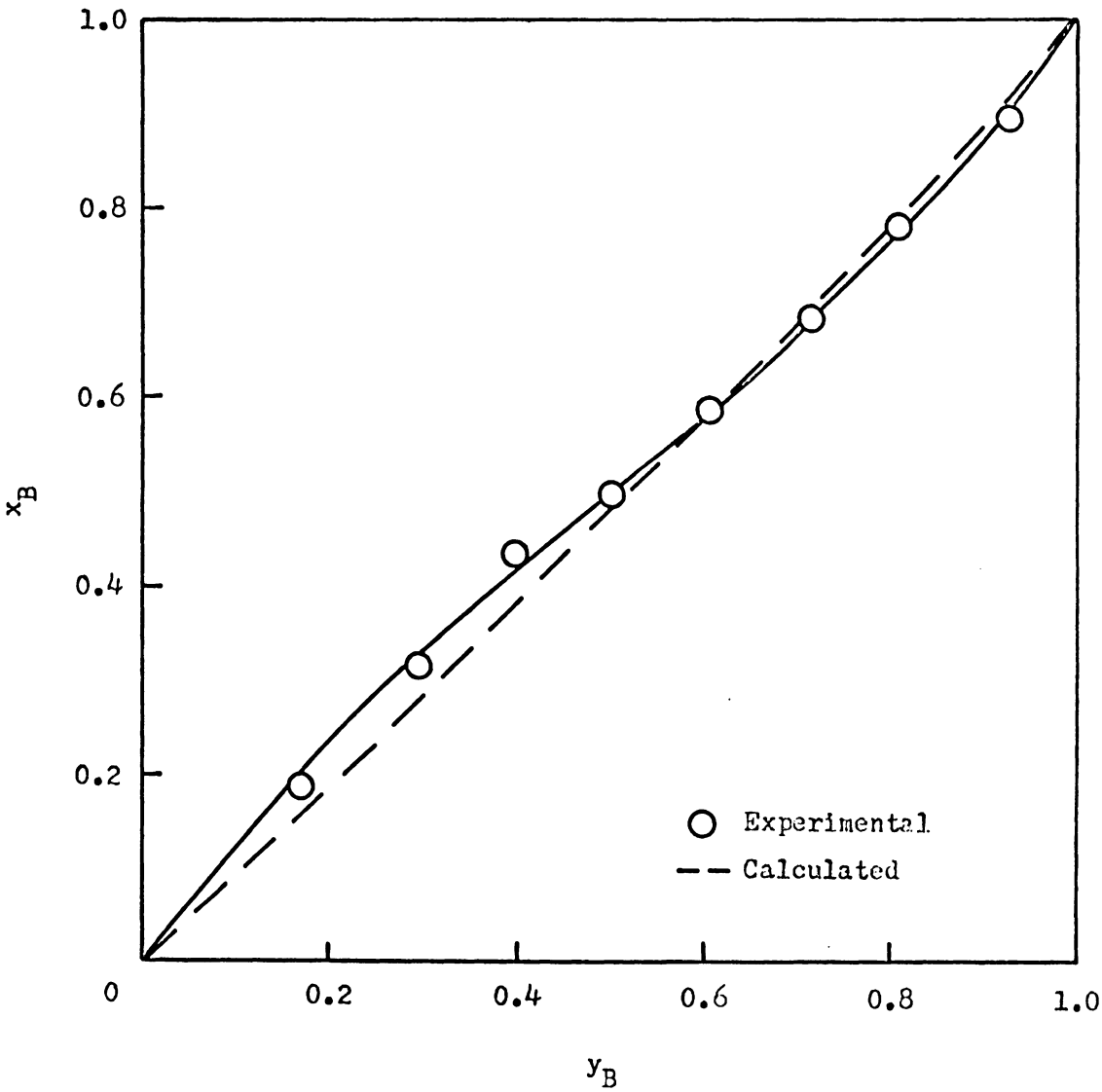

Figure 56. Calculated Benzene-Cyclohexane/Graphon Isotherm at 30°C

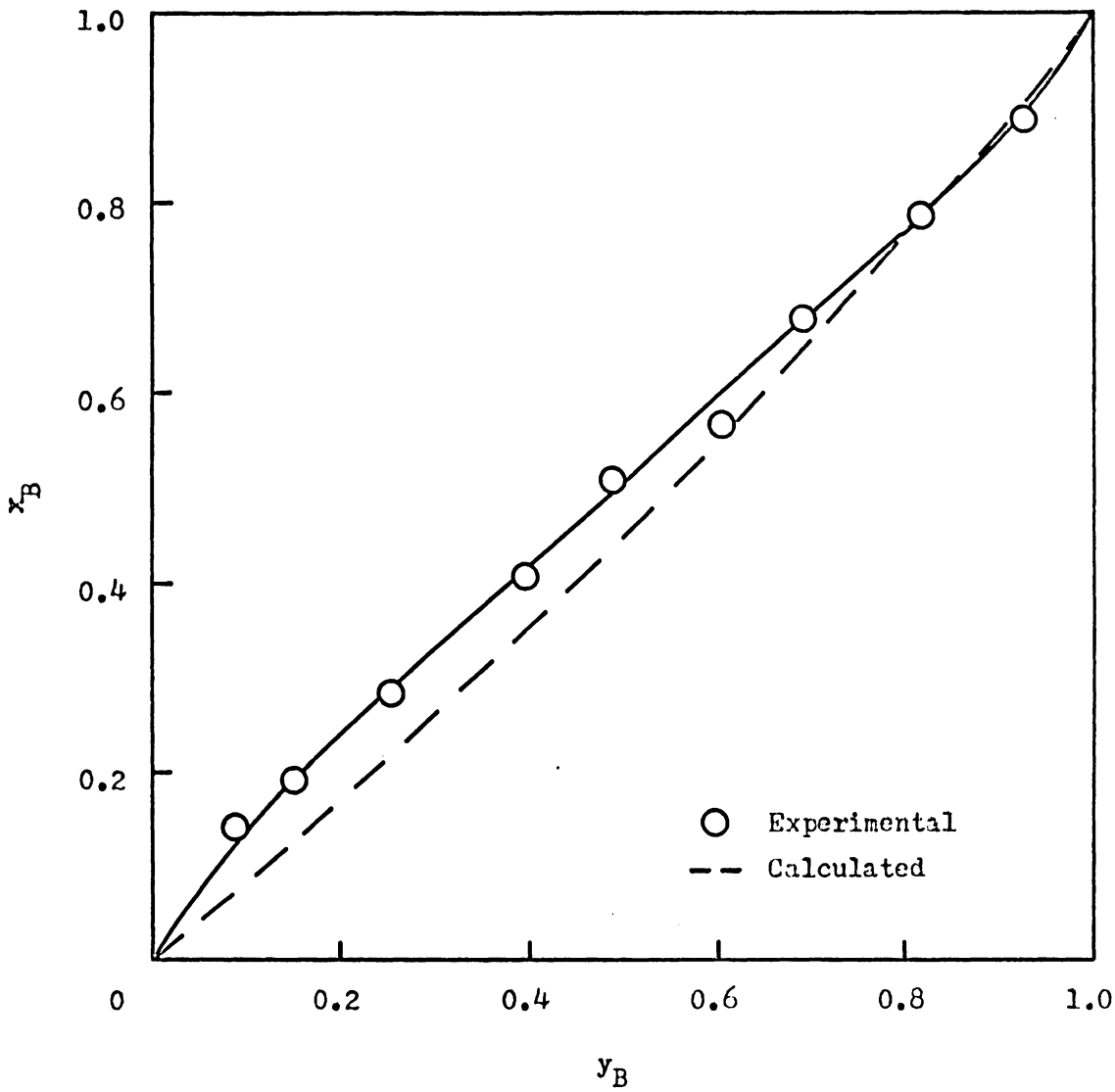

Figure 57. Calculated Benzene-Cyclohexane/Graphon Isotherm at 40°C

Figure 54 illustrates that the spreading pressure curves for ethanol and benzene on Graphon at 20°C cross at approximately 30 torr. Since the binary vapor adsorption isotherms were measured at a total pressure of 30 torr, the ideal adsorbed solution model predicts virtually no selective adsorption for the benzene-ethanol/Graphon system at 20°C. The spreading pressure curves for ethanol and cyclohexane also cross at about 30 torr. Comparisons between experimental and calculated isotherms for these two systems are shown in Figures 58 and 59. It has been observed previously (6) that an adsorption azeotrope will occur for a mixture if the pure component isotherms cross each other, as shown in Figure 14 for the pure vapor isotherms on Graphon. Examination of the spreading pressure curves for the pure components indicates at what approximate total pressure the azeotrope will occur. Thus, the ideal adsorbed solution model predicts that an azeotrope will occur, but cannot predict the composition of the azeotrope.

The spreading pressure curves for the three adsorbates on Graphon at 30 and 40°C are shown in Figures 60 and 61, respectively. At 30°C, the ethanol curve crosses the benzene and cyclohexane curves at about 55 torr, indicating that adsorption azeotropes would occur for the two mixtures if the total pressure were held constant at 55 torr. The 40°C spreading pressure curves indicate that azeotropes would be observed in isotherms measured at about 120 torr.

Since benzene-ethanol and cyclohexane-ethanol mixtures form nonideal adsorbed solutions on Graphon at 20°C, it would be expected that nonideal adsorbed solutions would also be obtained at 30 and 40°C. The benzene-ethanol/Graphon isotherms at 30 and 40°C calculated from the ideal

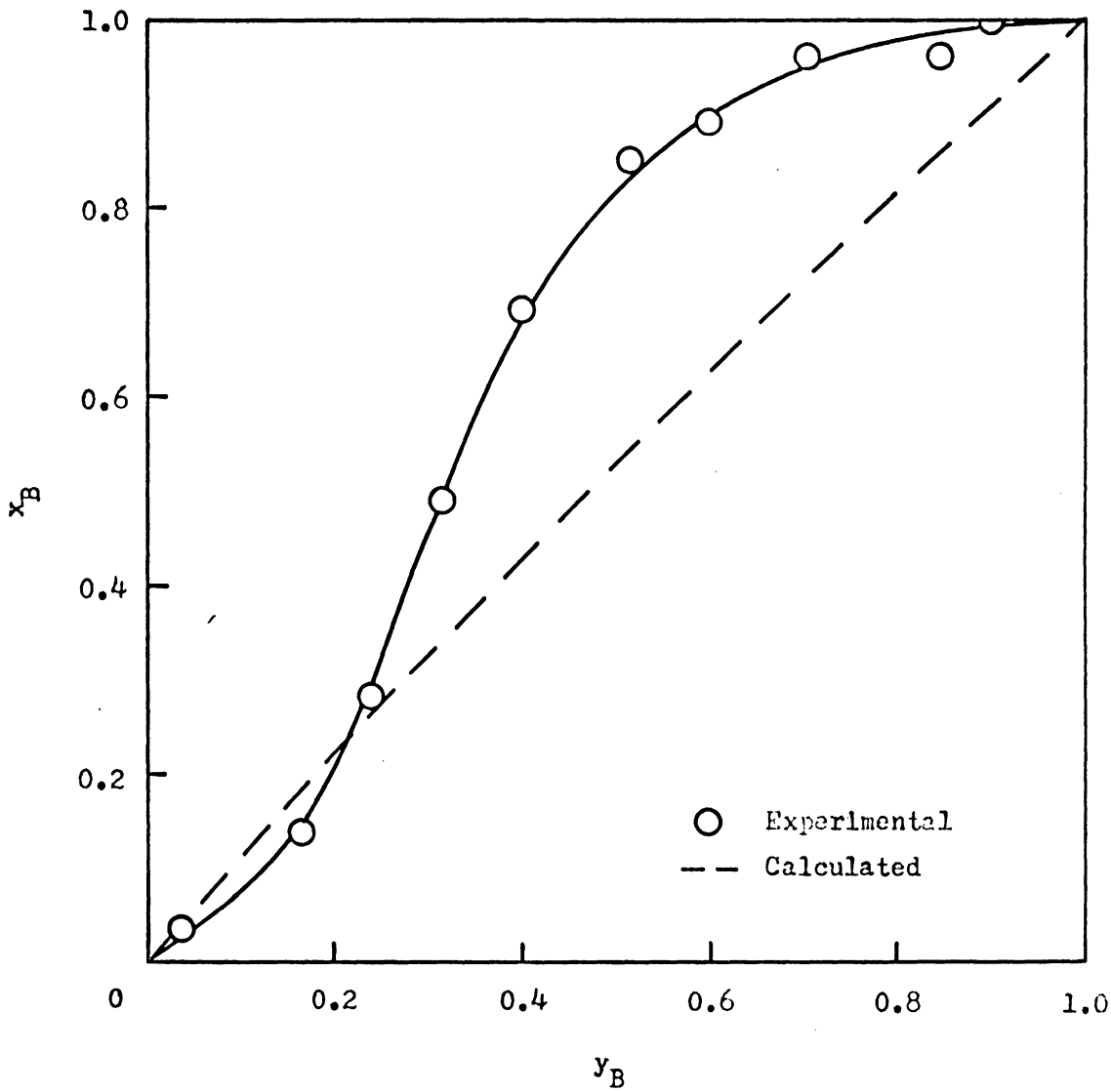

Figure 58. Calculated Benzene-Ethanol/Graphon Isotherm at 20°C

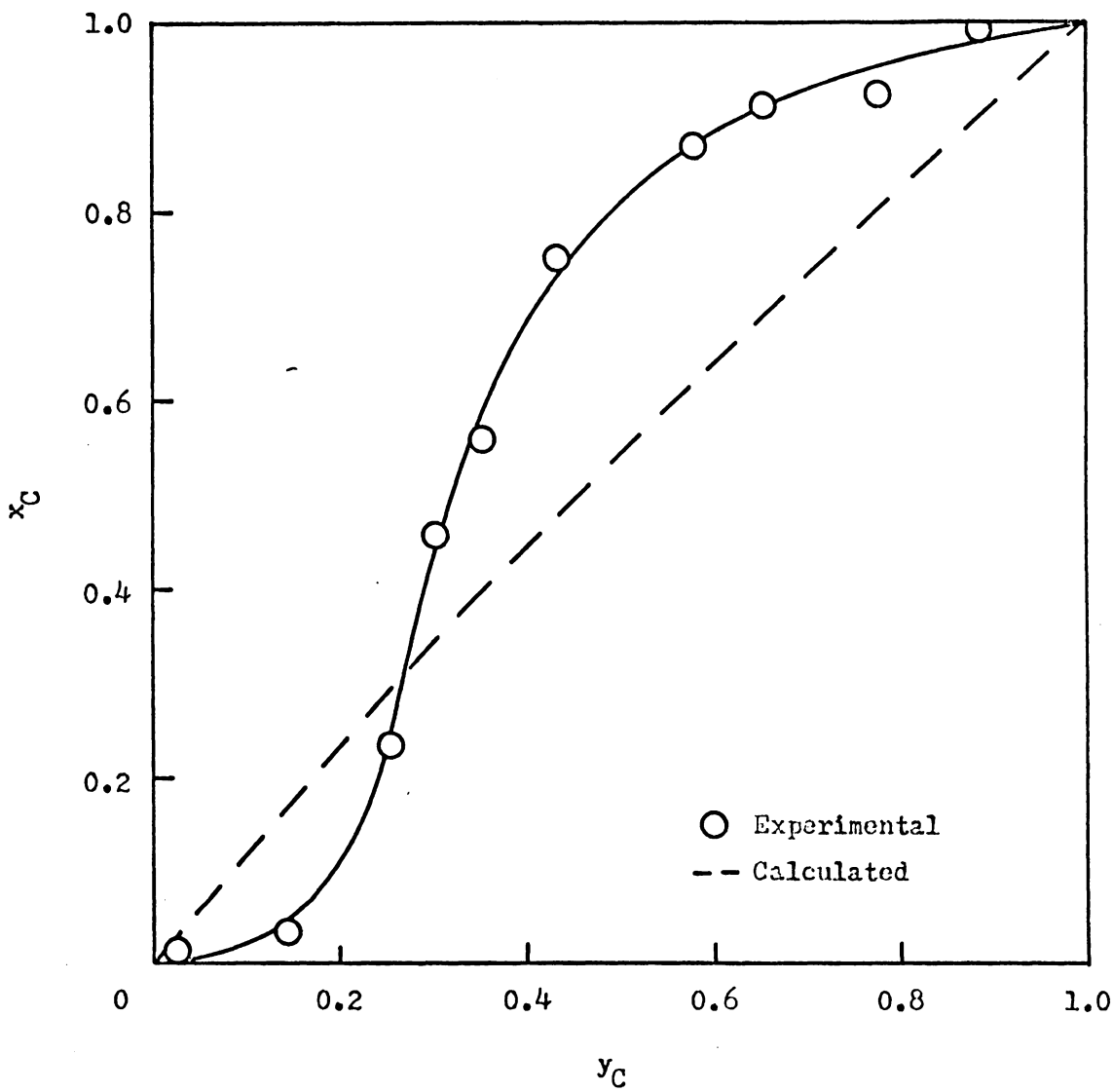

Figure 59. Calculated Cyclohexane-Ethanol/Graphon Isotherm at 20°C

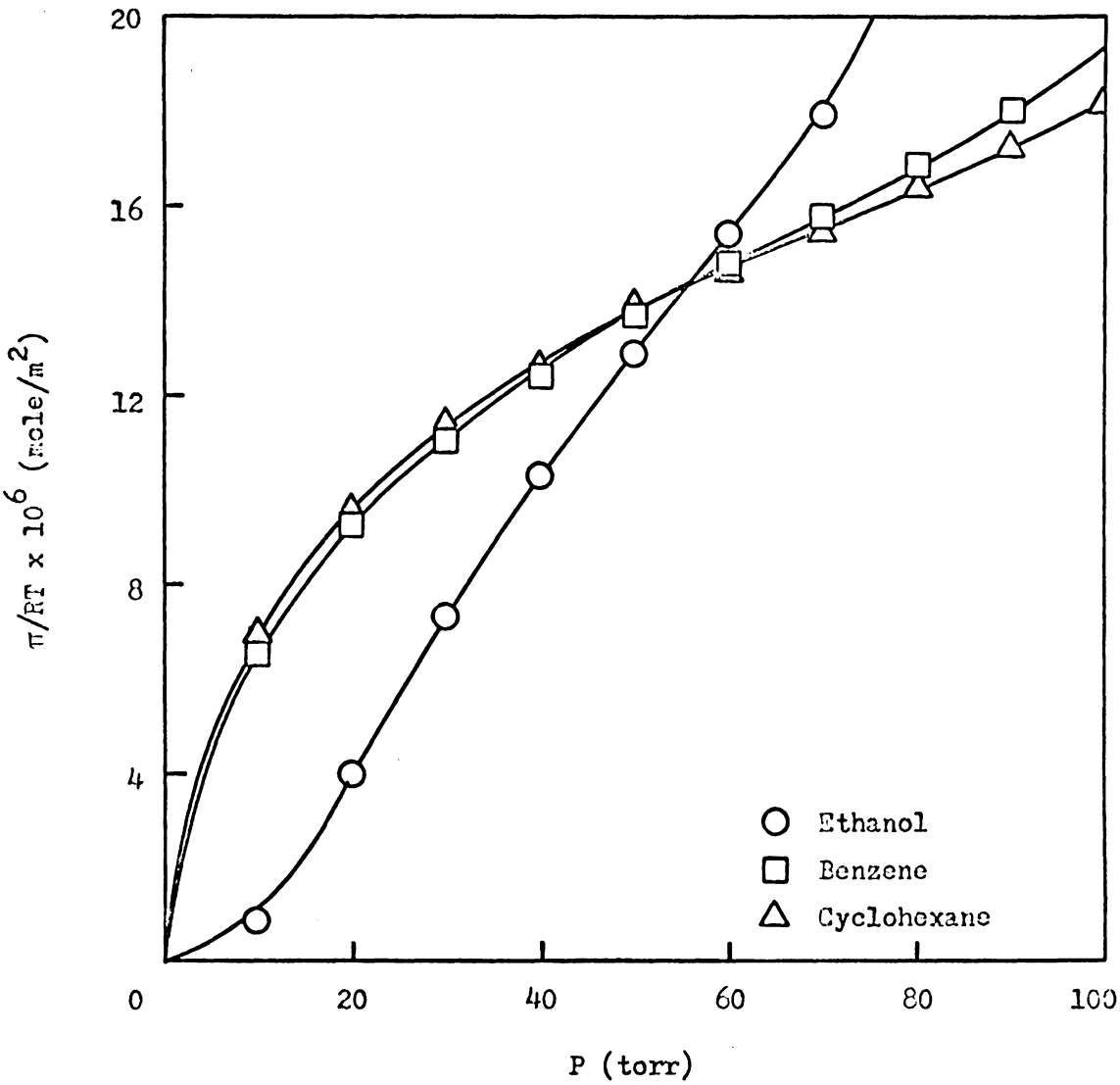

Figure 60. Spreading Pressure Curves for the Pure Adsorbates on Graphon at 30°C

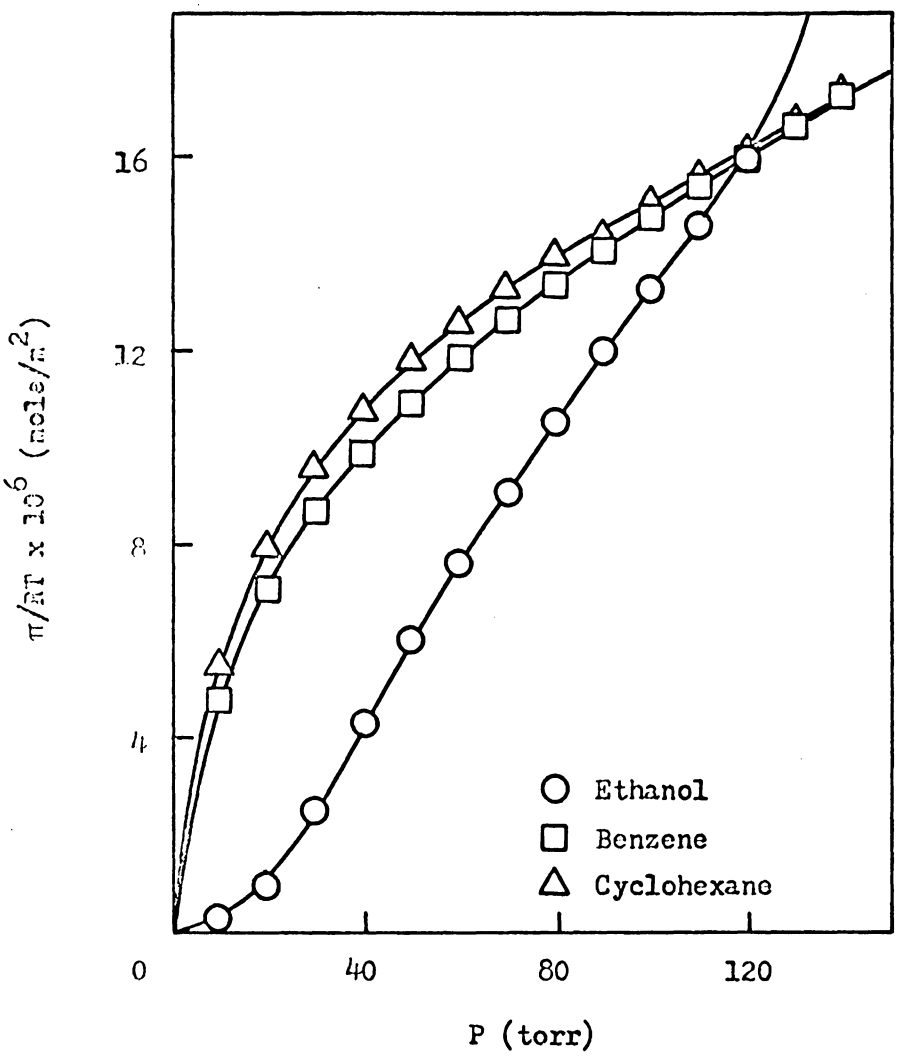

Figure 61. Spreading Pressure Curves for the Pure Adsorbates on Graphon at 40°C

adsorbed solution model are shown in Figures 62 and 63. The model predicts a smaller selective adsorption of benzene than actually occurs. Comparison of Figures 58, 62, and 63 illustrates that the agreement between experimental and calculated isotherms improves as the temperature increases. The calculated 30 and 40°C isotherms for cyclohexane-ethanol mixtures on Graphon, shown in Figures 64 and 65, show similar behavior. The predicted selective adsorption of cyclohexane is too low, with agreement between experimental and calculated isotherms improving with increasing temperature.

The fact that benzene-ethanol and cyclohexane-ethanol mixtures form nonideal adsorbed solutions on the Graphon surface is no doubt caused by structuring of ethanol in the adsorbed phase. Ethanol interacts weakly with the hydrophobic Graphon surface; hydrogen bonding interactions between ethanol molecules in the adsorbed phase are, therefore, extremely important. The presence of benzene or cyclohexane in the adsorbed phase disrupts the ethanol surface structure. Thus, ethanol is more volatile from the adsorbed mixture than from the pure state. The situation is analogous to the behavior of ethanol-benzene and ethanol-cyclohexane solutions.

It was observed that the benzene-ethanol and cyclohexane-ethanol adsorbed solutions on Graphon became closer to ideal as the adsorption temperature increased. At 20°C the total pressure of the mixture (30 torr) is fairly close to the saturation vapor pressure of ethanol (44 torr). Large amounts of ethanol are adsorbed, and structuring of ethanol in the adsorbed phase is highly developed. As the adsorption temperature increases the total pressure becomes further removed from the saturation

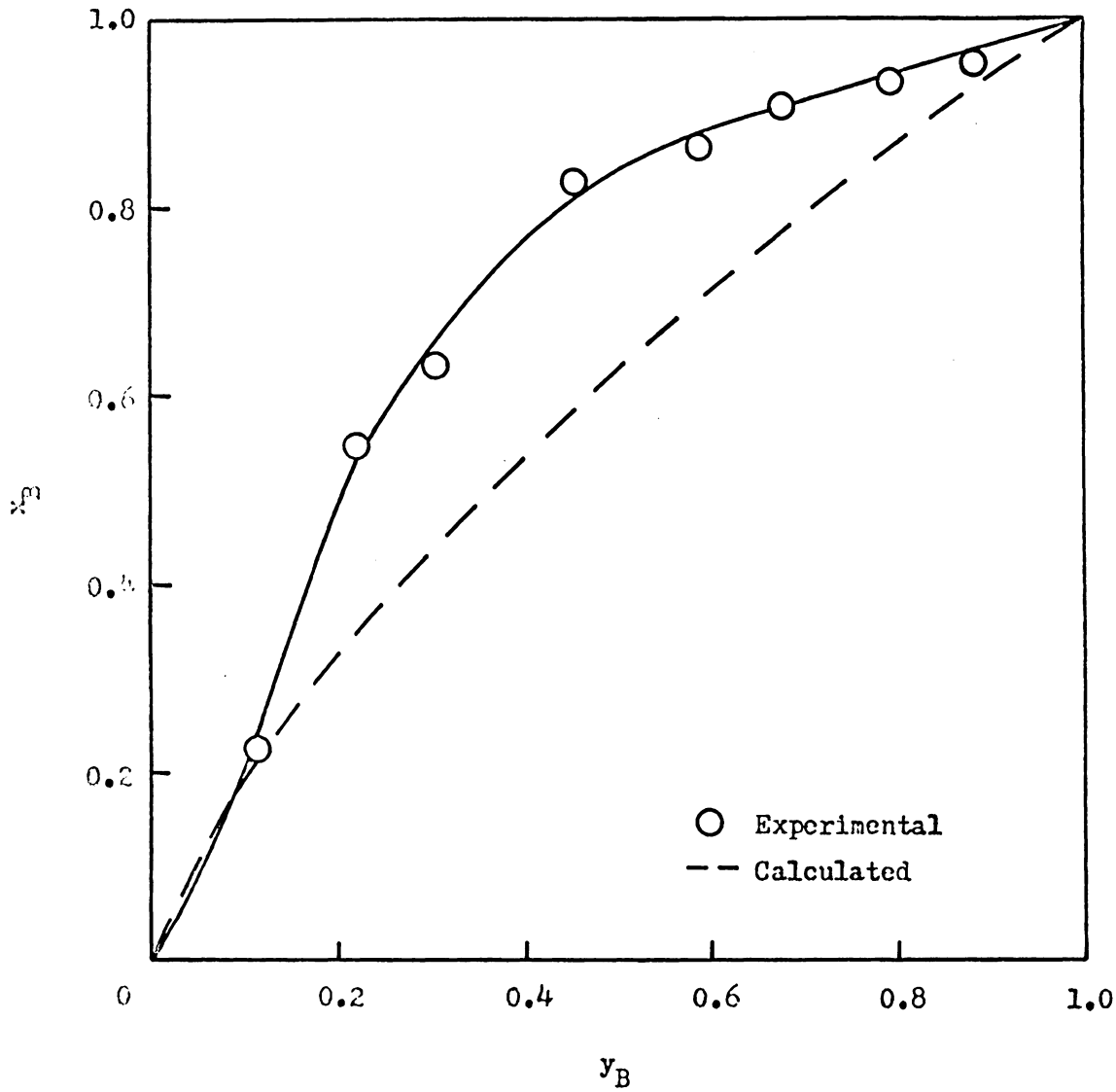

Figure 62. Calculated Benzene-Ethanol/Graphon Isotherm at 30°C

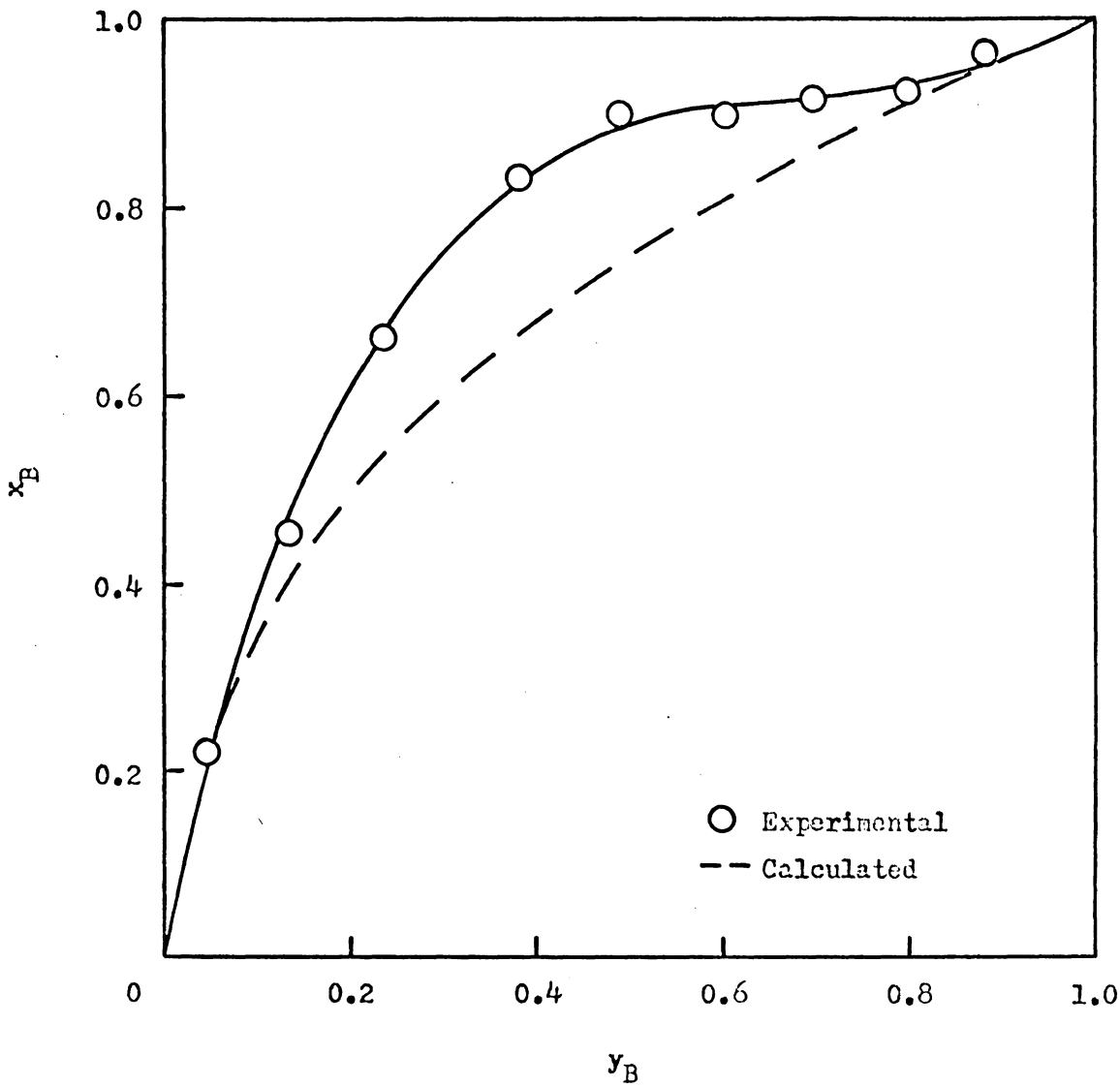

Figure 53. Calculated Benzene-Ethanol/Graphon Isotherm at 40°C

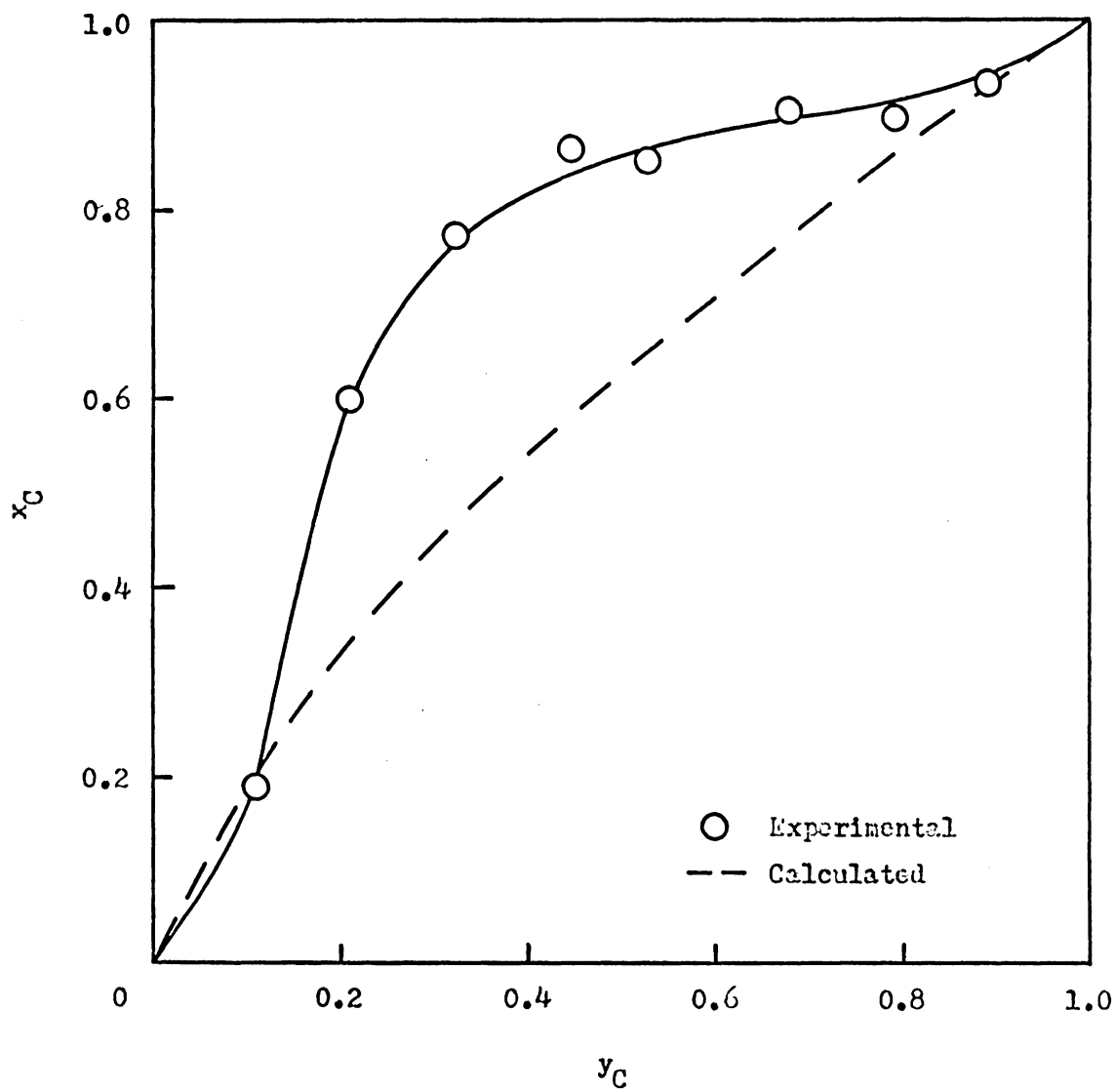

Figure 64. Calculated Cyclohexane-Ethanol/Graphon Isotherm at 30°C

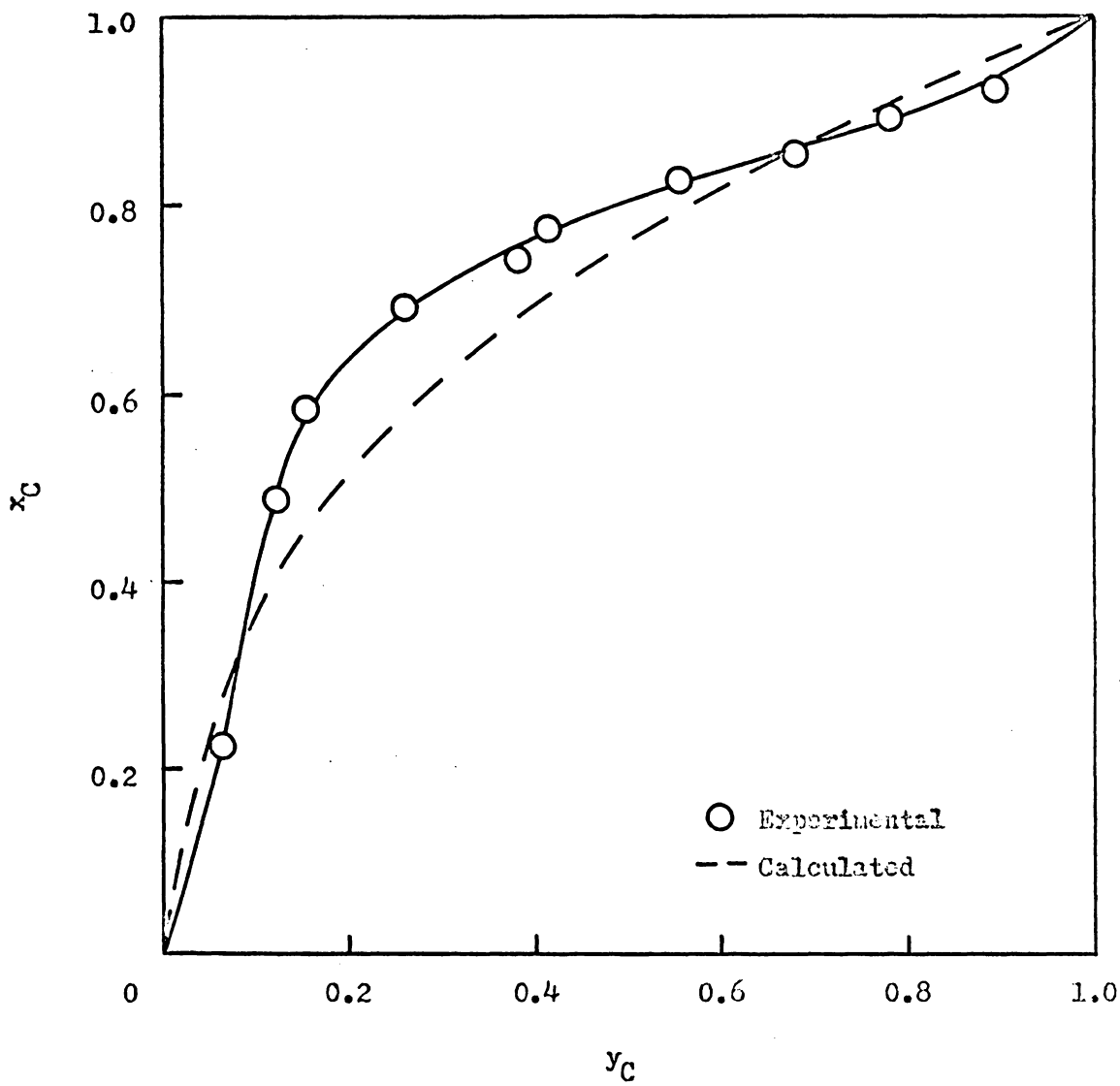

Figure 65. Calculated Cyclohexane-Ethanol/Graphon Isotherm at 45°C

vapor pressure of ethanol. Less ethanol is adsorbed, so that structuring of ethanol cannot develop to as great an extent.

V. SUMMARY

The pure vapor adsorption isotherms for ethanol, benzene, and cyclohexane on Cab-O-Sil and on Graphon, measured at 20, 30, and 40°C, all showed decreases in the amounts adsorbed with increasing temperature. The Cab-O-Sil isotherms were Type II; the amounts adsorbed followed the order ethanol > benzene > cyclohexane. From the initial shapes of the Cab-O-Sil isotherms it was concluded that ethanol interacts more strongly with the surface than do benzene or cyclohexane. The BET cross-sectional areas of ethanol, benzene, and cyclohexane on Cab-O-Sil were 37.5, 59.3, and 103 A^2, respectively. These values are much higher than the cross-sectional areas based on liquid molar volumes. It was concluded that the three adsorbates do not form close-packed monolayers on the Cab-O-Sil surface.

The maximum in the isosteric heat curve for ethanol on Cab-O-Sil was attributed to hydrogen bonding interactions between ethanol molecules in the adsorbed phase. The heat curves for benzene and cyclohexane both contained maxima at low coverages, but the data were not accurate enough to determine whether these maxima were significant. For the Cab-O-Sil systems no sharp changes in the isosteric heats of adsorption were observed at monolayer coverage, indicating that multilayer adsorption began before the first layers were completed.

The adsorption isotherms for benzene and cyclohexane on Graphon were Type II. From the initial shapes of these isotherms it was concluded that benzene and cyclohexane interact strongly with the Graphon surface. The ethanol/Graphon isotherms were intermediate between Types II and III.

The initial concavities in these isotherms indicated a weak interaction of ethanol with the hydrophobic Graphon surface. The amounts of benzene and cyclohexane adsorbed on Graphon were almost equal. Adsorption of ethanol was lower than benzene or cyclohexane at low pressures, becoming higher as pressure increased. The BET cross-sectional areas for benzene and cyclohexane on Graphon were 44.0 and 44.5 A^2, respectively. These values are much closer to the cross-sectional areas based on liquid molar volumes than were the values for these same adsorbates on Cab-O-Sil. The BET equation did not fit the ethanol/Graphon isotherms.

The isosteric heat curves for benzene and cyclohexane were similar, showing a decrease in the isosteric heat of adsorption with increasing surface coverage. The isosteric heat and the integral entropy of adsorption for ethanol on Graphon suggested that ethanol is adsorbed with the ethyl group lying on the surface, leaving the hydroxyl groups free for hydrogen bonding. Interactions could, therefore, occur between ethanol molecules in the first adsorbed layer, and also between ethanol molecules in the first and second layers.

The adsorption isotherms at 20, 30, and 40°C for ethanol-cyclohexane, ethanol-benzene, and benzene-cyclohexane vapor mixtures on Cab-O-Sil and on Graphon, measured at a total pressure of 30 torr, were compared to the pure component isotherms. For ethanol-cyclohexane and ethanol-benzene mixtures on Cab-O-Sil and for benzene-cyclohexane mixtures on Graphon, the amounts of the components adsorbed from the mixtures were generally less than from the pure states. For some of these systems, adsorption of a component from a mixture was greater than from the pure state at high vapor phase compositions of that component. For the benzene-

cyclohexane/Cab-O-Sil isotherms, the amounts adsorbed from the mixtures were greater than from the pure states. None of these enhancements in adsorption could be adequately explained.

For the benzene-ethanol/Graphon isotherms, adsorption of ethanol from the mixtures was much less than from the pure state. This behavior was attributed to the presence of benzene disrupting the structuring of ethanol on the Graphon surface. Adsorption of benzene from the mixtures was lower than from the pure state at low benzene mole fractions, becoming higher at the higher mole fractions. The enhancement in adsorption of benzene at high benzene concentrations was attributed to attractive interactions between the π electrons of benzene and the hydroxyl groups of adsorbed ethanol molecules. The cyclohexane-ethanol/Graphon isotherms were almost identical to those for benzene-ethanol mixtures on Graphon.

From the composition diagrams for the three vapor mixtures on Cab-O-Sil, it was concluded that selective adsorption of ethanol occurs from ethanol-cyclohexane and ethanol-benzene mixtures, and selective adsorption of benzene occurs from benzene-cyclohexane mixtures. Selectivities were highest for the ethanol-cyclohexane mixtures, and lowest for the benzene-cyclohexane mixtures. The benzene-cyclohexane/Graphon isotherms at 20, 30, and 40°C all showed adsorption azeotropes; very little selective adsorption of either component was observed. Adsorption azeotropes also occurred in the 20°C isotherms for benzene-ethanol and cyclohexane-ethanol vapor mixtures on Graphon. At 30 and 40°C, benzene and cyclohexane were selectively adsorbed over the entire composition range from benzene-ethanol and cyclohexane-ethanol mixtures, respectively. The

selectivities for these two mixtures were very similar. The variation of selectivity with temperature for both the Cab-O-Sil and the Graphon isotherms showed no particular trend.

Comparison of the 30°C binary vapor adsorption isotherms with the corresponding solution adsorption isotherms showed that selectivity is generally higher from solution. The enhanced selectivity from solution was attributed to intermolecular interactions in the liquid phase that are not present in the dilute vapor phase.

The experimental binary vapor adsorption isotherms were compared to those calculated from the pure component isotherms using the ideal adsorbed solution model. It was concluded that ethanol-cyclohexane and ethanol-benzene mixtures form ideal adsorbed solutions on the Cab-O-Sil surface. Benzene-cyclohexane mixtures form slightly nonideal adsorbed solutions on Cab-O-Sil. The ideal adsorbed solution model was correct in predicting that very little selective adsorption occurs for benzene-cyclohexane mixtures on Graphon, but it did not predict the adsorption azeotropes that are observed in these isotherms. Since the values of P_i^* for benzene and cyclohexane on Graphon are almost equal, very small nonidealities in the adsorbed solution could cause the azeotropes.

Since the 20°C isotherms for benzene-ethanol and cyclohexane-ethanol vapor mixtures on Graphon contained azeotropes, agreement between experimental and calculated isotherms for these two systems was poor. Nonidealities in the adsorbed solutions were attributed to the presence of benzene or cyclohexane disrupting the hydrogen bonding interactions between adsorbed ethanol molecules. Agreement between experimental and calculated isotherms for these two mixtures improved with increasing

adsorption temperature. This behavior was attributed to the fact that the structuring of adsorbed ethanol molecules on the Graphon surface is not highly developed at the higher temperatures. Although the ideal adsorbed solution model could not quantitatively predict the isotherms for these nonideal systems, it can predict the approximate total pressures at which adsorption azeotropes will occur. On the basis of this work, it may be concluded that the ideal adsorbed solution model is a useful one for predicting binary vapor adsorption equilibria.

LITERATURE CITED

1. S. Brunauer, "The Adsorption of Gases and Vapors," Vol. I, Princeton University Press, Princeton, N.J., 1943.

2. D. M. Young and A. D. Crowell, "Physical Adsorption of Gases," Butterworths, London, 1962.

3. J. R. Arnold, J. Amer. Chem. Soc., 71, 104 (1949).

4. W. K. Lewis, E. R. Gilliland, B. Chertow, and W. P. Cadogan, Ind. Eng. Chem., 42, 1319 (1950).

5. S. R. M. Ellis and D. W. Thompson, Birmingham Univ. Chem. Eng., 16, 99 (1965).

6. W. H. Cook and D. Basmadjian, Can. J. Chem. Eng., 43, 78 (1965).

7. "Calgon Water Report," Environ. Sci. Technol, 8, 871 (1974).

8. W. B. Innes and H. H. Rowley, J. Phys. Coll. Chem., 51, 1154 (1947).

9. W. B. Innes, R. B. Olney, and H. H. Rowley, J. Phys. Coll. Chem., 55, 1324 (1951).

10. M. R. Cines and F. N. Ruehlen, J. Phys. Chem., 57, 710 (1953).

11. N. M. Pavlyuchenko, Zh. Fiz. Khim., 44, 271 (1970); Russ. J. Phys. Chem., 44, 152 (1970).

12. J. N. Reeds and K. Kammermeyer, Ind. Eng. Chem., 51, 707 (1959).

13. W. J. Thomas and J. L. Lombardi, Trans. Inst. Chem. Eng., 49, 240 (1971).

14. L. Szepesy and V. Illes, Acta Chim. Acad. Sci. Hung., 35, 37 (1963).

15. L. Szepesy and V. Illes, Acta Chim. Acad. Sci. Hung., 35, 245 (1963).

16. A. B. Chernyshev, N. V. Kel'tsev, and A. L. Khalif, Dokl. Akad. Nauk SSSR, 82, 75 (1952); Chem. Abstr., 46, 4881h (1952).

17. T. L. Hill, Advan. Catal., 4, 211 (1952).

18. B. P. Bering, N. M. Pavlyuchenko, and V. V. Serpinskii, Vestsi Akad. Navuk Belarus. SSR, Ser. Khim. Navuk, 3, 5 (1970); Chem. Abstr., 73, 91742q (1970).

19. B. P. Bering, V. V. Serpinskii, and S. I. Surinova, Izv. Akad. Nauk SSSR, Ser. Khim., (12), 2611 (1967); Bull. Acad. Sci. USSR, Chem. Ser., (12), 2487 (1967).

20. J. Shen and J. M. Smith, Ind. Eng. Chem., Fundam., 7, 100 (1968).

21. M. Buelow, A. Grossmann, and W. Schirmer, Z. Chem., 12, 161 (1972).

22. S. Sircar and A. L. Myers, Chem. Eng. Sci., 28, 489 (1973).

23. T. L. Hill, J. Chem. Phys., 14, 265 (1946).

24. E. C. Markham and A. F. Benton, J. Amer. Chem. Soc., 53, 497 (1931).

25. A. J. Gonzalez and C. D. Holland, A.I.C.H.E.J., 16, 718 (1970).

26. R. J. Grant and M. Manes, Ind. Eng. Chem., Fundam., 5, 490 (1966).

27. A. L. Myers and J. M. Prausnitz, A.I.C.H.E.J., 11, 121 (1965).

28. A. L. Myers, Ind. Eng. Chem., 60, 45 (1968).

29. T. L. Henson and R. L. Kabel, A.I.C.H.E.J., 12, 606 (1966).

30. B. P. Bering, V. V. Serpinskii, and S. I. Surinova, Izv. Akad. Nauk SSSR, Ser. Khim., (1), 7 (1973); Bull. Acad. Sci. USSR, Chem. Ser., (1), 5 (1973).

31. A. J. Kidnay and A. L. Myers, A.I.C.H.E.J., 12, 981 (1966).

32. J. M. Fernbacher and L. A. Wenzel, Ind. Eng. Chem., Fundam., 11, 457 (1972).

33. H. C. van Ness, Ind. Eng. Chem., Fundam., 8, 464 (1969).

34. R. O. Friederich and J. C. Mullins, Ind. Eng. Chem., Fundam., 11, 439 (1972).

35. D. R. Bassett, E. A. Boucher, and A. C. Zettlemoyer, J. Colloid Interface Sci., 34, 436 (1970).

36. M. L. Hair and W. Hertl, J. Phys. Chem., 73, 4269 (1969).

37. R. W. Merriman, J. Chem. Soc., 103, 628 (1913).

38. J. M. Stuckey and J. H. Saylor, J. Amer. Chem. Soc., 62, 2922 (1940).

39. G. Scatchard, S. E. Wood, and J. M. Mochel, J. Phys. Chem., 43, 119 (1939).

40. S. Young and E. C. Fortey, J. Chem. Soc., 75, 873 (1899).

41. E. W. Washburn, Ed., "International Critical Tables," Vol. III, McGraw-Hill, New York, N.Y., 1928.

42. J. H. Whalen, J. Phys. Chem., 71, 1557 (1967).

43. C. Pierce and B. Ewing, J. Amer. Chem. Soc., 84, 4070 (1962).

44. A. L. McClellan and H. F. Harnsberger, J. Colloid Interface Sci., 23, 577 (1967).

45. R. A. Beebe and D. M. Young, J. Amer. Chem. Soc., 58, 93 (1954).

46. E. Borello, A. Zecchina, C. Morterra, and G. Ghiotti, J. Phys. Chem., 71, 2945 (1967).

47. J. A. Hockey and B. A. Pethica, Trans. Faraday Soc., 58, Part 10, 2017 (1962).

48. G. I. Berezin, A. V. Kiselev, R. T. Sagatelyan, and O. S. Chistozvonova, Zh. Fiz. Khim., 46, 756 (1972); Russ. J. Phys. Chem., 46, 432 (1972).

49. Yu. F. Berezkina, S. A. Kazaryan, O. G. Larionov, and K. V. Chmutov, Zh. Fiz. Khim., 47, 1331 (1973); Russ. J. Phys. Chem., 47, 756 (1973).

50. T. L. Hill, P. H. Emmett, and L. G. Joyner, J. Amer. Chem. Soc., 73, 5102 (1951).

51. J. Lopez-Gonzalez, F. G. Carpenter, and V. R. Deitz, J. Phys. Chem., 65, 1112 (1961).

52. D. R. Matayo and J. P. Wightman, J. Colloid Interface Sci., 44, 162 (1973).

53. A. V. Kiselev and L. F. Pavlova, Kolloidn. Zh., 25, 537 (1963); Chem. Abstr., 60, 6242d (1964).

54. A. V. Kiselev in "The Structure and Properties of Porous Materials," D. H. Everett and F. S. Stone, Eds., Butterworths, London, 1958, p. 195.

55. J. Timmermans, "Physico-chemical Constants of Binary Systems," Vol. II, Interscience, New York, N.Y., 1959.

56. E. Borello, A. Zecchina, and C. Morterra, J. Phys. Chem., 71, 2938 (1967).

57. C. Clark-Monks, B. Ellis, and K. Rowan, J. Colloid Interface Sci., 32, 628 (1970).

58. J. H. Hildebrand and R. L. Scott, "The Solubility of Nonelectrolytes," 3rd ed., Dover, New York, N.Y., 1964, p. 221.

APPENDIX I

Adsorption Data for Pure Ethanol on Cab-O-Sil

20°C: P (torr)	N x 10^6 (mole/m^2)
0.9	2.4
3.8	4.6
10.5	5.94
17.2	6.85
22.8	7.53
27.6	8.40
32.6	9.75
39.4	13.9
42.8	19.9

30°C: P (torr)	N x 10^6 (mole/m^2)
1.8	2.9
6.5	4.4
13.7	5.20
20.2	5.72
27.3	6.23
35.3	6.48
43.4	7.22
53.6	8.40
60.2	9.51
66.6	11.3
73.4	16.4

40°C: P (torr)	N x 10^6 (mole/m^2)
3.1	2.8
10.8	3.99
18.3	4.51
26.8	4.82
35.8	5.12
45.5	5.35
56.4	5.59
75.4	6.42
91.1	7.22
106.7	9.14
119.9	12.4
128.5	19.7

Adsorption Data for Pure Benzene on Cab-O-Sil

20°C: P (torr)	N x 10^6 (mole/m^2)
5.1	1.0
11.5	1.90
18.6	2.46
25.6	3.07
33.3	3.73
41.1	4.40
48.0	5.12
54.9	6.30
61.2	7.80
66.3	10.6
69.9	13.8
71.9	17.5

30°C: P (torr)	N x 10^6 (mole/m^2)
9.7	1.3
16.0	1.89
23.0	2.37
29.7	2.79
37.9	3.23
45.9	3.70
53.7	4.30
62.5	5.07
71.6	5.67
79.6	6.54
87.4	7.58
95.9	9.15
103.1	11.2

40°C: P (torr)	N x 10^6 (mole/m^2)
6.1	0.70
15.3	1.14
26.3	1.56
36.8	1.85
46.4	2.53
63.5	3.27
74.2	4.16
85.6	4.68
97.0	5.11
108.8	5.83
120.2	6.69
132.0	7.59
146.4	9.12
161.7	11.9
173.7	17.8

Adsorption Data for Pure Cyclohexane on Cab-O-Sil

20°C: P (torr)	N x 10^6 (mole/m^2)
4.1	0.55
11.2	1.09
18.6	1.56
25.6	2.08
32.9	2.86
40.6	3.36
48.0	4.13
56.4	5.65
65.2	7.96
72.6	14.3

30°C: P (torr)	N x 10^6 (mole/m^2)
6.0	0.44
15.9	0.502
25.4	1.11
35.1	1.46
44.6	1.78
53.9	2.22
65.1	2.72
76.1	3.30
86.8	4.15
100.4	6.14
112.7	10.6

40°C: P (torr)	N x 10^6 (mole/m^2)
7.5	0.27
18.1	0.395
28.8	0.609
40.6	0.852
52.3	1.10
65.2	1.43
79.0	2.11
101.5	2.83
118.2	3.40
135.2	4.22
143.1	4.62
157.1	6.17
169.5	8.27
177.9	12.8

Adsorption Data for Pure Ethanol on Graphon

20°C:

P (torr)	N x 10^6 (mole/m^2)
5.0	1.0
7.4	4.1
11.3	7.31
17.7	9.58
24.0	11.5
30.2	13.0
36.2	15.8
39.5	20.8
41.1	29.5

30°C:

P (torr)	N x 10^6 (mole/m^2)
3.9	0.24
10.7	2.23
14.6	4.76
21.0	7.35
28.6	9.09
36.4	10.6
46.5	12.2
57.2	13.7
69.1	19.1
73.1	28.3

40°C:

P (torr)	N x 10^6 (mole/m^2)
7.8	0.27
16.5	1.25
23.8	3.59
33.1	5.99
45.0	7.76
55.7	8.96
71.5	10.5
85.3	11.6
100.6	12.9
117.4	16.7
126.3	26.0

Adsorption Data for Pure Benzene on Graphon

20°C: P (torr)	N x 10^6 (mole/m^2)
2.0	2.4
6.9	3.7
16.1	4.60
26.1	5.17
34.6	5.83
41.2	6.62
47.6	7.87
56.8	10.3
63.9	13.2
71.2	21.5

30°C: P (torr)	N x 10^6 (mole/m^2)
4.3	2.8
14.3	3.91
24.6	4.49
36.1	4.98
47.8	5.55
60.3	6.31
71.5	7.24
82.6	8.78
94.5	11.4
107.1	17.2

40°C: P (torr)	N x 10^6 (mole/m^2)
4.9	2.2
15.8	3.51
29.0	4.11
45.9	4.68
63.8	5.06
84.0	5.86
106.1	6.84
124.3	8.01
147.4	10.3
168.7	14.8

Adsorption Data for Fure Cyclohexane on Graphon

20°C: P (torr)	N x 10^6 (mole/m^2)
2.6	3.3
10.2	4.02
18.0	4.28
23.9	4.53
32.4	4.95
40.7	5.58
48.2	6.80
55.5	8.82
62.7	12.7
67.5	18.9
70.3	31.0

30°C: P (torr)	N x 10^6 (mole/m^2)
4.5	2.9
15.8	4.01
29.7	4.39
43.1	4.78
55.5	5.18
66.5	5.65
78.0	6.65
89.8	8.42
101.1	11.5
111.3	17.4
116.8	24.7

40°C: P (torr)	N x 10^6 (mole/m^2)
3.7	2.00
14.5	3.64
28.8	4.03
42.2	4.32
55.5	4.48
71.5	4.78
88.9	5.17
113.3	5.59
134.7	7.79
152.6	11.3
167.2	20.0
173.7	32.3

Calculation of Pure Vapor Adsorption

Second point on ethanol/Cab-O-Sil isotherm at 20°C:

V_1 = 155 cc
V_2 = 36.0 cc
R = 6.24×10^4 cc-torr/mole-°K
T_1 = room temperature = 297.8°K
T_2 = adsorption temperature = 293.0°K
Σ = surface area of Cab-O-Sil sample = 16.2 m^2
P_i = 8.7 torr
P_f = 3.8 torr

From first point:
n_v = number of moles in vapor phase in V_2 = 1.77×10^{-6} mole
n_a = number of moles in adsorbed phase in V_2 = 3.91×10^{-5} mole

$$n_i = \frac{P_i V_1}{RT_1} + n_v + n_a = 1.134 \times 10^{-4} \text{ mole}$$

$$n_f = \frac{P_f V_1}{RT_1} + \frac{P_f V_2}{RT_2} = 3.918 \times 10^{-5} \text{ mole}$$

$$n = n_i - n_f = 7.42 \times 10^{-5} \text{ mole}$$

$$N = \frac{n}{\Sigma} = 4.6 \times 10^{-6} \text{ mole}/m^2$$

APPENDIX II

Isosteric Heat of Adsorption for Ethanol, Benzene, and Cyclohexane on Cab-O-Sil

Ethanol

θ	q_{st} (kcal/mole)
0.677	9.99 ± 1.16
0.790	12.4 ± 0.2
0.903	14.0 ± 1.6
1.02	15.4 ± 0.9
1.13	16.2 ± 1.6
1.35	16.7 ± 1.5
1.58	14.0 ± 0.5
1.81	12.2 ± 0.3
2.03	11.4 ± 0.2
2.26	11.1 ± 0.2
2.48	10.8 ± 0.2

Benzene

θ	q_{st} (kcal/mole)
0.286	8.11 ± 0.83
0.429	8.59 ± 1.45
0.571	9.16 ± 2.14
0.714	9.19 ± 2.16
0.857	8.68 ± 1.90
1.00	8.15 ± 1.57
1.14	7.55 ± 1.14
1.43	6.74 ± 0.78
1.71	6.45 ± 0.70
2.00	6.52 ± 0.55
2.29	6.73 ± 0.44
2.57	6.97 ± 0.42

Cyclohexane

θ	q_{st} (kcal/mole)
0.373	15.0 ± 1.9
0.497	15.2 ± 1.0
0.621	14.7 ± 0.7
0.745	14.0 ± 0.3
0.870	13.3 ± 0.4
0.994	12.5 ± 0.6
1.12	11.9 ± 0.8
1.24	11.3 ± 0.7
1.49	10.6 ± 0.8
1.74	10.1 ± 0.9
1.99	9.81 ± 0.93
2.24	9.62 ± 0.84
2.48	9.41 ± 0.71

Isosteric Heat of Adsorption for Ethanol, Benzene, and Cyclohexane on Graphon

Ethanol

θ	q_{st} (kcal/mole)
0.040	12.3 ± 0.2
0.080	10.3 ± 0.6
0.120	9.73 ± 0.94
0.160	9.75 ± 1.01
0.200	10.1 ± 1.1
0.240	10.5 ± 1.0
0.320	10.9 ± 0.6
0.400	11.5 ± 0.4
0.480	11.8 ± 0.4
0.560	12.0 ± 0.5
0.640	11.6 ± 0.9
0.720	11.5 ± 1.0
0.800	11.5 ± 1.0
0.880	11.4 ± 1.0
0.960	11.0 ± 0.8
1.04	10.5 ± 0.6

Benzene

θ	q_{st} (kcal/mole)
0.767	9.34 ± 1.66
0.844	8.94 ± 1.10
0.920	8.73 ± 0.46
0.997	9.46 ± 0.23
1.07	9.40 ± 0.18
1.15	9.26 ± 0.18
1.23	9.06 ± 0.17
1.30	8.59 ± 0.15
1.38	8.27 ± 0.29
1.46	8.14 ± 0.33
1.53	8.13 ± 0.36

Cyclohexane

θ	q_{st} (kcal/mole)
0.776	13.4 ± 3.4
0.854	12.1 ± 3.1
0.932	8.81 ± 1.32
1.09	7.96 ± 1.42
1.16	8.41 ± 1.39
1.24	8.10 ± 1.04
1.32	8.14 ± 0.69
1.40	8.36 ± 0.48
1.48	8.50 ± 0.27
1.55	8.59 ± 0.15

Integral Entropy of Adsorption for Ethanol on Graphon

θ	$S - S_L$ (cal/mole-$^\circ$K)
0.058	-0.657
0.106	-2.67
0.161	-2.64
0.226	-2.14
0.298	-1.75
0.361	-1.53
0.423	-1.72
0.480	-1.17
0.528	-1.09
0.609	-1.24
0.684	-1.05
0.755	-0.884
0.812	-1.09
0.899	-1.24
0.911	-1.12
0.954	-1.25
0.993	-1.63
1.03	-1.95
1.06	-1.84
1.14	-2.37
1.21	-2.46
1.29	-2.58
1.35	-2.78
1.50	-3.16
1.63	-3.23
1.76	-3.59
1.96	-3.67
2.23	-3.68

APPENDIX III

Adsorption Data for Ethanol-Cyclohexane Mixtures on Cab-O-Sil

T	P_E (torr)	$N_E \times 10^6$ (mole/m^2)	P_C (torr)	$N_C \times 10^6$ (mole/m^2)	y_E
20°C	3.6	2.9	26.2	0.206	0.123
	6.0	3.8	22.0	0.452	0.213
	9.9	4.9	17.7	0	0.359
	12.1	6.02	14.8	0.148	0.450
	16.0	6.80	10.2	0.140	0.611
	19.4	7.73	8.2	0.24	0.703
	21.3	8.00	5.4	0.22	0.796
	23.7	8.88	3.0	0.17	0.887
30°C	3.6	0.80	29.6	0.928	0.110
	4.1	1.1	20.0	0.275	0.171
	9.2	1.9	20.8	0.418	0.307
	10.4	2.75	16.1	0.364	0.392
	11.5	2.22	15.4	0.575	0.428
	15.7	2.95	10.4	0	0.602
	19.9	4.42	5.0	0	0.798
	21.4	5.24	2.5	0.13	0.894
40°C	2.3	1.1	29.2	0.0677	0.074
	5.0	2.1	26.8	0.163	0.156
	7.8	2.7	22.7	0	0.255
	9.9	3.4	21.0	0	0.320
	13.1	4.01	17.5	0	0.428
	18.3	4.21	12.0	0	0.604
	20.7	4.32	9.8	0	0.679
	24.6	4.94	5.9	0	0.808
	26.2	5.54	3.3	0.17	0.887

Adsorption Data for Ethanol-Benzene Mixtures on Cab-O-Sil

T	P_E (torr)	$N_E \times 10^6$ (mole/m^2)	P_B (torr)	$N_B \times 10^6$ (mole/m^2)	y_E
20°C	3.5	2.4	25.4	2.00	0.122
	6.4	3.6	20.2	0.778	0.239
	10.3	4.37	17.0	0.258	0.377
	13.5	4.84	13.9	0.186	0.493
	17.0	5.52	10.5	0.0477	0.618
	19.4	5.67	7.4	0	0.725
	21.9	6.57	4.8	0	0.822
	23.1	7.75	2.4	0.12	0.905
30°C	2.1	0.90	36.7	2.46	0.055
	3.3	1.5	22.9	1.99	0.127
	5.9	2.4	20.4	1.10	0.223
	9.8	3.0	15.6	0.762	0.386
	14.5	4.13	10.3	0	0.585
	17.4	4.27	7.2	0.066	0.708
	15.0	4.55	4.3	0.13	0.776
	26.1	5.64	2.2	0.066	0.922
40°C	1.7	0.64	38.5	3.04	0.043
	6.4	1.4	34.6	1.87	0.155
	8.3	1.9	31.8	1.72	0.207
	13.2	2.37	28.6	1.13	0.316
	17.4	2.81	23.3	0.618	0.428
	23.0	3.56	18.0	0.481	0.561
	26.4	3.50	14.5	0.544	0.645
	31.9	4.27	10.2	0.372	0.758
	35.2	4.65	6.8	0.18	0.839
	41.6	5.57	1.8	0.083	0.958

Adsorption Data for Benzene-Cyclohexane Mixtures on Cab-O-Sil

T	P_B (torr)	$N_B \times 10^6$ (mole/m^2)	P_C (torr)	$N_C \times 10^6$ (mole/m^2)	y_B
20°C	2.2	1.1	27.2	3.01	0.075
	4.2	1.6	24.6	2.68	0.147
	7.6	1.8	20.6	2.06	0.276
	10.4	2.16	17.8	1.65	0.369
	13.4	2.51	15.0	1.24	0.472
	16.4	2.78	12.0	0.913	0.577
	19.6	3.84	8.3	0.88	0.703
	22.1	4.32	5.8	0.64	0.793
	25.0	5.39	2.4	0.53	0.912
30°C	4.6	0.84	27.6	1.94	0.144
	8.7	1.4	23.8	1.59	0.268
	8.4	1.4	18.4	1.27	0.313
	8.4	1.47	13.9	1.01	0.376
	13.0	1.99	14.0	0.925	0.481
	17.5	1.98	9.4	0.59	0.651
	12.3	2.20	4.3	0.50	0.739
	27.4	3.06	4.4	0.40	0.861
40°C	2.1	0.63	29.8	1.10	0.066
	4.6	0.79	27.5	0.534	0.142
	9.5	1.2	22.7	0.489	0.295
	13.2	1.34	19.8	0.278	0.400
	15.8	1.40	15.6	0.361	0.503
	17.1	1.90	12.2	0.489	0.584
	21.1	2.51	9.0	0.30	0.701
	23.5	2.63	5.7	0.45	0.806
	29.4	3.21	2.6	0.24	0.919

Adsorption Data for Cyclohexane-Ethanol Mixtures on Graphon

T	P_C (torr)	$N_C \times 10^6$ (mole/m^2)	P_E (torr)	$N_E \times 10^6$ (mole/m^2)	y_C
20°C	0.6	0.20	20.0	12.9	0.027
	3.5	0.28	20.7	7.83	0.146
	6.8	1.2	19.7	4.01	0.256
	8.1	2.4	18.7	2.90	0.302
	9.4	3.2	17.3	2.53	0.352
	12.0	4.12	15.7	1.34	0.433
	15.8	4.76	11.3	0.696	0.583
	18.1	5.01	9.5	0.45	0.656
	21.9	5.35	6.3	0.42	0.778
	25.4	5.26	3.3	0.028	0.884
30°C	3.1	1.4	25.0	6.12	0.111
	6.4	2.5	23.9	1.64	0.210
	9.9	3.6	20.6	1.06	0.325
	13.5	3.96	16.7	0.613	0.447
	16.2	4.09	14.3	0.752	0.531
	20.9	4.93	9.8	0.50	0.681
	24.1	5.21	6.3	0.58	0.794
	27.4	5.68	3.3	0.39	0.892
40°C	1.9	1.5	26.4	5.24	0.068
	3.8	2.0	27.5	2.03	0.123
	4.6	2.3	25.8	1.67	0.153
	8.0	3.57	22.6	1.56	0.261
	11.4	3.65	18.5	1.25	0.381
	12.5	4.07	17.7	1.17	0.414
	16.5	4.09	13.3	0.836	0.554
	20.2	4.29	9.5	0.72	0.680
	23.9	4.43	6.3	0.50	0.792
	27.5	4.85	3.2	0.39	0.895

Adsorption Data for Benzene-Ethanol Mixtures on Graphon

T	P_B (torr)	$N_B \times 10^6$ (mole/m^2)	P_E (torr)	$N_E \times 10^6$ (mole/m^2)	y_B
20°C	0.8	0.36	20.1	11.0	0.039
	3.8	1.2	19.0	7.38	0.168
	5.8	2.0	18.5	5.24	0.237
	8.3	2.9	18.2	3.04	0.313
	10.8	3.76	16.3	1.67	0.399
	14.2	5.10	13.2	0.891	0.518
	15.2	5.21	10.3	0.641	0.596
	19.7	5.57	8.3	0.22	0.704
	23.0	6.04	4.1	0.25	0.847
	25.6	5.74	2.8	0	0.902
30°C	3.1	1.5	23.7	5.32	0.117
	6.3	2.7	21.8	2.23	0.223
	8.6	3.3	19.3	1.89	0.308
	13.0	3.93	15.5	0.808	0.456
	16.7	4.87	11.6	0.808	0.590
	19.2	5.04	9.1	0.50	0.679
	23.3	5.43	6.1	0.39	0.794
	25.6	5.57	3.4	0.28	0.882
40°C	2.6	1.1	26.9	3.73	0.046
	3.6	2.0	23.8	2.37	0.133
	6.9	2.5	22.1	1.28	0.238
	11.0	3.20	17.7	0.641	0.383
	14.3	3.82	14.8	0.418	0.491
	17.4	3.98	11.4	0.446	0.604
	21.1	4.37	9.0	0.39	0.701
	23.1	4.54	6.2	0.36	0.789
	26.4	4.76	3.5	0.17	0.882

Adsorption Data for Benzene-Cyclohexane Mixtures on Graphon

T	P_B (torr)	$N_B \times 10^6$ (mole/m^2)	P_C (torr)	$N_C \times 10^6$ (mole/m^2)	y_B
20°C	2.1	0.80	27.3	6.16	0.072
	4.8	1.4	25.2	5.46	0.161
	8.3	2.2	21.2	3.84	0.281
	11.0	2.51	18.0	3.37	0.379
	14.4	3.29	14.5	2.98	0.498
	17.4	4.09	10.8	2.48	0.617
	20.0	5.07	7.9	2.0	0.717
	22.5	5.15	4.8	1.3	0.826
	25.6	5.74	1.9	0.80	0.930
30°C	2.2	0.70	26.9	5.49	0.076
	5.0	1.1	23.9	4.82	0.172
	8.6	2.1	20.3	4.54	0.297
	11.8	2.73	17.8	3.57	0.399
	14.4	3.34	14.3	3.37	0.502
	17.6	3.57	11.4	2.51	0.607
	20.3	3.82	8.0	1.8	0.718
	23.4	4.48	5.4	1.2	0.811
	26.6	5.54	2.0	0.62	0.929
40°C	3.9	0.93	27.8	5.54	0.089
	4.4	1.3	25.2	5.43	0.150
	7.8	1.8	22.8	4.46	0.254
	12.5	2.28	19.0	3.29	0.397
	14.6	3.04	15.2	2.90	0.490
	17.8	3.51	11.5	2.67	0.608
	21.1	3.54	9.4	1.7	0.692
	23.8	4.74	5.2	1.3	0.819
	27.0	5.57	2.1	0.70	0.927

Calculation of Binary Vapor Adsorption

Amount of benzene adsorbed in benzene-cyclohexane/Graphon isotherm at 20°C for $y_B = 0.498$:

V_2 = 49.0 cc
V_3 = 6032 cc
V_s = volume of sample container = 271 cc
R = 6.24×10^4 cc-torr/mole-°K
T_1 = room temperature = 301.0°K
T_2 = adsorption temperature = 293.0°K
Σ = surface area of Graphon sample = 359 m^2
P_i = initial partial pressure of benzene in V_3 = 18.8 torr
P_f' = final partial pressure of benzene in $V_2 + V_3$ = 14.3 torr
P_f = final (equilibrium) partial pressure of benzene in V_3

$$P_f = \frac{P_f'(V_2+V_3)}{V_3} = 14.4 \text{ torr}$$

$$n_i = \frac{P_i V_3}{RT_1} = 6.02 \times 10^{-3} \text{ mole}$$

$$n_f = \frac{P_f V_3}{RT_1} + \frac{P_f V_s}{RT_2} = 4.84 \times 10^{-3} \text{ mole}$$

$$n = n_i - n_f = 1.18 \times 10^{-3} \text{ mole}$$

$$N = \frac{n}{\Sigma} = 3.29 \times 10^{-6} \text{ mole/m}^2$$

APPENDIX IV

Spreading Pressures for Ethanol on Cab-O-Sil

20°C: P (torr)	$\pi/RT \times 10^6$ (mole/m^2)
2	5.38
6	10.4
10	13.2
16	16.2
20	17.7
26	19.8
30	21.0
36	22.8
40	24.1
44	26.0

30°C: P (torr)	$\pi/RT \times 10^6$ (mole/m^2)
2	4.67
10	11.1
20	14.7
30	17.2
40	19.1
50	20.7
60	22.3
70	24.0
77	24.8

40°C: P (torr)	$\pi/RT \times 10^6$ (mole/m^2)
5	5.64
10	8.08
30	13.0
50	15.6
70	17.5
90	19.2
110	20.9
126	22.5
135	23.5

Spreading Pressures for Benzene on Cab-O-Sil

20°C: P (torr)	$\pi/RT \times 10^6$ (mole/m^2)
10	2.03
20	3.48
30	4.78
40	5.89
50	6.97
60	8.23
70	9.65
75	10.6

30°C: P (torr)	$\pi/RT \times 10^6$ (mole/m^2)
10	1.63
20	2.83
30	3.85
40	4.74
50	5.55
60	6.34
70	7.13
80	7.94
90	8.80
102	9.65
119	10.3

40°C: P (torr)	$\pi/RT \times 10^6$ (mole/m^2)
10	1.04
30	2.49
50	3.60
70	4.64
90	5.68
110	6.74
130	7.84
150	9.05
162	9.37
182	9.96

Spreading Pressures for Cyclohexane on Cab-O-Sil

20°C: P (torr)	$\pi/RT \times 10^6$ (mole/m^2)
10	1.26
20	2.18
30	3.02
40	3.84
50	4.69
60	5.66
72	7.30
77	8.25

30°C: P (torr)	$\pi/RT \times 10^6$ (mole/m^2)
10	0.796
20	1.32
30	1.77
40	2.19
50	2.59
60	3.00
70	3.42
80	3.85
90	4.32
100	4.87
114	5.94
121	6.50

40°C: P (torr)	$\pi/RT \times 10^6$ (mole/m^2)
10	0.367
30	0.889
50	1.31
70	1.74
90	2.22
110	2.75
130	3.33
150	3.98
170	4.81
178	5.27
185	5.80

Spreading Pressures for Ethanol on Graphon

20°C: P (torr)	$\pi/RT \times 10^6$ (mole/m^2)
6	1.09
10	3.21
16	6.89
20	9.05
26	12.0
30	13.8
36	16.3

30°C: P (torr)	$\pi/RT \times 10^6$ (mole/m^2)
10	0.931
20	4.00
30	7.34
40	10.3
50	12.9
60	15.4
70	17.9

40°C: P (torr)	$\pi/RT \times 10^6$ (mole/m^2)
10	0.302
20	0.977
30	2.52
40	4.31
50	6.04
60	7.65
70	9.16
80	10.6
90	12.0
100	13.3
110	14.6
120	16.0

Spreading Pressures for Benzene on Graphon

20°C: P (torr)	$\pi/RT \times 10^6$ (mole/m^2)
6	6.45
10	8.38
20	11.5
30	13.6
40	15.2
50	16.9
60	18.7

30°C: P (torr)	$\pi/RT \times 10^6$ (mole/m^2)
10	6.57
20	9.28
30	11.1
40	12.5
50	13.7
60	14.8
70	15.8
80	16.9
90	18.0

40°C: P (torr)	$\pi/RT \times 10^6$ (mole/m^2)
10	4.79
20	7.12
30	8.71
40	9.95
50	11.0
60	11.9
70	12.7
80	13.4
90	14.1
100	14.8
110	15.4
120	16.0
130	16.7
140	17.4

Spreading Pressures for Cyclohexane on Graphon

20°C: P (torr)	$\pi/RT \times 10^6$ (mole/m^2)
6	7.50
10	9.45
20	12.3
30	14.2
40	15.6
50	17.0
60	18.6
70	21.1

30°C: P (torr)	$\pi/RT \times 10^6$ (mole/m^2)
10	6.94
20	9.63
30	11.4
40	12.7
50	13.8
60	14.7
70	15.6
80	16.4
90	17.3
100	18.3
110	19.6

40°C: P (torr)	$\pi/RT \times 10^6$ (mole/m^2)
10	5.48
20	7.97
30	9.58
40	10.8
50	11.8
60	12.6
70	13.3
80	13.9
90	14.5
100	15.1
110	15.6
120	16.2
130	16.7
140	17.3
150	18.0
160	18.8
170	19.9

Saturation Spreading Pressures for Ethanol-Cyclohexane and Ethanol-Benzene Mixtures on Cab-O-Sil

	Ethanol-Cyclohexane		Ethanol-Benzene	
T	y_E	$\pi^s/RT \times 10^5$ (mole/m^2)	y_E	$\pi^s/RT \times 10^5$ (mole/m^2)
20°C	0	0.825	0	1.06
	0.098	1.00	0.104	1.38
	0.203	1.50	0.151	1.55
	0.283	2.09	0.304	2.20
	0.375	2.33	0.392	2.32
	0.485	2.43	0.499	2.37
	0.549	2.47	0.593	2.40
	0.679	2.53	0.697	2.44
	0.825	2.58	0.805	2.47
	1.00	2.60	0.896	2.50
			1.00	2.60
30°C	0	0.652	0	1.03
	0.094	0.867	0.105	1.37
	0.197	1.34	0.199	1.81
	0.302	1.91	0.300	2.16
	0.400	2.14	0.407	2.32
	0.509	2.24	0.503	2.40
	0.703	2.36	0.630	2.44
	1.00	2.48	0.720	2.45
			1.00	2.48
40°C	0	0.580	0	0.996
	0.103	0.831	0.098	1.36
	0.199	1.32	0.202	1.75
	0.302	1.74	0.297	2.15
	0.395	2.02	0.408	2.28
	0.518	2.18	0.520	2.30
	0.708	2.29	0.595	2.32
	1.00	2.35	0.702	2.34
			1.00	2.35

The vita has been removed from the scanned document

ADSORPTION OF BINARY VAPOR MIXTURES ONTO SOLIDS

by

Gracia Ann Perfetti

(ABSTRACT)

The adsorption isotherms for ethanol-cyclohexane, ethanol-benzene, and benzene-cyclohexane vapor mixtures on Cab-O-Sil and on Graphon at 20, 30, and 40°C were measured at constant total pressure. The adsorption isotherms for the pure components were also obtained. The ethanol/Graphon isotherms were intermediate between Types II and III; for the other systems, Type II isotherms were obtained. The amounts of the pure vapors adsorbed on Cab-O-Sil followed the order ethanol > benzene > cyclohexane. The adsorption isotherms for benzene and cyclohexane on Graphon were almost identical. Except at low relative pressures, the amount of ethanol adsorbed on Graphon was greater than the amounts of benzene or cyclohexane adsorbed.

Isosteric heats of adsorption and BET cross-sectional areas were calculated for the pure adsorbates on Cab-O-Sil and on Graphon. The data indicated that the three adsorbates do not form close-packed monolayers on the Cab-O-Sil surface. The isosteric heat and the integral entropy of adsorption for ethanol on Graphon suggested that ethanol forms a hydrogen-bonded structure on the Graphon surface.

The binary vapor adsorption isotherms were compared to the pure component isotherms. In several instances, the amounts of the components adsorbed from the mixtures were greater than from the pure states. For the Cab-O-Sil systems, selective adsorption of ethanol occurred from

ethanol-cyclohexane and ethanol-benzene mixtures; benzene was selectively adsorbed from benzene-cyclohexane mixtures. The adsorbate-vapor composition diagrams for benzene-cyclohexane mixtures on Graphon all contained adsorption azeotropes. Very little selective adsorption of either component occurred. In general, benzene and cyclohexane were selectively adsorbed from benzene-ethanol and cyclohexane-ethanol mixtures on Graphon. Adsorption azeotropes occurred in the 20°C isotherms for these two systems at high ethanol mole fractions. The temperature dependence of the selectivity for the systems studied followed no consistent trend. Comparison of the binary vapor adsorption isotherms with the analogous solution adsorption isotherms indicated that selectivity is generally higher in adsorption from solution.

The experimental binary vapor adsorption isotherms were compared to those calculated from the pure vapor adsorption isotherms using the ideal adsorbed solution model. It was found that the adsorbed solutions were ideal or slightly nonideal for all three mixtures on Cab-O-Sil and for benzene-cyclohexane mixtures on Graphon. The nonideal behavior observed for benzene-ethanol and cyclohexane-ethanol mixtures on Graphon was attributed to the presence of benzene or cyclohexane disrupting the hydrogen-bonded structure of ethanol on the Graphon surface. It was concluded that the ideal adsorbed solution model is a useful one for predicting binary vapor adsorption equilibria.